

**TOWARDS A BETTER UNDERSTANDING OF CONTAMINANT FATE
IN PLASTIC PLUMBING SYSTEMS AND THEIR REMEDIATION**

by
Xiangning Huang

A Dissertation

*Submitted to the Faculty of Purdue University
In Partial Fulfillment of the Requirements for the degree of*

Doctor of Philosophy



Lyles School of Civil Engineering

West Lafayette, Indiana

December 2018

**THE PURDUE UNIVERSITY GRADUATE SCHOOL
STATEMENT OF COMMITTEE APPROVAL**

Dr. Andrew J. Whelton, Chair

Lyles School of Civil Engineering, Purdue University

Division of Environmental and Ecological Engineering, Purdue University

Dr. Chad T. Jafvert

Lyles School of Civil Engineering, Purdue University

Division of Environmental and Ecological Engineering, Purdue University

Dr. Amisha Shah

Lyles School of Civil Engineering, Purdue University

Division of Environmental and Ecological Engineering, Purdue University

Dr. John A. Howarter

School of Materials Engineering, Purdue University

Division of Environmental and Ecological Engineering, Purdue University

Approved by:

Dr. Dulcy Abraham

Head of the Department Graduate Program

Dedicate to

My Dearest Parents Xiuqin and Chao

and

My Loving Husband Shou

ACKNOWLEDGMENTS

I am very grateful and blessed with my graduate student life at Purdue. The journey for me was not always straight forward. I constantly doubted about myself and I could have failed not once but twice. But luckily I met some amazing people who always believed in me and gave me courage and strength to continue my journey.

First, I would like to thank my major advisor Dr. Andrew J. Whelton, who took me during one of my hardest times and healed me as a better and happier person. He was always there for me and convinced me that I could do better and I was capable. After half a year I joined the group, magic happened, I started enjoying my work and the lab environment. And I started thinking more and want to learn more. Then everything just turned right to me. Even today, I still think joining Professor Whelton's group was one of the best choice I have ever made. He is the great mentor, excellent advisor and always be supportive and enthusiastic with students' achievements, big or small. Thanks are extend to my committee members Dr. Chad T. Jafvert, Dr. Amisha Shah and Dr. John Howarter. They not only guided me to solve some technical questions, but also helped me to define my research topics and shared insights on how to prepare my presentations. Without their help, the dissertation would not have been completely.

I would also like to thank my parents Xiuqin and Chao, who supported me throughout my graduate study, financially and mentally. Because of them, I always feel secure and I know they will be always there for me for ups and downs. Lastly, I thank my husband Shou for his unconditionally support and love. Our story started from the first day of college and since then we have grown so much, but luckily we always hold each other's hand and never give up. Shou is very productive in his research area, and he is helping me constantly to troubleshoot my experimental questions. He is the one that can comfort me when I am stressed out and also brings me so much joy and laugh. Lastly, I want to thank Purdue University for supporting diversity, respect and equality. As an international student, we do easily miss our home country, but Purdue provides a friendly and supportive environment that make me feel more comfortable and welcomed. I think I would miss Purdue a lot and I send my best wishes to Purdue.

TABLE OF CONTENTS

LIST OF TABLES	viii
LIST OF FIGURES	ix
ABSTRACT	xi
AUTHOR’S PREFACE & ATTRIBUTION	xiii
CHAPTER 1. CRUDE OIL CONTAMINATION OF PLASTIC AND COPPER DRINKING	
WATER PIPES	1
1.1 Introduction	1
1.2 Experimental	7
1.2.1 Pipe Materials, Chemicals and Preparation	7
1.2.2 Pipe Contamination	7
1.2.3 Pipe Decontamination	8
1.2.4 Water Quality and Statistical Analysis	8
1.3 Results and Discussion	10
1.3.1 BTEX Fate in Contact with Plastic and Copper Pipe Materials	10
1.3.2 The Role of Pipe Type on MAH Concentration	13
1.3.3 Leaching of Oil Related Contaminants other than BTEX	14
1.3.4 The Value of TOC Monitoring	16
1.3.5 Future Work	17
1.4 Conclusion	18
1.5 References	19
CHAPTER 2. COMPETITIVE HEAVY METAL ADSORPTION ONTO NEW AND AGED	
POLYETHYLENE UNDER VARIOUS DRINKING WATER CONDITIONS	23
2.1 Introduction	23
2.2 Materials and methods	26
2.2.1 Materials and reagents	26
2.2.2 Characterization	27
2.2.3 Metal adsorption test	28
2.3 Results and discussion	30
2.3.1 New and aged LDPE characterization	30

2.3.2 The plastic condition and water pH influenced metal adsorption	30
2.3.3 Metal species and concentrations influenced metal loading on LDPE.....	33
2.3.4 PEX-A pipe dissolved organic carbon reduced metal adsorption to LDPE	34
2.3.5 Free chlorine and corrosion inhibitor reduced metal adsorption to suspended LDPE ..	35
2.3.6 The presence of iron reduced the amount of copper and lead adsorbed onto LDPE....	36
2.3.7 Metal accumulation and speciation on the LDPE surface	37
2.4 Conclusion	39
2.5 References.....	40
CHAPTER 3. CORROSION OF UPSTREAM METAL PLUMBING COMPONENTS	
IMPACTS ON DOWNSTREAM PEX PIPE SURFACE DEPOSITS AND DEGRADATION 45	
3.1 Introduction.....	45
3.2 Materials and methods	47
3.2.1 Characterizing metal scale and deposition on exhumed pipes	47
3.2.2 Bench-scale experiment on metals leaching and deposition on PEX pipe surfaces.....	49
3.2.2.1 Materials and pipe apparatus	49
3.2.2.2 Water conditions.....	49
3.2.2.3 Sample collection and analytical methods.....	49
3.2.2.4 Characterization.....	50
3.2.2.4 Statistical methods.....	51
3.3 Results and discussion	51
3.3.1 Chemical composition of exhumed residential plumbing pipe surface deposits.....	51
3.3.2 Metals in aqueous phase and PEX pipe surface deposits were influenced by water pH, temperature, and brass and copper composition.....	56
3.3.3 PEX pipe organic carbon release was influenced by water temperature.....	59
3.3.4 Indications of PEX pipe degradation.....	60
3.4 Conclusion	62
3.5 References.....	63
CHAPTER 4. IN-SITU CLEANING OF HEAVY METAL CONTAMINATED PLASTIC	
WATER PIPES USING A BIOMASS DERIVED LIGAND	
4.1 Introduction.....	68
4.2 Materials and methods	71

4.2.1 Materials and conditions.....	71
4.2.2 Equipment.....	71
4.2.3 Synthesis of lignin derived DHEL.....	72
4.2.4 Bench scale metal-DHEL complexation experiment	72
4.2.5 Performance of DHEL to remove heavy metals from exhumed pipes.....	73
4.2.6 Statistical analysis.....	75
4.3 Results and discussion	76
4.3.1 Characterization of DHEL structure.....	76
4.3.2 Fe ³⁺ -DHEL complex stability constant and binding ratio	77
4.3.3 Variation of metal loading on the service line plastic pipe material	78
4.3.4 Preliminary test and SEM-EDS analysis of DHEL interaction with exhumed plastic pipe	80
4.3.5 Kinetic study of DHEL interaction with exhumed plastic pipe.....	82
4.3.6 DHEL metal removal performance with exhumed plastic pipes.....	84
4.3.7 Relationship between total metal loading and total metal removed on pipe segments	86
4.3.8 Proposed reaction mechanism	87
4.4 Conclusion	89
4.5 References.....	90
APPENDIX A.....	94
APPENDIX B	101

LIST OF TABLES

Table 1.1 Summary of select oil spills affecting surface and ground water supplies	3
Table 1.2 MAH and PAH composition of various crude oils and refined products	5
Table 1.3 SPME-GC/MS target compounds	9
Table 1.4 BTEX concentration for PEX-A, PEX-B, HDPE, and copper pipes	10
Table 1.5 BTEX concentration during 30 day decontamination study	12
Table 1.6 Statistical analysis of multi-variant parameters	17
Table 2.1 Metal adsorption to suspended LDPE pellets was affected by the presence of dissolved organic carbon, corrosion inhibitor and free chlorine	35
Table 3.1 Chemical composition of GIP scales and the connected PEX pipe deposits removed from the residential housing	55
Table 3.2 Total mass of Ca, Cu, Pb and Zn leached in water samples and deposited on PEX surfaces during the 21 day exposure period	58
Table 4.1 Mass of metal deposits ($\mu\text{g/g}$ solid scale) found on plastic water distribution pipes ...	69
Table 4.2 Kinetic parameters and regression coefficients for DHEL metal removal from exhumed plastic pipe	84

LIST OF FIGURES

Figure 1.1 Physiochemical processes of spilled oil in the environment	6
Figure 1.2 Benzene leaching data from different pipe materials	13
Figure 1.3 Total BTEX leaching from different pipe materials.....	14
Figure 1.4 Total ion chromatogram (TIC) of PAH standards containing 17 PAHs	15
Figure 1.5 Total ion chromatogram (TIC) of a) 0.3% crude oil mixture and b) on day 3 contaminated PEX-A pipe leaching water	16
Figure 2.1 SEM images of (a) New LDPE segment and (b) 10 hr aged LDPE pellets.	30
Figure 2.2 Loading of (a) Cu (b) Mn (c) Pb and (d) Zn onto New, 2 hr aged, 5 hr aged, and 10 hr aged LDPE pellets for the mixed metal solution	32
Figure 2.3 Metal speciation predicted by Visual MINTEQ ver. 3.1.....	32
Figure 2.4 Competitive metal adsorption on 10 hr aged LDPE pellets varied with pHs.....	33
Figure 2.5 Adsorbed metal loading varied by metal type and concentration	34
Figure 2.6 The percent of total mass of metal adsorbed to LDPE (a) in the absence of Fe and (b) in the presence of Fe	37
Figure 2.7 Comparison without Fe and with Fe XPS spectra.....	39
Figure 3.1 Image of inner wall metal scales on exhumed pipes.	54
Figure 3.2 Element distribution along the same length of an exhumed PEX cold water pipe.	54
Figure 3.3 XPS spectra of metal deposits on exhumed PEX pipe surfaces	56
Figure 3.4 Metal levels when plumbing rigs exposed to the pH 4 and pH 7.5 water.....	59
Figure 3.5 PBP and CBP organics leaching.....	60
Figure 3.6 Images of PEX pipes that harvested at the end of 21 days.....	61
Figure 3.7 FTIR spectra for PEX pipe surfaces	62
Figure 4.1 Proton and carbon NMR spectra of DHE based DHEL.	76
Figure 4.2 UV-spectra of Fe ³⁺ -DHEL complex.....	77
Figure 4.3 Job's plot of a 1:1 Fe-DHEL complex at a) pH 4 and b) pH 7.....	78
Figure 4.4 Total metal loading along the same length of exhumed PEX-A pipes.....	80
Figure 4.5 Cross-section images of one year old PEX-A potable water pipe segments.....	81
Figure 4.6 SEM and EDS analysis of metals on exhumed plastic pipe surfaces.....	81
Figure 4.7 Percentage of metal removed kinetic test.....	83

Figure 4.8 DHEL performance test.....	86
Figure 4.9 The correlation between metal desorption with amount of metal loadings.....	87
Figure 4.10 Proposed DHEL metal removal mechanism from exhumed plastic pipe.....	89

ABSTRACT

Author: Huang, Xiangning. PhD

Institution: Purdue University

Degree Received: December 2018

Title: Towards A Better Understanding of Contaminant Fate in Plastic Plumbing Systems and Their Remediation

Committee Chair: Andrew J. Whelton

This dissertation focused on better understanding the fundamental processes that control organic and inorganic contaminant interaction with plastic plumbing pipes. Plastic pipes are increasingly being installed for drinking water plumbing, but their role in affecting drinking water quality has received little study. It is well-known that plastic pipes can sorb and release organic contaminants and be difficult to decontaminate. Several problems were identified in the literature and through discussions with industry: (1) Past guidance issued to communities affected by petroleum contaminated water does not seem to specifically consider plastic plumbing pipe remediation, (2) investigators have also identified heavy metals can accumulate on pipe inner walls, (3) Others have proposed certain heavy metals can catalyze plastic water pipe degradation, (4) No nondestructive cleaning methods were found for removing metal scales from plastic pipes. These topics were a basis for studies conducted because lack of information inhibits greater protection of public health, safety, and welfare.

This dissertation involved the application of knowledge and techniques from the environmental engineering and science, polymer engineering, and material science disciplines. Chapter 1 focused on the response of copper and plastic pipes (i.e., chlorinated polyvinylchloride (cPVC), high-density polyethylene (HDPE), crosslinked polyethylene (PEX)) exposed to petroleum contaminated drinking water. Bench-scale results revealed that pipe rinsing followed by a single 3 day water stagnation period removed target monoaromatic hydrocarbons (MAH) from copper pipes, but much longer (≥ 15 days) time was required for decontaminating cPVC, HDPC, and PEX pipes. Benzene, trimethylbenzene and polynuclear aromatic hydrocarbons, some of which are not typically considered in drinking water contamination investigations, were found desorbed into clean drinking water from pipes. Future plumbing decontamination guidance should consider the conditions necessary for plastic pipe remediation. Chapter 2 describes the influence of drinking

water conditions on heavy metal contaminant – low density polyethylene (LDPE) pellet surface interactions. Mixed metal drinking water solutions were applied and contained Cu, Fe, Mn, Pb and Zn at 30 µg/L. LDPE was selected as the model polymer because of its prior use for piping in Europe, use in bench-scale studies by others, and similarity to products used for the manufacture of more complex materials in the USA (HDPE, PEX). As expected, metal loadings were about 5 times greater for aged LDPE pellets suspended in solution compared to new LDPE pellets. This difference was attributed to the aged plastic surfaces having oxygen containing functional groups, increased surface area, and enhanced hydrophilicity. Metal loading was lower at pH >9.5 and in the presence of dissolved organic contaminants. The presence of free chlorine and corrosion inhibitor also decreased metal adsorption onto LDPE pellets. These factors likely enabled metal precipitation thereby not allowing metal species to adsorb to LDPE pellets suspended in water. XPS results showed deposited metals (i.e., Cu, Pb, Zn) primarily consisted of hydroxides and oxides. To further understand heavy metal – plastic pipe interactions, Chapter 3 involved the use of metal and plastic pipe rigs and exhumed PEX plumbing pipes. Exhumed cold and hot water PEX pipes contained a noticeable amount of heavy metals (i.e., most abundant metals were 2049 mg/m² Fe, 400 mg/m² Ca, 438 mg/m² Zn and 150 mg/m² P). Metal release and deposition onto PEX pipe was examined using bench-scale pipe rigs that contained new PEX pipe, brass valves, and copper pipe. Two water matrices (pH 4 and 7.5) and two temperatures (23°C and 55°C) were explored. The pH 4 water often accelerated metal leaching from brass valves, and a greater amount of heavy metals deposited on PEX pipes at high water pH and temperature (pH 4 and 55°C) conditions. Oxygen containing functional groups were detected on PEX pipes connected to a brass valve or a brass valve combined copper pipe, but were not found on PEX pipe only (controls) samples, indicating that certain configurations may facilitate plastic pipe degradation. The last chapter describes the ability of a new lignin derived ligand to remove metal deposits from exhumed PEX plumbing pipes. When the ligand concentration was ≥ 5mM, more than 95% of sorbed metals (i.e., Cu, Fe, Mn, Pb and Zn) were removed. The ligand favored certain metals over others (Cu > Zn > Fe > Mn > Pb) and heavy metal removal mechanisms were proposed. This dissertation provides insights into the role of plastic pipes on drinking water quality. As plastic pipes continue to be installed, it is in the interest of public health, welfare, and safety to understand their role in positively and negatively affecting drinking water safety.

AUTHOR'S PREFACE & ATTRIBUTION

Four manuscripts are enclosed as four separate studies (chapters) in this dissertation. The topics covered in this dissertation relate to drinking water safety, water chemistry and polymer science. For each study, the literature was reviewed, knowledge gaps and objectives were identified. Experiments were designed and conducted based on the knowledge-gaps identified and results were presented and thoroughly discussed.

Financial support for the efforts described in each chapter are as follows: Chapter 1 was funded by the Water Research Foundation and American Water Works Association's Water Industry Technical Action Fund (WITAF). Chapters 2 and 3 were funded by the United States Environmental Protection Agency (USEPA) (grant number: R836890). Chapter 4 was funded by the United States National Science Foundation (grant number: CBET-1228615) and Purdue Research Foundation Innovation Research Fund.

Attribution

A concise description of coauthors' contributions is listed as below. Xiangning Huang and Dr. Andrew J. Whelton (Associate Professor in Lyles School of Civil Engineering and Division of Environmental and Ecological Engineering, Purdue University) contributed to all chapters.

Chapter 1

This work was published in Journal of Hazardous Materials in 2017.

Ms. Stephane Andry (Division of Environmental and Ecological Engineering, Purdue University) contributed to conduct the literature search work.

Mr. Jessica Yaputri (Division of Environmental and Ecological Engineering, Purdue University) assisted experiment preparation and cleaning work.

Mr. Devin Kelly (Division of Environmental and Ecological Engineering, Purdue University) helped the experimental preparation and water samples collection.

Dr. David A. Ladner (Department of Environmental Engineering and Earth Sciences, Clemson University) made the contribution to solve technical problems and provided paper feedbacks.

Chapter 2

Mr. Dmitry Y. Zemlyanov (Birck Nanotechnology Center, Purdue University) assisted with XPS and SEM measurements.

Ms. Susana Diaz-Amaya (School of Materials Engineering, Purdue University) made the contribution to BET test.

Dr. Maryam Salehi (Department of Civil Engineering, The University of Memphis) helped with FTIR test.

Dr. Lia Stanciu (School of Materials Engineering, Purdue University) helped to solve technical problems during the BET test.

Chapter 3

Dr. Kelsey J. Pieper (Department of Civil and Environmental Engineering, Virginia Polytechnic Institute and State University) contributed to experimental design and statistical analysis.

Dr. H. Kory Cooper (Department of Anthropology) helped with pXRF measurements.

Ms. Susana Diaz-Amaya (School of Materials Engineering, Purdue University) assisted with FTIR test.

Mr. Dmitry Y. Zemlyanov (Birck Nanotechnology Center, Purdue University) assisted with XPS measurements.

Chapter 4

This work was published in Journal of Environmental Chemical Engineering in 2017.

Dr. Shou Zhao (Department of Chemistry and Biochemistry, University of California, Santa Barbara) contributed to synthesize lignin derived ligand.

Dr. Mahdi Abu-Omar (Department of Chemical Engineering and Department of Chemistry & Biochemistry, University of California, Santa Barbara) help to solve technical problems during the ligand synthesis.

CHAPTER 1. CRUDE OIL CONTAMINATION OF PLASTIC AND COPPER DRINKING WATER PIPES

1.1 Introduction

Oil spills pose threats to drinking water utilities, infrastructure, and community water supplies. For the year 2016, the U.S. National Response Center estimated that there were 23,170 chemical incidents in the U.S. Of those incidents, almost half (11,937) contaminated a water resource and about 60% were related to oil products [1]. Oils and related products such as crude, diesel, No. 2 fuel, and gasoline are often transported using hazardous material pipelines, trucks, and railcars [2-4]. As spills from these transport vessels have been previously demonstrated, contaminated source water can pass through drinking water treatment plants and water distribution systems, entering premise plumbing undetected [5-7] (Table 1.1).

A literature review demonstrated that oil spills in the U.S. and Canada have contaminated both surface and ground water supplies (Table 1.1). Oil spills commonly prompted communities to shut their intake (when warning was provided), truck in clean water, and/or switch to a backup water supply. Several incidents were first detected after contaminated water had passed through treatment plants and the water distribution system, and had reached customer taps [5, 7, 8]. A wide range of delays between the spill (e.g., pipe rupture) and detection were found (immediate detection vs. after 17 hr.) [9]. To protect public health and infrastructure, preventing oil contaminated water from reaching the water distribution system and customer infrastructure is desired, but evidence shows this does not always occur [10, 11].

Plastic water pipes are being chosen for new construction and water piping, which typically contain the largest surface area for contaminant sorption in distribution infrastructure. Plastic pipes

used for drinking water conveyance include crosslinked polyethylene (PEX) types A and B, high-density polyethylene (HDPE), and chlorinated polyvinylchloride (CPVC).

A previous study conducted by Marshutz (2001) showed that copper (90%) was the most widely used plumbing material in the U.S., compared to PEX (7%) and CPVC (2%) [18]. However, a more recent survey conducted in the southeastern United States revealed that PEX (54%) was the most common material for 59 households that replumbed followed by copper (9%) and CPVC (7%) [19]. The trend implies an increasing use of plastic pipes due to their flexibility and low cost. While some studies have shown oil contaminated soil or groundwater can externally permeate plastic water pipes (over long time), a short exposure period (hours to days) caused by conveyance of contaminated water has not been studied [20-24]. Because plastic pipes chemically differ from one another, water utilities that use some or all of these materials may have quite different experiences when trying to decontaminate their piping [25-27]. Furthermore, the degree of chemical leaching from oil contaminated pipes into clean water after the contaminated water has been flushed out has not been studied. The potential for contaminants to exceed drinking water maximum contaminant levels (MCLs), taste and odor limits also deserve scrutiny. Also, an important water quality parameter, total organic carbon (TOC) has been used to characterize the treatment efficiency of oil-field and natural gas produced water [28-30]. But TOC has not been evaluated as the potential indicator under the oil contaminated drinking water scenario.

Table 1.1 Summary of select oil spills affecting surface and ground water supplies used for drinking water

Location	Year	Pop.	Spill Details			Water System Details				
			Cause	Product	Delay, hr	Est. Vol. ^a , gal	Dist., mi	Alert?	Assets	Actions
Nibley, UT	15	5,000	Truck	Diesel	na	nr	nf	No	WTP, DS, PS	Water stations in nearby cites
Mt. Carbon, WV	15	2,000	Rail	Crude: Light	na	378,000	nf	Yes	nc	Ran out; Trucked-in
Greenbrier Co., WV	15	12,000	Truck	Diesel	na	4,000	nf	Yes	WTP	Ran out; Trucked-in
Longueuil, CAN	15	300,000	AST	Diesel	na	7,500	nf	No	WTP, DS, PS	Trucked-in
Glendive, MT	15	5,500	Pipe	Crude: Light	nf	30,000	nf	No	WTP, DS, PS	Trucked-in
Lynchburg, VA	14	492,900	Rail	Crude: Light	na	29,600	nf	Yes	nc	Alt source
Mayflower, AR	13	-	Pipe	Crude: Heavy	12	> 210,000	nf	Yes	nc	N/A
Sundre, CAN	12	-	Pipe	Crude: Light	2.3	12,600	25	No	WTP	Trucked-in
Marshall, MI	10	-	Pipe	Crude: Heavy	>17	>800,000	25	Yes	nc	n/a
Reston, VA	93	1,000,000	Pipe	#2 Fuel oil	> 0	477,436	60	Yes	WTP	Alt source
Simpsonville, SC	91	10,500	Pipe	#2 Fuel oil	>0	550,000	32	Yes	WTP	Alt source; Trucked-in
Pittsburgh, PA	88	23,000	AST	Diesel	na	>800,000	600	Yes	WTP	Alt source; Trucked-in
Atlanta, GA	63	625,000	Pipe	Kerosene	nf	60,000	nf	No	WTP	Trucked in

a. Volume of spilled oils are approximate values

AST = Above ground storage tank; WTP = water treatment plant; DS = Distribution system; PS = Building plumbing systems; nc = not contaminated

Reproduced with permission by the Water Research Foundation (2016).

Crude oils and their related products are complex mixtures that contain organic, inorganic, and radionuclide compounds. Monoaromatic (MAH) and polycyclic aromatic hydrocarbons (PAH) represent the majority of oil products by mass, and their compositions vary widely by geographical location and source [31, 32]. As shown in Table 1.2, crude oil and the related products can contain high organic chemical concentration and compounds have a wide range of physiochemical properties.

For regulated drinking water contaminants, the maximum contaminant concentration present in oils can be as much as 2.2×10^6 times greater than the corresponding drinking water MCLs (e.g., benzo(a)pyrene). Even when spilled oil might be diluted in the receiving water, there is still the risk that the drinking water standards could be exceeded for some oil-related contaminants. It is noteworthy that some compounds present in oils do not have federal drinking water standards (Table 1.2). However, as the 2014 chemical spill in West Virginia made clear, contaminants without federal drinking water standards can also pose health risks [33]. Therefore, it is important for emergency responders to fully characterize which contaminants are present in the spilled oil and contaminated water so health officials can conduct the appropriate risk assessments. Once oil enters a water, the fate of oil contaminants is a function of contaminant physiochemical properties, environmental conditions, and other materials that contact the contaminants (Figure 1.1). It is well-known that volatilization is a major mass transfer pathway for gasoline and kerosene spills because these liquids contain a great amount of high volatility constituents [34, 35]. However, dissolution of volatile contaminants also occurs simultaneously and fate of these contaminants in the water column is also important.

Table 1.2 MAH and PAH composition of various crude oils and refined products

Contaminant Detected in Oil	U.S. Drinking Water Limit, mg/L	Concentration in Oil, mg/L	Max Concentration in Oil/ Drinking Water Limit Ratio	Property		
				VP at 25°C, mmHg	C _w at 25°C, mg/L	Log K _{ow} at 23°C
<i>Monoaromatic Hydrocarbons (MAHs)</i>						
Benzene ^a	0.005 ^b	0-2866	573,200	94.8	1,790	2.13
Toluene	1 ^b	136-5,928	5,928	28.4	526	2.73
Ethylbenzene	0.7 ^b	58-1,319	1,884	9.6	169	3.15
Total Xylenes	10 ^b	396-6,187	618	6.61	178	3.12
C ₃ -Benzenes	-	940-13,780	-	-	-	-
Total MAH	-	1,570-21,920	-	-	-	-
<i>Polycyclic Aromatic Hydrocarbons (PAHs)</i>						
Naphthalene ^a	0.02 ^c	3,939-20,852	1,042,600	8.50 x 10 ⁻²	31	3.30
Phenanthrene	-	1,296-22,779	-	1.21 x 10 ⁻⁴	1.15	4.46
Dibenzothiophene	-	609-2,033	-	2.05 x 10 ⁻⁴	1.47	4.38
Fluorene	0.04 ^c	513-4,986	124,650	6.00 x 10 ⁻⁴	1.69	4.18
Chrysene	-	167-11,887	-	6.23 x 10 ⁻⁹	2.00 x 10 ⁻³	5.81
Biphenyl	-	7-839	-	-	-	-
Acenaphthylene	-	7-34	-	6.68 x 10 ⁻³	16.1	3.94
Acenaphthene	0.06 ^c	2.86-167	2,783	2.15 x 10 ⁻³	3.9	3.92
Anthracene	0.3 ^c	0.99-217	723	6.53 x 10 ⁻⁶	0.0434(24°C)	4.45
Fluoranthene	-	0.27-80	-	9.22 x 10 ⁻⁶	0.26	5.16
Pyrene	0.03 ^c	4.10-552	18,400	4.50 x 10 ⁻⁶	0.135	4.88
Benz(a)anthracene ^a	-	0.25-551	-	-	-	-
Benzo(b)fluoranthene ^a	-	0.12-125	-	5.00 x 10 ⁻⁷	1.50 x 10 ⁻³	5.78
Benzo(k)fluoranthene ^a	-	0.12-34	-	9.65 x 10 ⁻¹⁰	8.00 x 10 ⁻⁴	6.11
Benzo(e)pyrene	-	0.12-221	-	5.70 x 10 ⁻⁹	6.30 x 10 ⁻³	6.44
Benzo(a)pyrene ^a	0.0002 ^b	0.12-449	2,245,000	-	-	-
Perylene	-	0-159	-	5.25 x 10 ⁻⁹	4.00 x 10 ⁻⁴	6.25
Indeno(1,2,3c,d)pyrene ^a	-	0-25	-	-	-	-
Dibenz(a,h)anthracene ^a	-	0-68	-	-	-	-
Benzo(g,h,i)perylene	-	0-83	-	1.00 x 10 ⁻¹⁰	2.60 x 10 ⁻⁴	6.63

Sources: [12-14]. a. Substance defined as a known or probable human carcinogen by the IARC and NTP. [15, 16]; b. U.S. EPA Maximum Contaminant Level of Drinking Water (MCL) (mg/L) [17]; c. Reference dose proposed by U.S. EPA Drinking Water Health Advisories (mg/kg/day) [14]; VP-Vapor Pressure, mmHg; C_w-Water Solubility, mg/L; Log K_{ow}- Octanol-Water Partition Coefficient; Dash (-) represents no Drinking Water Standards or Health Advisories available for that contaminant. Reproduced with permission by the Water Research Foundation (2016).

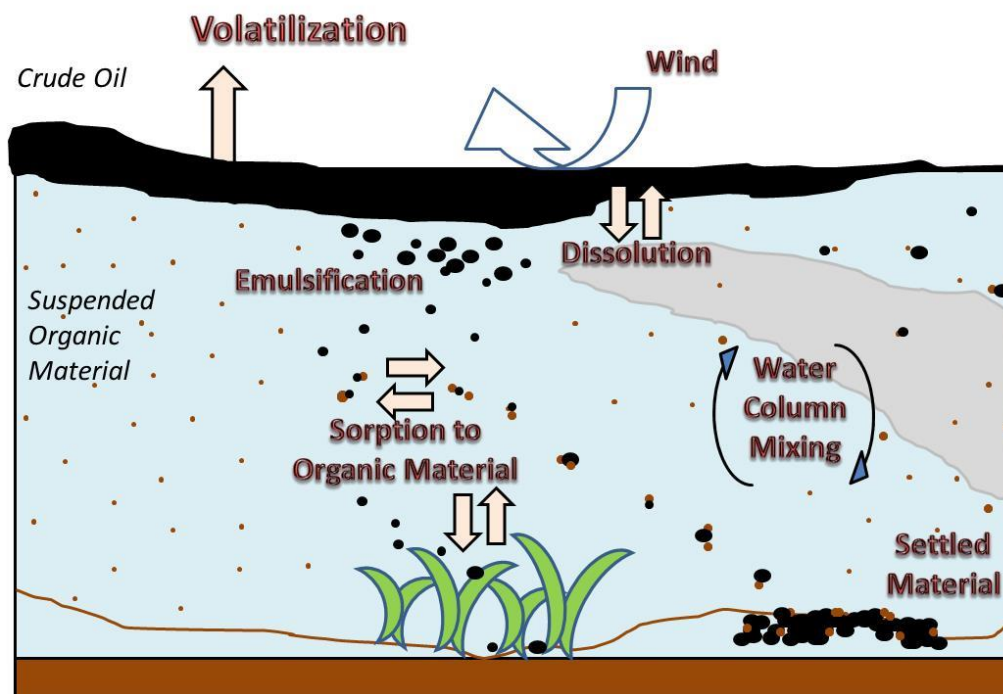


Figure 1.1 Physiochemical processes of spilled oil in the environment. Reproduced with permission by the Water Research Foundation (2016).

This study was initiated to understand the degree to which plastic and copper pipes become contaminated by oil and subsequent leaching of sorbed contaminants into the water supply. The goal of this work was to investigate which plumbing materials were more susceptible (easier to sorb and desorb contaminants) during the short duration contamination events and the duration required for contaminants in the water back to the safe level. The specific objectives were to (1) assess the potential of benzene, toluene, ethylbenzene, and xylenes from crude oil contaminated water to sorb and desorb from the PEX, HDPE, CPVC, and copper pipes over a 30-day leaching period, (2) determine if other crude oil related contaminants (e.g. MAHs and PAHs) can be sorbed and desorbed from PEX-A pipe, and (3) evaluate whether TOC concentration is a good indicator for oil contaminated water.

1.2 Experimental

1.2.1 Pipe Materials, Chemicals and Preparation

PEX-A, PEX-B, HDPE, CPVC and copper potable water pipes were purchased from regional pipe supply companies with different inner diameters: 1.70, 1.68, 2.09, 1.77 and 2.06 cm, respectively. PEX-A pipe was manufactured with a medium-density polyethylene (PE) resin while PEX-B pipe was manufactured with a high-density PE resin. HDPE pipe was also manufactured with a high-density resin. All pipes were labeled as certified for potable water with a National Sanitation Foundation International [36] logo. BTEX (e.g. benzene, toluene, ethylbenzene and total xylene) (SKU-43728) and trimethylbenzene isomer analytical standards were purchased from Sigma Aldrich. The DEP(MA)-PAH mix was obtained from AccuStandard (1000 μ g/mL in CH₂Cl₂). Louisiana light sweet crude (LLSC) oil used for the experiments was obtained from a crude oil processing facility in Mobile, AL.

Before pipe contamination experiments were conducted, all new pipes were tap water rinsed and disinfected similar to field protocols [37]. Pipes were flushed for 10 min. with tap water then were filled with a 200 mg/L free chlorine solution (made from 5.65-6% wt% of NaOCl, Fisher Chemical). The laboratory prepared tap water was a low alkalinity water recipe adopted from prior work, with the pH adjusted in the range of 6 to 8 [38, 39]. Teflon[®] wrapped silicon stoppers were used to keep the water in place and prevent leaking. After 3 hr. stagnation, pipes were drained and flushed again using tap water for 3 min.

1.2.2 Pipe Contamination

Pipes were contaminated with one of two crude oil / contaminated water solutions: (1) 0.05% v/v solution and (2) 0.3% v/v solution. The 0.3% solution was adopted from an ongoing U.S. EPA crude oil-cast iron water pipe contamination study [40]. An oil-water solution 50 times less

concentrated (i.e. 0.05%) was also examined in the present study. Oil-water solutions were prepared by 20 hr. of mixing LLSC and synthetic tap water in aspirator bottles [41]. After 5 hr. of stagnation, aliquots were removed through the bottom aspirator valve to obtain water with the soluble fraction of oil. Pre-conditioned pipe coupons were filled with oil solutions without headspace, capped and remained stagnant for 3 days. This exposure duration was based on prior Do Not Use drinking water orders which typically lasted 2 to 3 days, but for some cases the contaminated water could be remained in place for up to 30 days [42]. A control group was prepared by filling pipe coupons with synthetic tap water only. All the experiments were conducted in triplicate.

1.2.3 Pipe Decontamination

After the pipe contamination period, each pipe was drained and rinsed with about 200 mL synthetic tap water to remove any residue on the pipe inner wall. Next, pipes were filled and replaced with freshly prepared synthetic tap water. This draining and refilling procedure was repeated every three days for up to 30 days [38, 43]. At day 3, 6, 9, 15, and 30, water drained from the pipe was collected and characterized for BTEX, other MAHS, potential PAHs and TOC concentration. After sampling process on certain day, pipe segments would be refilled with clean water. Leaching results were expressed in two forms: (1) BTEX/TOC aqueous concentrations, $\mu\text{g/L}$ or mg/L and (2) conversion of BTEX/TOC levels to $\mu\text{g}/\text{dm}^2$ so pipe diameter differences were considered. For more details, BTEX/TOC leaching data were calculated by multiplying measured concentration ($\mu\text{g/L}$) by volume of the pipe coupon (L) and divided by pipe inner surface area (dm^2).

1.2.4 Water Quality and Statistical Analysis

Headspace solid phase microextraction-gas chromatography/mass spectrometry (HS-SPME-GC/MS) was used to quantify aqueous BTEX (benzene, toluene, ethylbenzene and xylene, total)

concentration [44, 45] (Table 1.3). Method details are shown elsewhere [11]. A Supelco SPME fiber assembly (100 μm PDMS, fused silica 23 Ga) was selected to extract the volatile compounds. The fiber was pre-conditioned with a hot injector inlet (250 $^{\circ}\text{C}$) for 30 min. The GC column was Zebron ZB-WAX from Phenomenex (diameter 0.32 mm, length 30 m, film 0.5 μm) coupled with multipurpose MS detector. BTEX standard and synthetic tap water were used to make standard solutions. Calibration curves were developed for both low (0.2-10 $\mu\text{g/L}$) and high range (50-2,000 $\mu\text{g/L}$) of BTEX solutions with the correlation coefficient of 0.99 or greater. The total xylene concentration was calculated as counting *o*-, *m*-, and *p*-xylene isomers and reported in this study. The liquid-liquid extraction technique was performed as described from a past study and the concentrate was analyzed by GC-MS [46]. Peaks detected from concentrates were confirmed with BTEX, trimethylbenzene and PAHs standards (e.g. retention time and parent ion), coupled with mass spectral library. TOC concentration was determined using a Shimadzu TOC-L CPH analyzer with a calibration standard curve ranging up to 10 mg/L (USEPA method 415.1) [47, 48]. NCSS software was applied to perform single and multi-variate analysis of variance (ANOVA) with a $\alpha = 0.05$ significance level.

Table 1.3 SPME-GC/MS target compounds

Compounds	RT (min)	Quantification ions (m/z)	MDL ^b ($\mu\text{g/L}$)
Benzene	2.84	78, 77, 52	0.24
Toluene	4.38	91, 92, 65	0.18
Ethyl benzene	5.98	91, 106, 51	0.16
Xylene, total	Various ^a	91, 106, 105	0.44

a. RT, retention time for *o*-, *m*-Xylene and *p*-Xylene ranged from 6.10 to 7.40 min.; b. MDL, minimum detection limit for each compound was calculated based on 7 replicates, MDL = Std. dev * $t_{(n-1)}$.

Reproduced with permission by the Water Research Foundation (2016).

1.3 Results and Discussion

1.3.1 BTEX Fate in Contact with Plastic and Copper Pipe Materials

After oil contaminated water contacted pipes for three days, aqueous MAH concentration was significantly reduced (Table 1.4) ($p < 0.01$). The initial BTEX concentrations for the crude oil water were: benzene ($935 \pm 41 \mu\text{g/L}$), toluene ($284 \pm 13 \mu\text{g/L}$), ethylbenzene ($205 \pm 3 \mu\text{g/L}$), and total xylenes ($1,139 \pm 32 \mu\text{g/L}$). After the 3 day exposure period, BTEX levels were much lower for all plastic pipe solutions compared to copper pipe solution. These results indicated that plastic pipes have more affinity to BTEX compounds than copper pipes. It is well-known BTEX compounds can permeate the plastic pipes studied, but this short duration exposure and head-to-head experiment underscores how different the materials perform under a similar contamination scenario. Additional experiments were conducted to evaluate pipe decontamination and leaching for a 30 day period.

Table 1.4 BTEX concentration for PEX-A, PEX-B, HDPE, and copper pipes exposed in the 0.05% oil mixture for 3 days

Pipe Material	Concentration ($\mu\text{g/L}$)			
	B	T	E	X
PEX-A	255 ± 35	21 ± 4	95 ± 1	384 ± 3
PEX-B	269 ± 35	24 ± 5	96 ± 1	389 ± 4
HDPE	214 ± 10	17 ± 0	95 ± 2	378 ± 9
Copper	397 ± 74	107 ± 23	141 ± 7	718 ± 33

Data shown represents the mean (standard deviation) for triplicate pipe samples. Results for CPVC initial and after 3 days BTEX levels in the crude oil mixture were not able to be measured.

Reproduced with permission by the Water Research Foundation (2016).

As expected, the greatest BTEX concentrations were detected for all pipes on day 3, but BTEXs were only detected on day 3 for copper pipes (Table 1.5). Absence of BTEX on subsequent testing days is likely due to residual contaminants that had adhered to the copper pipe surface and were not removed during contaminated pipe tap water rinsing. For all plastic pipes, benzene and toluene were detected in water for up to 15 days. This result indicated that those contaminants had

permeated and were desorbing from the plastic pipes. Except for CPVC pipe, benzene and toluene were detected for all PE pipes for 30 days. 3. Copper drinking water pipe is a common material used to replacement plastic pipes that have been externally permeated due to petroleum product spills [26, 49].

As simulated water use continued, lower concentrations of BTEXs were found. PEX-A pipe was the most susceptible to contamination as reflected by the greatest amount of BTEX desorbed during the study. This finding indicates that the type of water pipe even within the same water distribution system or building plumbing could influence why different drinking water contaminant levels are detected during after contaminated drinking water has been flushed out. Water utilities and health officials should consider the type of water pipe material in contact with contaminated drinking water when determining the time needed to return infrastructure to safe use. A review of drinking water contamination incidents indicated this phenomenon has not been incorporated into water distribution and building plumbing decontamination procedures [42].

During the 30 day decontamination study for the plastic and copper pipes examined, benzene was the only compound found to exceed its MCL. For the 0.3% oil mixture condition, all four plastic pipes exceeded the benzene MCL on day 9 (Table 1.5). Even on day 15, all polyethylene pipes leached benzene above its corresponding MCL. Copper pipe was the least affected (MCL only exceeded on day 3). PEX-A pipe consistently resulted in the greatest benzene concentration throughout the 30 day study. For the less concentrated oil water mixture (0.05%) condition, the detected benzene concentration was much lower, but still exceeded its MCL for 11 of 25 pipe-exposure duration pairs. Again, benzene levels from PEX-A pipe were markedly greater than for PEX-B, HDPE, and CPVC pipes. MCLs for toluene (1,000 $\mu\text{g/L}$), ethylbenzene (700 $\mu\text{g/L}$), and total xylene (10,000 $\mu\text{g/L}$) were not exceeded or approached for either oil-water condition.

However, on day 3 TEX compounds exceeded their taste and odor thresholds for the 0.3% crude oil contamination scenario (Table 1.5). Even though TEX compounds were below their health based MCLs, their presence would have contributed to taste and odor problems for polyethylene materials. In contrast, for the 0.3% oil mixture condition TEX levels for CPVC and copper pipes slightly exceeded taste and odor thresholds for day 3 only.

Table 1.5 BTEX concentration during 30 day decontamination study for PEX-A, PEX-B, HDPE, CPVC, and Copper pipes

Material	Mean Desorbed Concentration (µg/L)							
	B	T	E	X ^a	B	T	E	X
	<u>0.3% oil mixture Day 3</u>				<u>0.05% oil mixture Day 3</u>			
PEX-A	1,434.4	140.2	2.43 ^o	73.00 ^o	77.0	12.6	-	-
PEX-B	1,167.9	116.8 ^{oT}	1.68	66.80 ^o	36.0	3.53	-	-
HDPE	1,274.1	129.0 ^{oT}	2.07 ^o	58.50 ^o	39.6	1.61	-	-
CPVC	81.03	38.88 ^o	2.42 ^o	10.36	9.22	0.76	-	-
Copper	5.45	7.90	2.18 ^o	22.60 ^o	0.46	0.85	-	-
	<u>0.3% oil mixture Day 6</u>				<u>0.05% oil mixture Day 6</u>			
PEX-A	121.1	9.10	1.09	8.72	56.7	4.61	-	-
PEX-B	80.2	2.89	0.47	3.68	25.4	3.03	-	-
HDPE	100.5	1.56	-	2.38	24.2	2.02	-	-
CPVC	10.63	0.98	-	-	2.38	0.51	-	-
Copper	-	-	-	-	-	-	-	-
	<u>0.3% oil mixture Day 9</u>				<u>0.05% oil mixture Day 9</u>			
PEX-A	51.3	11.1	-	-	25.4	0.61	-	-
PEX-B	37.6	9.82	-	-	5.33	0.28	-	-
HDPE	47.4	9.13	-	-	5.03	0.33	-	-
CPVC	5.12	0.42	-	-	1.26	0.43	-	-
Copper	-	-	-	-	-	-	-	-
	<u>0.3% oil mixture Day 15</u>				<u>0.05% oil mixture Day 15</u>			
PEX-A	21.0	9.46	-	-	6.14	-	-	-
PEX-B	16.5	5.33	-	-	3.01	-	-	-
HDPE	18.5	7.63	-	-	2.10	-	-	-
CPVC	1.74	0.28	-	-	0.70	0.37	-	-
Copper	-	-	-	-	-	-	-	-
	<u>0.3% oil mixture Day 30</u>				<u>0.05% oil mixture Day 30</u>			
PEX-A	0.23	0.48	-	-	0.79	-	-	-
PEX-B	0.34	0.20	-	-	0.54	-	-	-
HDPE	0.28	0.26	-	-	0.25	-	-	-
CPVC	-	-	-	-	-	-	-	-
Copper	-	-	-	-	-	-	-	-

a Xylene represents total xylene, which counts for o-, m-, p-isomers; - represents the value is less than detection limit or not detectable; Red and bolded text represents a concentration that exceeds an MCL; ^o Concentration is greater than the odor threshold; ^T Concentration is greater than the taste threshold.

Reproduced with permission by the Water Research Foundation (2016).

1.3.2 The Role of Pipe Type on MAH Concentration

To determine the role of pipe type on leaching performance, BTEX concentrations were normalized using each pipe's inner wall surface area ($\mu\text{g}/\text{dm}^2\text{-time}$). MAH flux, mass/surface area-time, from PE materials was initially orders of magnitude greater than flux from CPVC and copper pipes (Figures 1.2 and 1.3). Differences were less noticeable by day 30. When the inner pipe wall surface area exposed to contaminated water was normalized across pipes, the PEX-A material was still the most susceptible to BTEX permeation and leaching. For the 0.05% oil contamination scenario, the rank of most to least contaminated pipe materials was PEX-A > HDPE > PEX-B > CPVC > copper ($p < 0.01$) (Table 1.6).

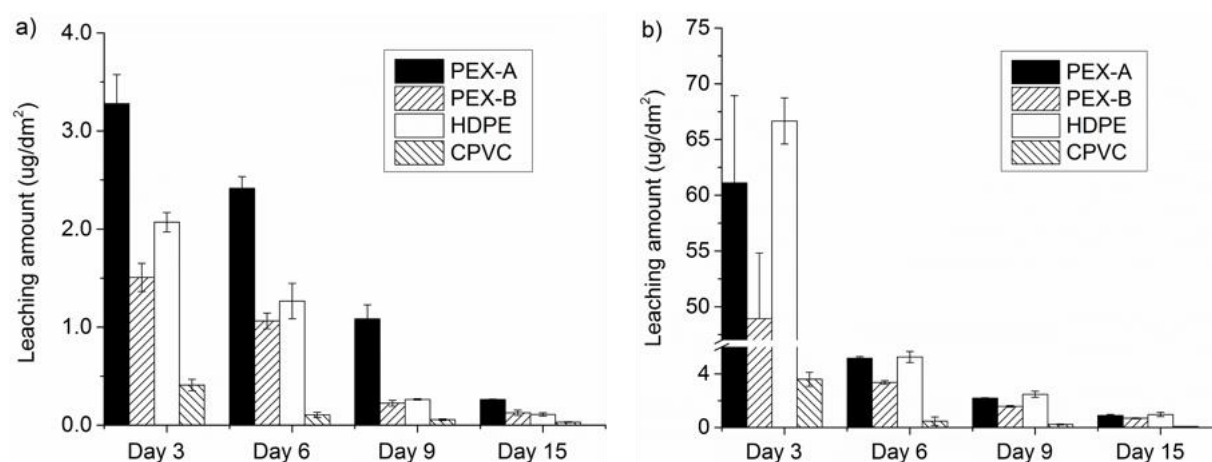


Figure 1.2 Benzene leaching data from different pipe materials, presented as mass per unit surface area, during decontamination process from two contamination scenarios: a) 0.05% oil mixture contamination scenario and b) 0.3% oil mixture contamination scenario. For each pipe material, 3 pipe coupon replicates were adopted to measure the consistency. Column height is the average and the error bars show the standard deviation. Reproduced with permission by the Water Research Foundation (2016).

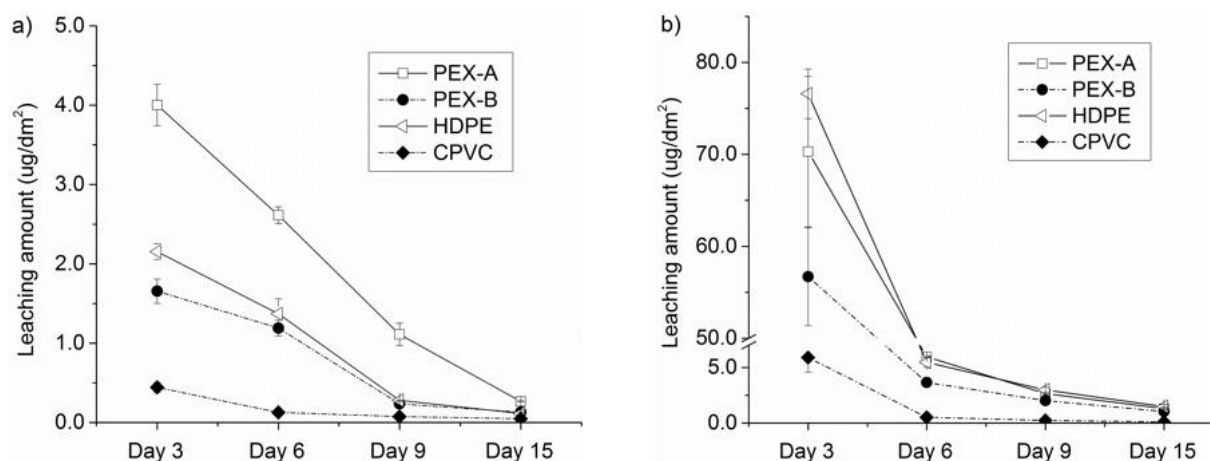


Figure 1.3 Total BTEX leaching from different pipe materials, presented as mass per unit surface area, during decontamination process from two contamination scenarios: a) 0.05% oil mixture contamination scenario; b) 0.3% oil mixture contamination scenario. For each pipe material, three pipe coupon replicates were adopted to measure the consistency. Symbols represent the average and the error bars show the standard deviation. Reproduced with permission by the Water Research Foundation (2016).

BTEX leaching from pipe materials depended on the initial drinking water oil exposure concentration, the type of plumbing materials, as well as the exposure duration after contamination occurred (Table 1.6). When the oil concentration was increased to 0.3% v/v, no difference was found between PEX-A and HDPE pipes ($p = 0.896$). The remaining materials had lower fluxes than both PEX-A and HDPE pipes during the study period: PEX-B > CPVC > Copper ($p < 0.05$). Copper pipe sorbed and desorbed much less contaminant compared to all plastics studied (Table 1.5).

1.3.3 Leaching of Oil Related Contaminants other than BTEX

Because PEX-A pipe was the most susceptible material to BTEX contamination, leaching from this pipe was studied in greater detail. Analytical standards were used to identify the tentatively identified compounds in both the crude oil/water mixture and water samples exposed to contaminated pipes (Figure 1.4). After the simulated 3 day Do Not Use drinking water condition with the 0.3% v/v crude oil-water mixture, PEX-A pipe on day 3 leached a variety of oil related

compounds (Figure 1.5). In addition to BTEX several other MAHs and PAHs had sorbed and desorbed into drinking water. Contaminants that were confirmed include 1,3,5-trimethylbenzene, 1,2,4-trimethylbenzene, 1,2,3-trimethylbenzene, naphthalene, 2-methylnaphthalene and 1-methylnaphthalene. None of these contaminants have drinking water MCLs [17]. A limitation of this study is that drinking water disinfectants were not present in the test water for this experiment. Although, analytical methods oil constituents are susceptible to halogenation during water treatment [52], and could be transformed into other compounds also not routinely screened for during standard analytical methods. Results show that once contaminated water is suspected, chemical analysis is needed to thoroughly identify the compounds present [11]. Negative emergency response, public health, and public confidence consequences of issuing water safety guidance without appropriately identifying chemicals in the contaminated drinking water can be found elsewhere [54].

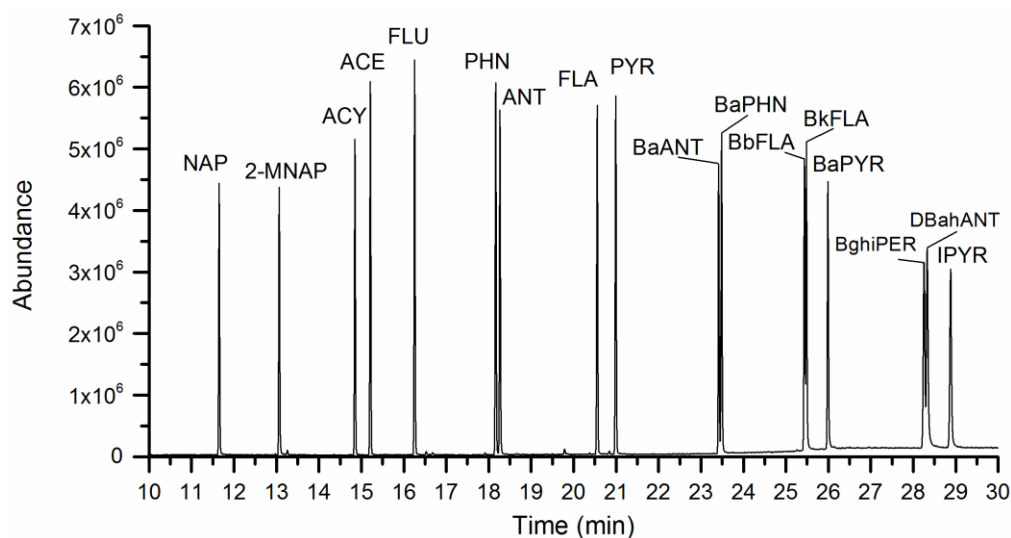


Figure 1.4 Total ion chromatogram (TIC) of PAH standards containing 17 PAHs with peaks labeled as: NAP: naphthalene (rt=11.65, m/z=128); 2-MNP: 2-methylnaphthalene (rt=13.07, m/z=142); ACY: acenaphthylene (rt=14.85, m/z=152); ACE: acenaphthene (rt=15.21, m/z=154); FLU: fluorene (rt=16.25, m/z=165); PHN: phenanthrene (rt=18.17, m/z=178); ANT: anthracene (rt=18.27, m/z=178); FLA: fluoranthene (rt=20.56, m/z=202); PYR: pyrene (rt=20.99, m/z=202); BaANT: benzo(a)anthracene (rt=23.42, m/z=228); BaPHN: benzo(a)phenanthrene (rt=23.49, m/z=228); BbFLA: benzo(b)fluoranthene (rt=25.44, m/z=252); BkFLA: benzo(k)fluoranthene (rt=25.49, m/z=252); BaPYR: benzo(a)pyrene (rt=25.99, m/z=252); BghiPER: Benzo(g,h,i)perylene (rt=28.25, m/z=276); DBahANY: Dibenzo(a,h)anthracene (rt=28.33, m/z=278) and IPYR: Indeno(1,2,3-cd)pyrene (rt=28.88, m/z=276). rt stands for retention time. m/z is the parent ion for the contaminant.

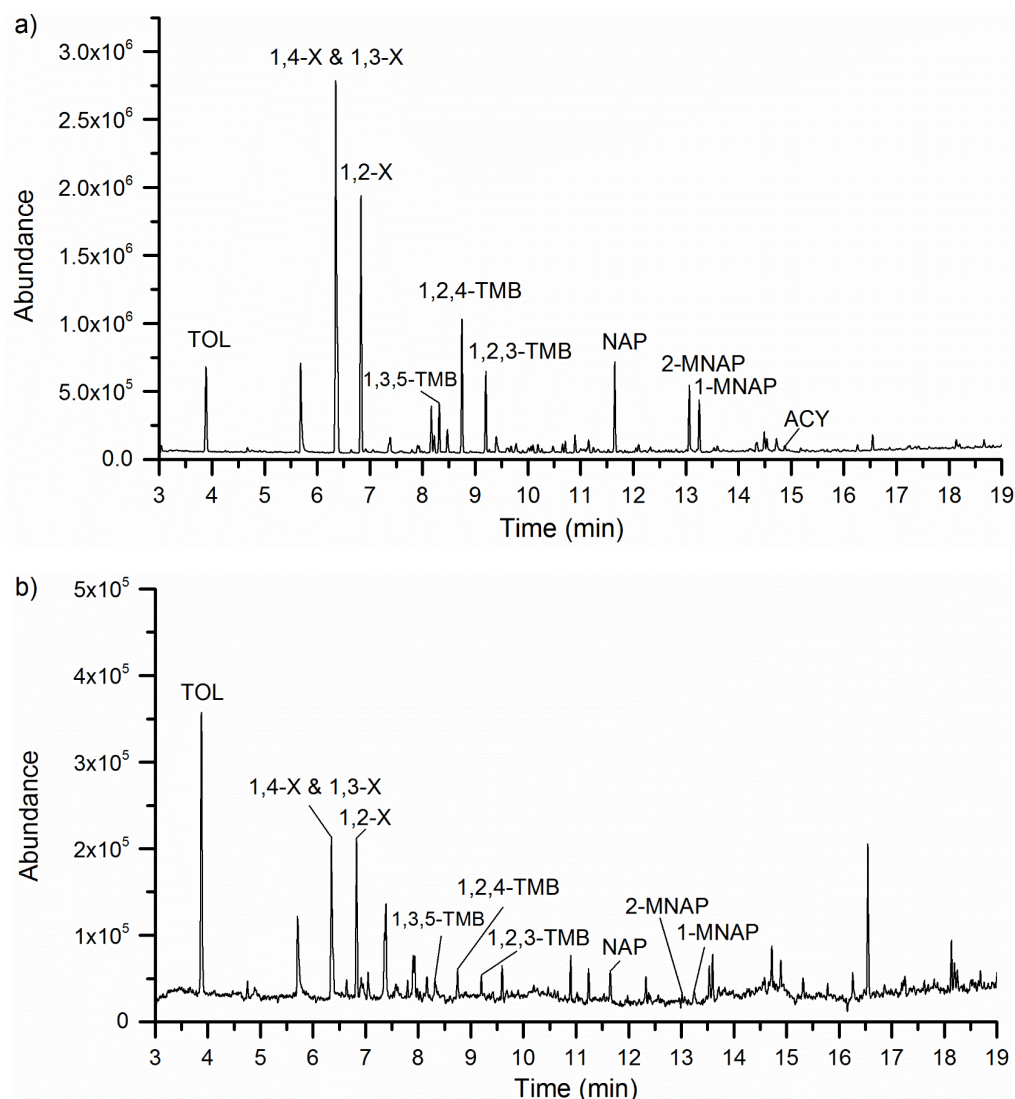


Figure 1.5 Total ion chromatogram (TIC) of a) 0.3% crude oil mixture and b) on day 3 contaminated PEX-A pipe leaching water sample with peaks labeled as: TOL: toluene (rt = 3.89 min); 1,4-X: 1,4-xylene (rt = 6.35 min); 1,3-X: 1,3-xylene (rt = 6.38 min); 1,2-X: 1,2-xylene (rt = 6.83 min); 1,3,5-TMB: 1,3,5-trimethylbenzene (rt = 8.32 min); 1,2,4-TMB: 1,2,4-trimethylbenzene (rt = 8.75 min); 1,2,3-TMB: 1,2,3-trimethylbenzene (rt = 9.20 min); NAP: naphthalene (rt = 11.65 min); 2-MNAP: 2-methylnaphthalene (rt = 13.07 min); 1-MNAP: 1-methylnaphthalene (rt = 13.25 min) and ACY: acenaphthylene (rt = 14.85 min). These contaminants were not detected from new PEX-A pipe leaching water sample. Benzene not shown as it eluted before the solvent cut off time. rt stands for retention time.

1.3.4 The Value of TOC Monitoring

Due to high background organic carbon released from the plastic pipes, TOC monitoring was not effective for estimating MAH reductions. TOC concentrations in control groups were greatest for new PEX-A pipes (> 6.5 mg/L), while other types of piping materials had TOC levels less than

1 mg/L. This finding agreed well with the past study, where PEX-A pipes also founds leached more TOC than other pipe materials (e.g. PEX-B and PEX-C) [38]. The normalized TOC leaching data failed to differentiate the 0.3% and 0.05% oil mixture contamination scenario from control groups (Table 1.6).

Table 1.6 Statistical analysis of multi-variant parameters

Parameters	BTEXs ($\mu\text{g}/\text{dm}^2$)		TOC ($\mu\text{g}/\text{dm}^2$)	
	<i>p</i> value	Significant or not?	<i>p</i> value	Significant or not?
<i>Main effect</i>				
Oil concentration	<0.05	Yes	0.73	No
Pipe Material	<0.05	Yes	<0.05	Yes
Exposure duration	<0.05	Yes	0.15	No
<i>Interaction effect</i>				
Conc. and material	<0.05	Yes	0.30	No
Conc. and time	<0.05	Yes	0.13	No
Material and time	<0.05	Yes	<0.05	Yes

Reproduced with permission by the Water Research Foundation (2016).

1.3.5 Future Work

To effectively recover water distribution system assets and building plumbing, results show the following information is important: the type of pipe/materials exposed, chemicals present, their initial concentration, and the duration of contaminated water exposure. These factors will influence the time needed to desorb chemicals and return infrastructure to safe use. Other factors not examined in this study but likely would influence the time needed to desorb chemicals from infrastructure include water temperature, pipe scales, biofilms, other materials such as gaskets, fixtures, valves, appliances, and water heaters in the plumbing system. As reported by others, flushing is a commonly applied pipe cleaning method, but sometimes infrastructure replacement was conducted [35]. Surfactants have shown to be inefficient for removing BTEX from copper and PEX-A pipe [53]. Also found was that some surfactant solutions can damage plastics. It is recommended that additional work be conducted to determine what actions are needed to safely decontaminate oil contaminated distribution and plumbing infrastructure.

1.4 Conclusion

The goal of this study was to investigate the susceptibility of plastic and copper service lines to short-term oil contamination and assess their subsequent ability to leach contaminants into the water supply. Results showed that copper was the least susceptible to contamination, but did desorb BTEX compounds during the first 3 day leaching period. PEX, HDPE, and CPVC pipe materials sorbed and desorbed much greater levels of BTEXs into drinking water than copper pipe. PEX-A and HDPE pipes were more vulnerable to contamination than PEX-B pipe, while CPVC exhibited the least susceptibility among the plastics. Benzene accounted for the majority of the total leached MAHs for all types of pipe materials and often exceeded the MCL; taste and odor thresholds were also exceeded. Non-BTEX compounds like trimethylbenzene isomers and PAH contaminants were also found desorbing from a PEX-A pipe.

The ability of a water distribution system to return contaminated pipes to service will be influenced by several factors. These include the type of pipe contaminated, the composition of crude oil contaminated water, aqueous concentration of contaminants, and the time since the contaminated water was removed from the pipe. A drinking water's TOC concentration was not a good indicator of oil contaminated water. Other water characterization techniques (e.g. GC-MS) were needed to better characterize the target contaminants and the levels in the water. Tentative identification of compounds enabled the authors to then purchase analytical standards and confirm the presence of MAHs and PAHs.

Results of this study are specific to the crude oil tested. Difference composition of oils could result in different aqueous concentrations. Considering the complex composition of oil products (i.e., MAHs, PAHs, metals and radionuclides), other contaminants should also be monitored and studied. Future work is recommended to examine the short-term interaction of contaminants with

water distribution system materials under different water hydraulic conditions (i.e., various flow and pressure conditions).

1.5 References

- [1] J.L. Weidhaas, A.M. Dietrich, N.J. DeYonker, R. Ryan Dupont, W.T. Foreman, D. Gallagher, J.E. Gallagher, A.J. Whelton, W.A. Alexander, Enabling Science Support for Better Decision-Making when Responding to Chemical Spills, *J. Environ. Quality*, 45 (2016) 1490-1500.
- [2] C.E. Restrepo, J.S. Simonoff, R. Zimmerman, Causes, cost consequences, and risk implications of accidents in US hazardous liquid pipeline infrastructure, *Int. J. Crit. Infr. Protect.*, 2.1 (2009): 38-50.
- [3] D. Yuhua, Y. Datao, Estimation of failure probability of oil and gas transmission pipelines by fuzzy fault tree analysis, *J. Loss Prevent. Process Ind.*, 18.2 (2005): 83-88.
- [4] Pipeline and Hazardous Materials Safety Administration (PHMSA), Pipeline Safety: Hazardous Liquid Pipelines Transporting Ethanol, Ethanol Blends, and other Biofuels. [http://www.phmsa.dot.gov/staticfiles/PHMSA/DownloadableFiles/Files/EthanolNotice7.07%20\(Policy%20Statement%20to%20convert\).pdf](http://www.phmsa.dot.gov/staticfiles/PHMSA/DownloadableFiles/Files/EthanolNotice7.07%20(Policy%20Statement%20to%20convert).pdf), 2007 (accessed 15.08.06).
- [5] A. Anselmo, J. Sullivan, DME: The Best Fuel, Period, *ChemBioPower* . <http://static1.squarespace.com/static/54a07d7ae4b093269b63ac5c/t/54e514a3e4b0773025013b38/1424299171380/CBP-WhitePaper-v5.pdf>, 2015 (accessed 15.10.13).
- [6] Montana Department of Environmental Quality (DEQ), Bridge Pipeline's Oil Spill on the Yellowstone River near Glendive. <http://www.deq.mt.gov/yellowstonespill2015.mcp#Updates>, 2015 (accessed 15.02.03).
- [7] D. Luther, Another American Water Emergency: Utah Municipal Water Supply Tainted by Chemical Spill, *Freedomoutpost*. <http://freedomoutpost.com/2015/04/another-american-water-emergency-utah-municipal-water-supply-tainted-by-chemical-spill/>, 2015 (accessed 15.05.01).
- [8] Agency for Toxic Substance & Disease Registry (ATSDR), 2015 Yellow River Oil Spill, http://www.atsdr.cdc.gov/yellowstone_river.html, 2015 (accessed 15.01.20).
- [9] National Transportation Safety Board (NTSB), Enbridge Incorporated Hazardous Liquid Rupture and Release. <http://www.nts.gov/investigations/AccidentReports/Reports/PAR1201.pdf>, 2010 (accessed 15.04.15).
- [10] T.M. Brody, P.D. Bianca, J. Krysa, Analysis of inland crude oil spill threats, vulnerabilities, and emergency response in the midwest United States, *Risk Anal.*, 32 (2012) 1741-1749.
- [11] X. Huang, A.J. Whelton, S. Andry, J. Yaputri, D. Kelly, D.A. Ladner, Interaction of Fracking and Crude Oil Contaminants with Water Distribution Pipes, EO 2014-07, Water Research Foundation (WRF), 2016.
- [12] Environmental Canada, ETC Spills Technology Databases, Oil Properties Database. <http://www.etc.cte.ec.gc.ca/databases/oilproperties/>, 2001 (accessed 15.02.21).
- [13] Syracuse Research Corporation (SRC), FatePointers Search Module. <http://esc.srcinc.com/fatepointer/search.asp>, 2013 (accessed 15.02.10).

- [14] U.S. Environmental Protection Agency (EPA), 2012 Edition of the Drinking Water Standards and Health Advisories. <http://water.epa.gov/action/advisories/drinking/upload/dwstandards2012.pdf>, 2012 (accessed 15.02.13). Washington, D.C.
- [15] International Agency for Research on Cancer (IARC). Agents Classified by the IARC Monographs, Volumes 1–111. World Health Organization. 2015.
- [16] U.S. Department of Health and Human Services, 13th Report on Carcinogens. <http://ntp.niehs.nih.gov/pubhealth/roc/roc13/index.html>, 2014 (accessed 15.03.02).
- [17] U.S. Environmental Protection Agency (EPA), National Primary Drinking Water Regulations. <http://water.epa.gov/drink/contaminants/upload/mcl-2.pdf>, 2009 (accessed 15.01.10). Washington, D.C.
- [18] S. Marshutz, Hooked on copper: A comparison shows the gap is narrowing with PEX gaining popularity as a preferred material in new construction and repiping work, Reeves Journal, (2001).
- [19] J. Lee, E. Kleczyk, D.J. Bosch, A.M. Dietrich, V.K. Lohani, G. Loganathan, Homeowners' decision-making in a premise plumbing failure-prone area (PDF), J. Am. Water Works Assoc., 105.5 (2013): E236-E241.
- [20] American Water Works Association (AWWA), Permeation and Leaching. <https://www.epa.gov/sites/production/files/2015-09/documents/permeationandleaching.pdf>, 2002 (accessed 15.06.08).
- [21] A.R. Berens, J.P. Pfau, D.E. Crum, K.E. Carns, Prediction of Organic Chemical Permeation Through PVC Pipe [with Discussions], J. Am. Water Works Assoc., (1985): 57-65.
- [22] K.P. Chao, P. Wang, Y.T. Wang, Diffusion and solubility coefficients determined by permeation and immersion experiments for organic solvents in HDPE geomembrane, J. Hazard. Mater., 142.1 (2007): 227-235.
- [23] T.M. Holsen, J.K. Park, D. Jenkins, R.E. Selleck, Contamination of potable water by permeation of plastic pipe, J. Am. Water Works Assoc., (1991): 53-56.
- [24] F. Mao, J.A. Gaunt, C.L. Cheng, S.K. Ong, Permeation of BTEX compounds through HDPE pipes under simulated field conditions, J. Am. Water Works Assoc., 102.3 (2010): 107.
- [25] A.J. Whelton, A.M. Dietrich, D.L. Gallagher, Impact of chlorinated water exposure on contaminant transport and surface and bulk properties of high-density polyethylene and cross-linked polyethylene potable water pipes, J. Environ. Eng., 137.7 (2011): 559-568.
- [26] S.K. Ong, J. Gaunt, F. Mao, C.L. Cheng, L. Esteve-Agelet, C. Hurburgh, Impact of hydrocarbons on PE/PVC pipes and pipe gaskets, J. Am. Water Works Assoc., (2008).
- [27] I. Skjevrak, A. Due, K.O. Gjerstad, H. Herikstad, Volatile organic components migrating from plastic pipes (HDPE, PEX and PVC) into drinking water, Water Res., 37.8 (2003): 1912-1920.
- [28] X. Zhao, Y. Wang, Z. Ye, A.G. Borthwick, J. Ni, Oil field wastewater treatment in biological aerated filter by immobilized microorganisms, Process Biochem., 41.7 (2006): 1475-1483.
- [29] Y.S. Li, L. Yan, C.B. Xiang, L.J. Hong, Treatment of oily wastewater by organic–inorganic composite tubular ultrafiltration (UF) membranes, Desalination, 196.1 (2006): 76-83.
- [30] L.M. Jackson, J. Myers, Design and construction of pilot wetlands for produced-water treatment, in: SPE Annual Technical Conference and Exhibition, 2003.
- [31] U.S. Environmental Protection Agency (EPA), Crude Oil Category: Category Assessment Document. <http://www.epa.gov/hpv/pubs/summaries/crdoilct/c14858ca.pdf>, 2011 (accessed 15.02.18). Washington, D.C.

- [32] W.K. Seifert, J.M. Moldowan, Paleoreconstruction by biological markers, *Geochim. Cosmochim. Acta*, 45.6 (1980): 783-794.
- [33] A.J. Whelton, L. McMillan, M. Connell, K.M. Kelley, J.P. Gill, K.D. White, R. Gupta, R. Dey, C. Novy, Residential Tap Water Contamination Following the Freedom Industries Chemical Spill: Perceptions, Water Quality, and Health Impacts, *Environ. Sci. Technol.*, 49.2 (2015): 813-823.
- [34] W.E. Coleman, J.W. Munch, R.P. Streicher, H.P. Ringhand, F.C. Kopfler, The identification and measurement of components in gasoline, kerosene, and no. 2 fuel oil that partition into the aqueous phase after mixing, *Arch. Environ. Con. Tox.*, 13.2 (1984): 171-178.
- [35] M. Reed, The physical fates component of the natural resource damage assessment model system, *Oil Chem. Pollut.*, 5.2-3 (1989): 99-123.
- [36] National Sanitation Foundation International/American National Standards Institute (NSF/ANSI), NSF/ANSI 61-2016 Drinking water system components-Health effects. http://www.nsf.org/newsroom_pdf/NSF-ANSI_61_watemarked.pdf, 2016 (accessed 16.10.12). Ann Arbor, MI.
- [37] K.M. Kelley, A.C. Stenson, R. Cooley, R. Dey, A.J. Whelton, The cleaning method selected for new PEX pipe installation can affect short-term drinking water quality, *J. Water Health*, 13.4 (2015): 960-969.
- [38] K.M. Kelley, A.C. Stenson, R. Dey, A.J. Whelton, Release of drinking water contaminants and odor impacts caused by green building cross-linked polyethylene (PEX) plumbing systems, *Water Res.*, 67 (2014): 19-32.
- [39] Y. Zhang, M. Edwards, Accelerated chloramine decay and microbial growth by nitrification in premise plumbing, *J. Am. Water Works Assoc.*, 101.11 (2009): 51.
- [40] H. John, Methods used by EPA to create crude oil contaminated drinking water for contamination studies. 2016, February 11. Personal Communication.
- [41] J. Anderson, J. Neff, B. Cox, H. Tatem, G.M. Hightower, Characteristics of dispersions and water-soluble extracts of crude and refined oils and their toxicity to estuarine crustaceans and fish, *Mar. Biol.*, 27.1 (1974): 75-88.
- [42] K.S. Casteloos, R.H. Brazeau, A.J. Whelton, Decontaminating chemically contaminated residential premise plumbing systems by flushing, *Environ. Sci.: Water Res. Technol.*, 1.6 (2015): 787-799.
- [43] E.J. Kim, J.E. Herrera, D. Huggins, J. Braam, S. Koshowski, Effect of pH on the concentrations of lead and trace contaminants in drinking water: A combined batch, pipe loop and sentinel home study, *Water Res.*, 45.9 (2011): 2763-2774.
- [44] J. Pawliszyn, Applications of solid phase microextraction, *Roy. Soc. Chem.*, 1999.
- [45] I. Arambarri, M. Lasa, R. Garcia, E. Millán, Determination of fuel dialkyl ethers and BTEX in water using headspace solid-phase microextraction and gas chromatography-flame ionization detection, *J. Chromatogr. A*, 1033.2 (2004): 193-203.
- [46] M.L. Tabor, D. Newman, A.J. Whelton, Stormwater chemical contamination caused by cured-in-place pipe (CIPP) infrastructure rehabilitation activities, *Environ. Sci. Technol.*, 48.18 (2014) 10938-10947.
- [47] J. Aitkenhead-Peterson, M.K. Steele, N. Nahar, K. Santhy, Dissolved organic carbon and nitrogen in urban and rural watersheds of south-central Texas: land use and land management influences, *Biogeochemistry*, 96.1-3 (2009): 119-129.
- [48] R.J. Miltner, H.M. Shukairy, R.S. Summers, Disinfection by-product formation and control by ozonation and biotreatment, *J. Am. Water Works Assoc.*, (1992): 53-62.

- [49] F. Goodfellow, S. Ouki, V. Murray, Permeation of Organic Chemicals Through Plastic Water-Supply Pipes, *Water and Environ. J.*, 16.2 (2002): 85-89.
- [50] World Health Organization (WHO), Guidelines for drinking-water quality, fourth edition. 2011.
- [51] U.S. Department of Health and Human Services (HHS), Toxicological profile for benzene, Atlanta, GA: Agency for Toxic Substances and Disease Registry (ATSDR), (1993).
- [52] H. Shiraishi, N.H. Pilkington, A. Otsuki, K. Fuwa, Occurrence of chlorinated polynuclear aromatic hydrocarbons in tap water, *Environmental Sci. Technol.*, 19.7 (1985): 585-590.
- [53] K.S. Casteloes, G.P. Mendis, H.K. Avins, J.A. Howarter, A.J. Whelton, The interaction of surfactants with plastic and copper plumbing materials during decontamination, *J. Hazard. Mater.*, 325.5 (2016): 8-16.
- [54] A.J. Whelton, L. McMillan, C.L-R. Novy, K.D. White, X. Huang. Case Study: The crude MCHM chemical spill, West Virginia. *Environ. Sci.: Wat. Res. Technol.* DOI: 10.1039/C5EW00294J

CHAPTER 2. COMPETITIVE HEAVY METAL ADSORPTION ONTO NEW AND AGED POLYETHYLENE UNDER VARIOUS DRINKING WATER CONDITIONS

2.1 Introduction

Predicting the type and concentration of drinking water contaminants at a building faucet is a growing U.S. focus area. In particular, drinking water health concerns for heavy metals such as lead and copper [1-3] as well as aesthetic issues caused by other metals (Fe, Mn, Zn) have resulted in U.S. drinking water standards for these contaminants [4, 5]. As water distribution system and building plumbing pipes such as galvanized steel/iron, copper, and lead have been replaced [6], plastic pipes have increased in popularity. Often, plastic pipes are selected as a replacement material because they do not leach metals into the bulk water. Though, a growing body of evidence suggests that plastic drinking water pipes can accumulate heavy metal deposits. Therefore, to predict heavy metal concentration at a building faucet, the fate of heavy metals in plastic piping systems should be understood.

Unlike recently discovered metal deposits on plastic drinking water pipes, scales on metals pipes have been extensively studied where Cu_2O , CuO , $\alpha\text{-FeOOH}$, Fe_3O_4 , MnO_2 , and PbCO_3 have been reported [7-9]. Evidence has shown that a variety of heavy metals including Cu, Fe, Mn, Pb, and Zn can deposit onto plastic drinking water pipes used for buried water mains (i.e., polyvinylchloride [PVC]) [7, 10], service lines (i.e., PVC and high-density polyethylene [HDPE] pipes) [11, 12], and building plumbing (i.e., crosslinked polyethylene [PEX]) [13]. Lead and copper loadings were found as high as 9.68 mg Pb/ g scale and 1.14 mg Cu/ g scale on exhumed PVC pipes from drinking water distribution systems [10]. Other common metals found on plastic pipes were 0.11-2.33 mg Al/g scale, 2.86-28.86 mg Ca/g scale, 5.16-460.14 mg Fe/g scale, 0.29-

5.14 mg Mn/g scale, 4.07-10.45 mg Si/g scale and 1.85-541.56 mg Zn/g scale [10-12]. Iron has often been found as the most abundant element in piping scales and can co-precipitate with other metals [10-12, 14]. For example, up to 443 mg Fe/g solid scale was found on PVC drinking water distribution pipe and goethite was identified as the major form of iron present [10]. Salehi et al. (2017) found varied Fe loadings (0.7-19.7 mg Fe/m²) on a one-year old PEX plumbing pipes [13]. So the impact of iron on metals (i.e., Cu, Mn, Pb and Zn) adsorption to plastics should also be examined. The type and characteristics of metal deposits is likely influenced by source water quality variation, system operations, and upstream piping materials or fittings. To better understand heavy metal fate in plastic drinking water piping systems, factors that control heavy metal-plastic interaction should be elucidated.

Because few studies have identified the factors that control metal adsorption onto plastic drinking water pipes, micro/macroplastic [15-23] and plastic sampling container [24, 25] studies were reviewed. Both plastic surface characteristics and the solution conditions may affect the metal adsorption process, such as plastic type (i.e., PET, PE, PVC, and PP) [17, 20, 22], plastic aging (i.e., virgin vs aged plastic pellets) [13, 16, 19, 23], water pH (i.e., 4-11) [16, 21, 23, 24], and water source quality (i.e., marine, fresh and estuarine water) [16, 17, 19, 23]. Whereas, few studies have been conducted to investigate metal-plastic interactions under drinking water conditions. A recent study designed with drinking water showed Pb was electrostatically bound to oxidized carbon on aged the low-density polyethylene (LDPE) [21]. However, the study limitation was that the role of metal competition and presence of dissolved organics (i.e., NOM) were not examined. In addition, free chlorine and orthophosphate are often used as a disinfectant and corrosion inhibitor in drinking water systems, but their role on metal deposits on plastic pipes has not been examined. Further, several prior metal-plastic interaction studies have proposed mechanisms but directly

conflict with one another: (1) The plastic surface acquired a negative charged surface when immersed in fresh or salt water solution, which caused metal ion adsorption [16, 23], (2) The plastic surface became more negatively charged with increasing water pH, resulting in greater electrostatic attractions between metal species and the plastic, (3) Increased water pH promoted metal hydrolysis and resulted in less metal cations available for adsorption [16]. The mechanism of metal-plastic interactions has not been thoroughly studied. Neither the effect of organic constituents nor has the presence of corrosion inhibitor or free chlorine on metal-plastic interactions been studied. Since these variables are important drinking water characteristics, they warrant examination.

The study goal was to identify which factors can influence the type and magnitude of copper (Cu), iron (Fe), lead (Pb), manganese (Mn), and zinc (Zn) loading on new and aged low-density polyethylene (LDPE) under various drinking water conditions. These metals were selected because they are commonly found in plumbing systems and in previously exhumed plastic pipe deposits. The hypothesis was that both plastic properties (i.e., state of aging) and water conditions (i.e., pH, the presence of organic carbon, free chlorine, corrosion inhibitor and iron) would affect the amount of metal adsorbed onto the plastic's surface. Since plastic pellets are often used as the raw materials to manufacture plastic piping materials (i.e., PVC, PE, PP and PEX) and prior plastic pollution studies, in the current work, low density polyethylene (LDPE) pellets were adopted. While the LDPE piping is not used in the U.S., it was previously used in United Kingdom water distribution systems [26].

2.2 Materials and methods

2.2.1 Materials and reagents

Low density polyethylene (LDPE) pellets and sheets were purchased from Sigma Aldrich, MO, whereas aged plastics were obtained based on the previous work [21]. For more details, 99.5% purity oxygen was supplied as the ozone generator feeding gas. New LDPE plastics (25 g) were added into 250 ml of nanopure water in a flat-bottom three-necked flask. The aging process was conducted at 85 °C (within a water bath), with a 4 mg/min ozone mass flowrate. Aging duration was varied from 2 to 10 hr. Before metal interaction experiments, new and aged pellets were pre-conditioned (stirring with 500 ml nanopure water) for 24 hr and air dried.

In the current study, a synthetic tap water recipe was adopted to better simulate the tap water matrix [27]. Millipore Mili-Q water (MQW) (18.2 M Ω cm) was used to prepare all solutions. Reagents used throughout the study were analytical grade or higher. Metal stock solutions (i.e., Cu, Fe, Mn, Pb and Zn) were 1,000 mg/L ICP-MS standards (Ricca Chemical, TX), and desired concentrations were achieved through series of dilutions. NaOH and HNO₃ were used to adjust solution pHs. Na₂HPO₄·7H₂O (Catalog No. AC206515000) was used as the representative corrosion inhibitor, which was purchased from Fisher Scientific, NH. Whereas, sodium hypochlorite (10-15%, reagent grade) (supply part No. 425044) was obtained from Sigma-Aldrich, MO and used to test the free chlorine effect. The aquatic Suwannee River NOM (SRNOM) was purchased from the International Humic Substances Society (IHSS) (Catalog No. 2R101N). PEX-A (i.e., cross-linked medium density polyethylene) pipes with 3/4" diameter were from SupplyHouse.com (product No. F1040750).

2.2.2 Characterization

The Fourier transform infrared (FTIR) spectroscopy (Perkin Elmer spectrum 100 FTIR spectrometer) was used to provide functional groups information on new and aged LDPE pellets surfaces. Past studies showed that the presence of polar functional groups (i.e., $>C=O$, $-OH$, and $>C=O<$) on aged plastics could be responsible for the higher metal uptake [16, 21, 28]. The FTIR spectrum was obtained in the wavelength range of $600-4000\text{ cm}^{-1}$, with a 1 cm^{-1} resolution and samples were scanned in triplicate. The surface wettability for both new and aged LDPE segments (dimension: $1\times 1\text{ cm}^2$) was achieved through the goniometer (Rame-hart Instrument Co., NJ). During the measurement, a $2\text{ }\mu\text{L}$ DI water droplet was deposited onto the sample surface. Then the image was taken and the contact angel was measured by the DROPimage Advanced software. The surface areas of plastics were determined by the Brunauer-Emmett-Teller (BET) method. In this process, 15 pellets were adopted with the averaged weight varied from $0.48-0.52\text{ g}$. And N_2 gas adsorption-desorption was conducted by the Micromeritics TriStar 3020 Analyzer system. Prior the BET test, pellets samples were weighted in Micromeritics sample tubes and went through degassing process for 5 hr at $70\text{ }^\circ\text{C}$ [29]. For the following two tests, new LDPE pellets were exposed to 5 mg/L mixed metal solutions (for 24 hr) and dried in the anaerobic chamber. The morphology of deposited metals was examined by scanning electron microscopy-energy dispersive X-ray spectroscopy (SEM-EDS) (Hitachi S-4800 Field Emission SEM). To enhance each samples' conductivity, plastic pellets were sputter-coated with a thin carbon film and the conductive tape was also used [15]. X-ray photoelectron spectroscopy (XPS) (Kratos AXIS Ultra DLD Imaging X-ray Photoelectron Spectrometer) was used to characterize the metal deposit speciation on new LDPE pellets. The measurement was conducted by using an $\text{Al K}\alpha$ X-ray source (1486.7 eV of protons) and a high vacuum chamber (10^{-8} Torr). All binding energies were referred

to 284.6 eV C 1s peak to compensate the surface charging effect. Visual MINTEQ ver. 3.1 was adopted to predict metal speciation in the solution [30].

2.2.3 Metal adsorption test

For the kinetic study, 50 pre-conditioned LDPE pellets (i.e., new and aged) were added into a 50 ml Teflon (PTFE) bottle. In order to simplify metal speciation in the solution, the water was purged beforehand (with N₂) to remove oxygen and all experiments were conducted within an anaerobic chamber. To initiate the metal adsorption process, 20 ml of 30 µg/L of oxygen free metal solutions (i.e., Cu, Mn, Pb, Zn with/without Fe) were added into each bottle. The ratio of plastic pellet surface area to the solution volume (S/V) was estimated as 1.5 cm²/ml, which was comparable to the S/V ratio for 2.54 cm (1 inch) diameter plastic drinking water pipes. Then the water pH was adjusted to 7.5 by using NaOH and HNO₃ solutions. Kinetic studies were conducted in duplicate for up to 24 hr, and at room temperature with stirring speed of 250 rpm. Although trace metal levels are varied in different drinking water conditions, overall the selected metal concentration (i.e., 30 µg/L) was comparable to drinking water in the United States [31]. Periodically, pellets were removed from the reactor and placed into a 15 ml metal-free polypropylene centrifuge tube. The plastic centrifuge tube was pre-filled with 10 ml of 2% HNO₃ and the digestion duration was the minimum of 48 hr [32]. Then digested solutions were analyzed by inductively coupled plasma-optical emission spectroscopy (ICP-OES) (Perkin Elmer). The method report limits (MRL) were 1 µg Cu/L, 2 µg Fe/L, 1 µg Mn/L, 2 µg Pb/L, and 1 µg Zn/L, respectively.

To study water conditions influences on metal-plastic adsorption process, SRNOM, plastic leaching, free chlorine (i.e., NaOCl), corrosion inhibitor (i.e., Na₂HPO₄) and iron were also studied with the same manner. The 18 mg/L (as DOC) SRNOM and plastic leaching water were adopted. The concentrated plastic leaching water was achieved by filling the clean synthetic water into a

new PEX-A pipe and left at the 55 °C constant room for one month. Then the desired DOC level could be reached by dilutions. Free chlorine was selected within the range of 0.5-2 mg/L as Cl₂. The role of corrosion inhibitor was examined from 1-5 mg/L as PO₄³⁻. 30 µg/L iron was added in the solution to test the influence on other metals adsorption behavior. The metal loss percentage (C_b%) to PTFE bottle walls was estimated from the control group (i.e., no pellets were added). Calculations were conducted by subtracting the metals remaining in solution (i.e., at 24 hr) (C_l, µg/L) from the initial metal concentration (C_o, µg/L) ($C_b \% = \frac{C_o - C_l}{C_o} \times 100\%$). Started with 30 µg/L mixed metal solution (without Fe), the C_b% was 9.4% Cu, 1.2% Mn, 4.9% Pb and 6.2% Zn, respectively.

Effect of solution pH and metal concentration on metal loadings were also tested by adding 50 ten hour aged LDPE pellets in 20 ml of 30 µg/L mixed metal solutions in an anaerobic chamber. The initial pH was adjusted from 5.5 to 10.5. At the end of the experiment (up to 24 hr), pellets were digested by using the previous method (i.e., 2% of HNO₃ for 48 hr). Metal concentration effect was also studied in the same manner by adding 50 ten hour aged LDPE pellets in 20 ml of 5-100 µg/L mixed metal solutions at pH 7.5. After 24 hr, pellets were digested and along with left over metal solutions were analyzed by ICP-OES. The multivariate analysis of variance (MANOVA) test was conducted (with 95% confidence interval and $\alpha=0.05$) by using the NCSS statistical software. In addition, Langmuir and Freundlich isotherm models were used to study metals concentration and the pseudo-first model was adopted to study the iron effect (Appendix A).

2.3 Results and discussion

2.3.1 New and aged LDPE characterization

As expected, the aging process altered LDPE surface chemistry, increased surface hydrophilicity and surface area. ATR-FTIR results showed that oxygen-containing bonds were not detected on the new polymer while -OH bend [939 and 1411 cm^{-1}], ether (C-O-C stretch) [1105 and 1170 cm^{-1}] and ketone (C=O bend) [at 1708 cm^{-1}] bonds were found on the aged LDPE (Figure A.1) [29, 33]. The aging process also changed the LDPE surface from hydrophobic ($\theta > 90^\circ$) to one that was more hydrophilic ($\theta < 90^\circ$) (Figure A.2). The 10 hr aging procedure also changed LDPE surface morphology from smooth to one that contained visible dents and surface area was increased from 0.0493 (new LDPE) to 0.1036 m^2/g (aged LDPE) (Figure 2.1).

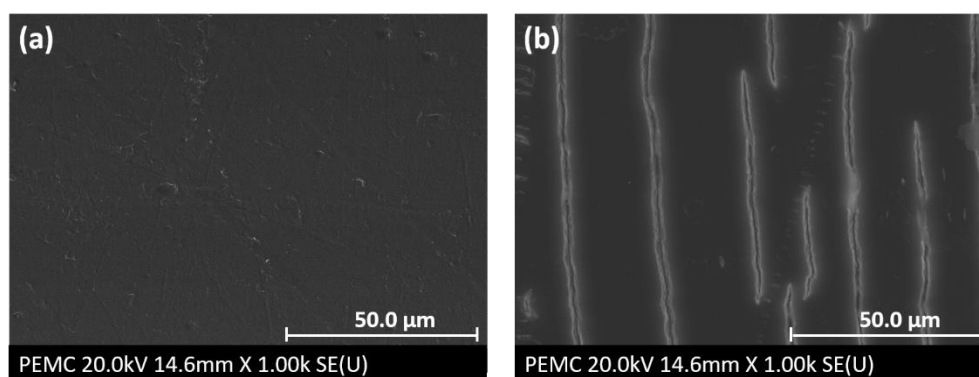


Figure 2.1 SEM images of (a) New LDPE segment and (b) 10 hr aged LDPE pellets.

2.3.2 The plastic condition and water pH influenced metal adsorption

Results showed that the longer the LDPE was aged, the greater metal loadings of Cu, Mn, Pb, and Zn ($\frac{\text{Mass of adsorbed metal } (\mu\text{g})}{\text{Surface area of plastic pellets } (\text{m}^2)}$) occurred (Figure 2.2 and Figure A.3). For new LDPE, metal adsorption reached equilibrium within 2 hr, whereas the 5 and 10 hr aged plastics did not reach the equilibrium until 10 hr. Aged LDPE adsorbed about a five-fold greater mass of metals than new LDPE. Because surface area only increased 2.1 fold for 10 hr aged LDPE pellets, but there was a 4.8, 4.5 and 3.8 fold increase for Cu, Pb and Zn loading, respectively, the increased

adsorption was likely due to more than a change in LDPE surface area. Other plastic surface characteristics such as polar functional groups (i.e., -OH, C-O-C and C=O) [16, 29] and increased hydrophilicity [15, 34] have been previously attributed to higher metal loadings on plastics.

Because metal loading was quantified on the LDPE and many forms of metal species were likely present in the solution, results were qualitatively interpreted. Cu was found in the greatest loading on LDPE followed by Pb, Zn > Mn (Figure 2.2). As the MINTEQ prediction indicated, a majority of each metal was present in ionic form at pH 6.8 (Figure 2.3), but other species were also likely present (i.e., oxyhydroxides). Metal characteristics such as ionic radius [Pb^{2+} (1.12 Å) > Mn^{2+} (0.8 Å) > Zn^{2+} (0.74 Å) > Cu^{2+} (0.72 Å)] [32, 35, 36], and electronegativity [Zn^{2+} (28.84 eV) \approx Cu^{2+} (28.56 eV) > Pb^{2+} (26.18 eV) > Mn^{2+} (24.66 eV)] [35, 37] likely influenced adsorption. Additional experiments revealed that metal adsorption behavior was significantly influenced by water pH at levels (Figure 2.4). Reasons for these differences could be due to (1) differences in the affinity of different metal species (Table A.1) on the plastic surface, (2) differences in competition between metal ions and protons on the plastic surface [38], (3) the plastic surface provided nucleation sites for metal oxide precipitation (i.e., $\text{Pb}(\text{OH})_2(\text{s})$) [21], and the (4) co-precipitation of metals at elevated pH (i.e., Zn) [39, 40]. To understand metal deposits on plastic surfaces, additional work is recommended to understanding the fundamental factors that control metal specie and plastic interaction in multi-metal solutions.

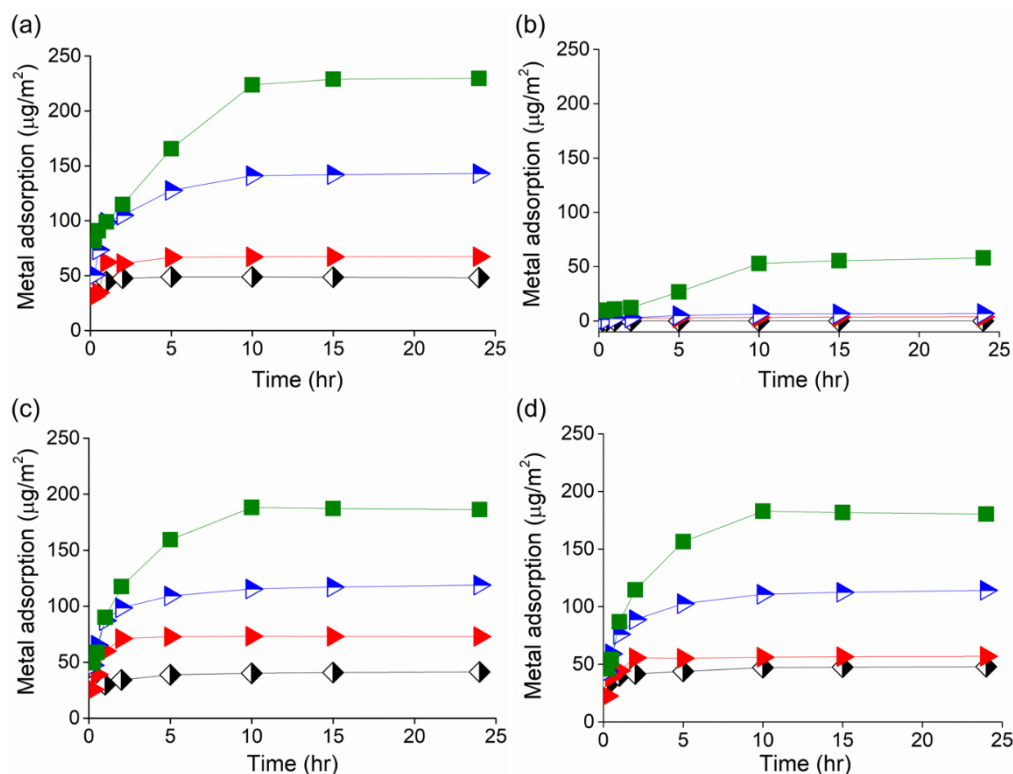


Figure 2.2 Loading of (a) Cu (b) Mn (c) Pb and (d) Zn onto \blacklozenge New, \blacktriangleright 2 hr aged, \blacktriangleleft 5 hr aged, and \blacksquare 10 hr aged LDPE pellets for the mixed metal solution. Initial metal concentration was $30 \mu\text{g}/\text{L}$ for each metal, equilibrium pH was at 6.8.

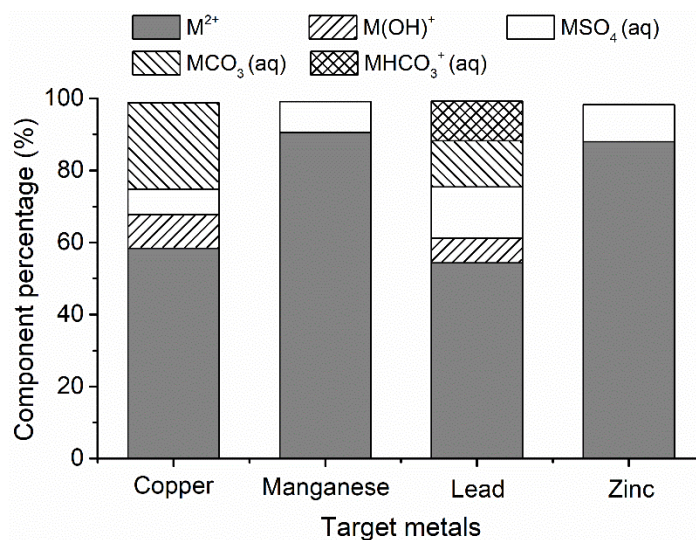


Figure 2.3 Metal speciation in the metal mixed solution as predicted by Visual MINTEQ ver. 3.1. Initial metal concentration was $30 \mu\text{g}/\text{L}$ for each metal, equilibrium pH was at pH 6.8.

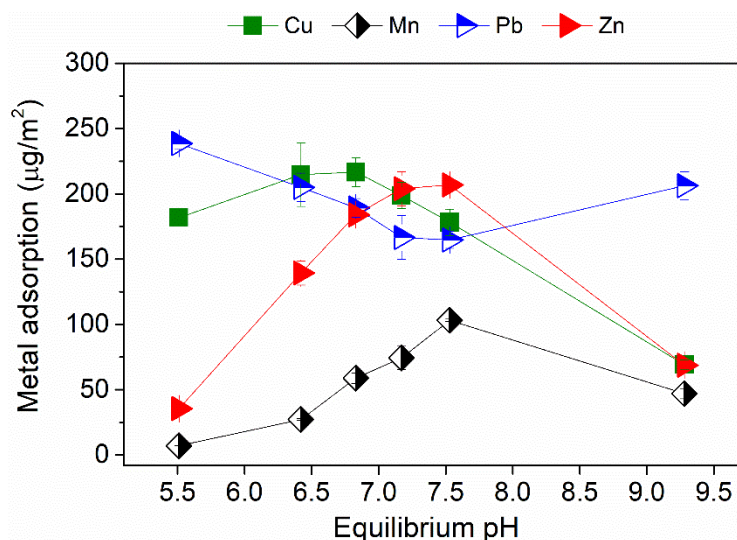


Figure 2.4 Competitive metal adsorption (■ Cu, * Fe, ◆ Mn, ▲ Pb, and ▼ Zn) on 10 hr aged LDPE pellets varied with pHs. Drinking water pH is typically between 6.5 and 8.5. Initial metal concentration was 30 µg/L for each metal.

2.3.3 Metal species and concentrations influenced metal loading on LDPE

As the amount of total metals in solution increased, a greater metal loading was found on the LDPE surface (Figure 2.5). This result was mainly driven by the enhanced metal concentration gradient in the solution and the availability of LDPE surface bonding sites. Both Langmuir and Freundlich isotherm models revealed high coefficients of determination ($r^2 > 0.9$) for the aqueous metal concentration measurements (Table A.2). The Langmuir isotherm model predicted the LDPE's maximum metal adsorption capacity was Cu ($1,109 \mu\text{g}\cdot\text{m}^{-2}$) > Pb ($1,038 \mu\text{g}\cdot\text{m}^{-2}$) > Zn ($893 \mu\text{g}\cdot\text{m}^{-2}$) > Mn ($199 \mu\text{g}\cdot\text{m}^{-2}$). Limited available testing of exhumed plastic water pipes has shown different orders of metal surface loading: Zn > Pb > Mn > Cu [10] and Mn > Cu > Zn > Pb [13]. It is likely that many additional factors not examined in this study (i.e., biofilm, different source water chemistry, temperature and hydraulic fluctuations) could influence plastic pipe metal loading. Though, the calculated Freundlich constant ($1/n$) revealed that as aqueous metal concentration increased, the adsorption rate decreased due to less available bonding sites [41].

Therefore, the type and concentration of metals in solution will influence metal loading on plastic pipes.

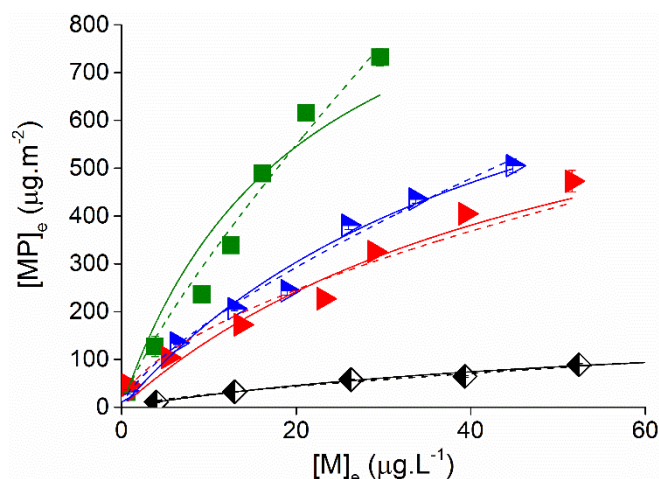


Figure 2.5 Adsorbed metal loading (■ Cu, ◆ Mn, ▲ Pb, and ▲ Zn) varied by metal type and concentration. Experiments were conducted in triplicate using 10 hr aged LDPE pellets. Solid lines represent the Langmuir isotherm model fitting, dash lines represent the Freundlich isotherm model fitting. Initial metal concentration was 30 μg/L for each metal, equilibrium pH was 6.8.

2.3.4 PEX-A pipe dissolved organic carbon reduced metal adsorption to LDPE

As expected, when SRNOM was present, the amount of metals adsorbed to LDPE was reduced (-12.4% Pb to -70.1% Cu). But also found that organics leached from PEX-A pipes reduced metal adsorption (Table 2.1). When SRNOM was present, the reduced metals adsorption to LDPE was likely due to SRNOM constituents forming metal complexes [42, 43]. SRNOM is mainly composed of fulvic and humic acids that contain multiple functional groups (i.e., carboxyl, amine, and phenolic), that can form metal complexes [32, 44]. Interestingly, organic constituents leached from PEX-A pipes also reduced metal adsorption, but to a much lesser degree than SRNOM. Copper, the metal most affected by SRNOM (-70.1% adsorption), was also the metal that most affected by the presence of PEX-A pipe dissolved organic carbon (-43.8% adsorption) (Table 2.1 and Figure A.4). Cu^{2+} had the smallest ionic radius and greatest electronegativity compared to the other metals present, and prior studies have shown humic acid forms stable

complexes in the following order: Cu > Pb > Zn > Mn [45]. Adsorption of other metals was reduced by 5.7% to 9.1% in the presence of PEX-A pipe organic constituents. Limited information is available about the organic compounds leached by PEX pipes into drinking water [26], but past studies have identified compounds that have phenolic and carboxylic functional groups (i.e., 2,4-di-*tert*-butylphenol and benzenepropanoic acid in the PEX pipe contacted water) [46, 47]. It is possible that dissolved organic constituents leached by PEX pipe may also form complexes with metal species. Additional studies are recommended to better characterize PEX pipe leaching chemicals and their role in heavy metal fate in drinking water piping systems.

Table 2.1 Metal adsorption to suspended LDPE pellets was affected by the presence of dissolved organic carbon, corrosion inhibitor and free chlorine.

Target metals	<i>Water conditions (adsorbed metal/plastic surface area) ($\mu\text{g}/\text{m}^2$)</i>						
	LDPE only	18 mg/L NOM	18 mg/L Plastic leaching ^b	1 mg/L PO_4^{3-}	5 mg/L PO_4^{3-}	0.5 mg/L Cl_2	2 mg/L Cl_2
Cu	230	69 (-70.1%)	129 (-43.8%)	161 (-29.8%)	152 (-34.0%)	152 (-33.7%)	143 (-38.0%)
Mn	58	43 (-26.7%)	54 (-6.5%)	60 (ND)	57 (-1.3%)	43 (-26.4%)	41 (-29.6%)
Pb	186	163 (-12.4%)	176 (-5.7%)	123 (-34.2%)	76 (-59.4%)	145 (-22.1%)	119 (-36.0%)
Zn	180	148 (-17.8%)	164 (-9.1%)	164 (-8.9%)	139 (-22.8%)	159 (-12.0%)	146 (-18.9%)

a. Experimental condition: 30 $\mu\text{g}/\text{L}$ of Cu, Mn, Pb and Zn, the equilibrium pH was 6.8.

b. Organics leaching solution was obtained from new PEX-A pipes at 55°C constant temperature room.

ND represents there was no reduction be found.

2.3.5 Free chlorine and corrosion inhibitor reduced metal adsorption to suspended LDPE

The presence of free chlorine and corrosion inhibitor reduced metal loadings on suspended LDPE pellets (Table 2.1 and Figure A.5). Free chlorine mostly affected Cu loading (up to 38%) and Zn adsorption was influenced the least (less than 20%). Even free chlorine is the strong oxidation agent, but based on the MINTEQ prediction, under the experimental condition (i.e., anaerobic and equilibrium at pH 6.8), about 83.2% OCl^- existed as HOCl (aq) form and 16.8% as OCl^- . There was no metal speciation changes nor precipitates formed. However, the excess of ions

(i.e., Na^+) and molecules (i.e., HOCl) could also compete with target metals to adsorb onto plastic surfaces and resulted the metal loadings reduction. Other long term studies revealed free chlorine could oxidize metals in the form as CuO and MnO_2 , PbO_2 and Zn(OH)_2 [48-50]. Because the free chlorine concentration used in the current study was fairly low (i.e., ≤ 2 mg/L) and experiments were conducted in a short duration (i.e., 24 hrs, at room temperature), the plastic surface degradation was negligible.

By adding 1 and 5 mg/L corrosion inhibitor (as PO_4^{3-}), Pb resulted the most reduction (up to 59.4%), followed by Cu, Zn and Mn (Table 2.1). The 1mg/L PO_4^{3-} did not alter much for metal speciation in the solution. Except, 0.3-1.3% metals presented as MHPO_4 (aq), which reduced the charge attraction to plastic surfaces compared with M^{2+} . When PO_4^{3-} level elevated to 5 mg/L, 44.6% Pb precipitated as $\text{Pb}_3(\text{PO}_4)_2$ (s) that largely reduced Pb soluble forms in water solution (Figure A.5). Cao et al. (2002) had the similar finding, who successfully applied phosphate to transform available Pb in soils from available phase into the residual phase [51]. Because pellets were suspended in the solution, metal precipitates may have settled out in the water column or precipitation forms were not favorable to plastic surfaces. In addition, 6.1% Cu was in the form as CuHPO_4 , compared with less than 2% ZnHPO_4 and MnHPO_4 . An interesting finding was the addition of corrosion inhibitor did not much influence the Mn adsorption (ND-1.3% reduction). This was mainly due to less affinity of manganese speciation on plastic surfaces and high soluble manganese phosphate forms at neutral pH and room temperature [52].

2.3.6 The presence of iron reduced the amount of copper and lead adsorbed onto LDPE

Iron's presence did not seem to affect Mn and Pb metal adsorption, which also showed the good fitting with the pseudo-first-order model prediction ($r^2 > 0.9$) (Figure A.6 and Table A.3). In contrast, adsorption of Cu, Fe and Zn did not predicted well by the model, and this has also been reported when researchers studied Cu and Zn adsorption onto polyethylene microplastics in fresh

water and marine environment [16, 19]. Direct quantification of the metals adsorbed on the LDPE surface revealed that Cu and Pb loading were reduced by 4% and 4.5%, respectively after Fe addition (Figure 2.6). Mn (-0.2%) and Zn (-0.8%) loadings were less affected by iron's presence. This observation might be due to the affinity of metal species to the plastic surface. While LDPE can provide nucleation sites for iron species [13], it is unknown if other metal species were similarly affected. Additional studies are recommended to explore the role of plastic surface properties on nucleation kinetics.

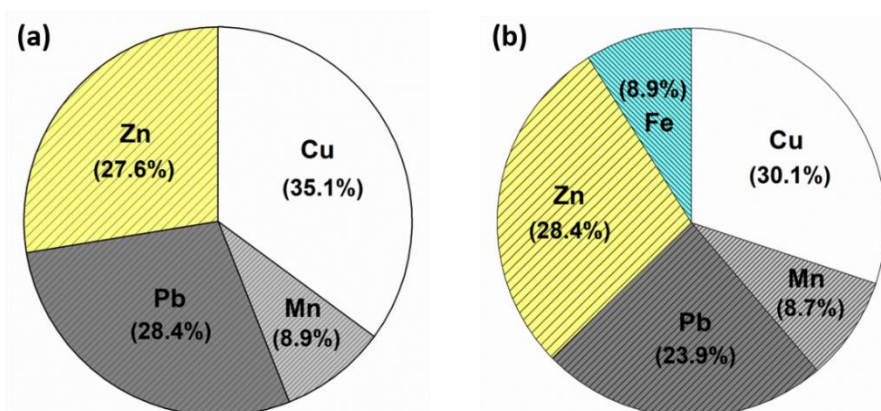


Figure 2.6 The percent of total mass of metal adsorbed to LDPE (a) in the absence of Fe and (b) in the presence of Fe. Initial metal concentration was 30 $\mu\text{g/L}$ for each metal, and the equilibrium pH was 6.8.

2.3.7 Metal accumulation and speciation on the LDPE surface

While the morphology of aged LDPE (i.e., dents) did not affect the author's ability to extract deposited metals into an acidic solution, dents inhibited representative SEM-EDS and XPS analysis of the LDPE surface. For this reason, the form of metals that were present on new LDPE pellets at pH 6.8 were examined. SEM-EDS and XPS further confirmed target metals (Cu, Mn, Pb, and Zn) sorbed onto LDPE (Figure A.7 and Figure 2.7). When Fe was added to the solution, Cu, Pb and Zn LDPE surface loadings were reduced (Figure 2.7 and Table A.4). Due to the fairly low

level of Fe and Mn on LDPE surface, these two metals were not detected by XPS (results not shown), however their presence on plastic surfaces did detect by EDS.

A variety of metal oxides and hydroxide previously found on plastic drinking water pipes exhumed from the field were also found in the present study. High resolution XPS spectra revealed CuO, Cu(OH)₂, PbO, Pb(OH)₂ and ZnO were major metal forms that found on the LDPE surface (Figure 2.7 (b)-(d)). The Cu 2p_{3/2} and Cu 2p_{1/2} shake-up satellites were observed at 944 eV and 964 eV, respectively. In addition, the Cu 2p_{3/2} characteristic peak located at 934.9 eV indicated the presence of Cu²⁺ oxides (Cu 2p_{3/2} at 934.6 eV) and Cu²⁺ hydroxides (Cu 2p_{3/2} at 935.1 eV) [53, 54]. The high resolution Pb 4f spectrum showed two distinguishable peaks that located at 138.4 eV (Pb 4f_{7/2}) and 143.2 eV (Pb 4f_{5/2}), with an energy separation of 4.8 eV. From which the lead speciation could be attributed to PbO (Pb 4f_{7/2} at 138.3 eV) and Pb(OH)₂ (Pb 4f_{7/2} at 138.6 eV), respectively [55, 56]. Last but not the least, the Zn 2p_{3/2} peak in this study was found at 1021.8 eV that corresponded well with ZnO (Zn 2p_{3/2} at 1021.7 eV) [53].

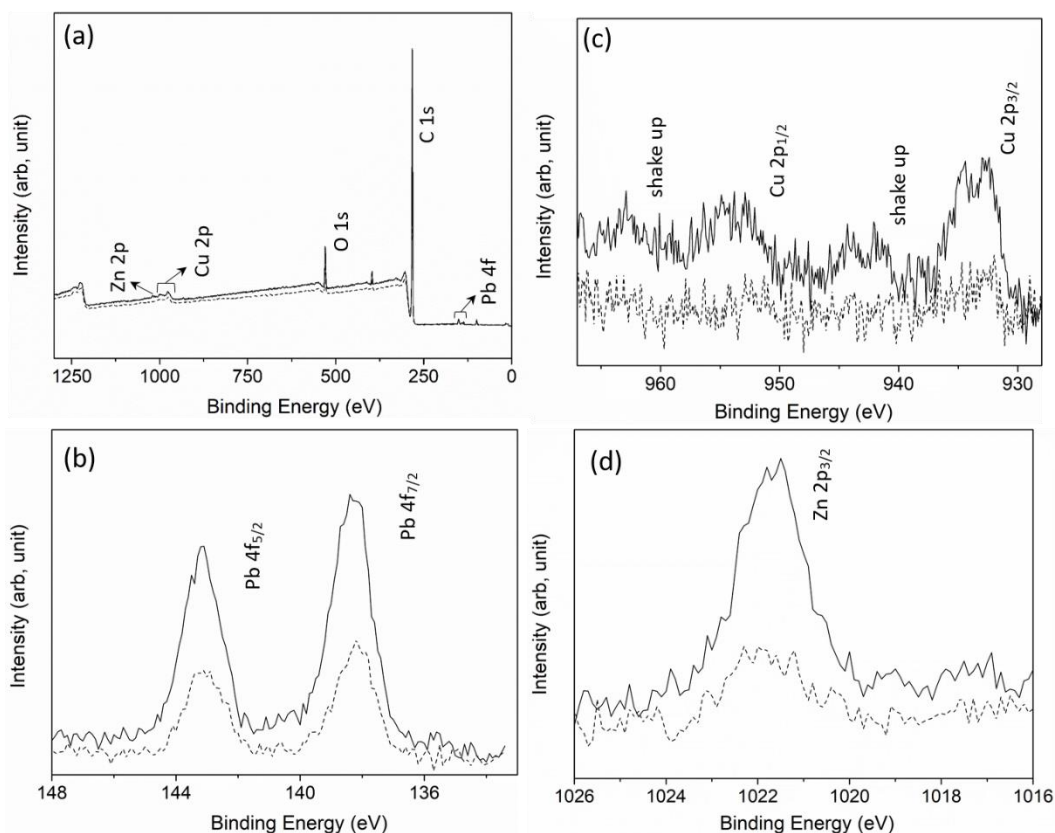


Figure 2.7 Comparison — without Fe and with Fe XPS spectra of (a) wide scan (b) Cu 2p (c) Pb 4f and (d) Zn 2p on new LDPE pellets. Iron and manganese were not detected by XPS.

2.4 Conclusion

To understand drinking water quality within plastic drinking water system, there is a need to study heavy metal interaction with plastic materials. In the present work, Cu, Fe, Mn, Pb and Zn competitive metal adsorption onto new and aged LDPE was studied under various drinking water conditions. Aging process enhanced surface area and resulted more polar, hydrophilic and uneven surface characteristics. In the absence of organics, corrosion inhibitor, free chlorine and iron, 10 hr aged LDPE pellets adsorbed 5 times more metals than new pellets. Due to metal speciation, metal ion properties, and affinity of metals to plastic surfaces, Cu was adsorbed the most, followed by Pb, Zn and Mn. And change of solution pH altered metals adsorption differently. As expected, metal adsorption increased as increasing mixed metal concentration (5-100 $\mu\text{g/L}$).

By adopting the Langmuir isotherm model, the 10 hr aged LDPE pellets maximum metal adsorption capacity was $\text{Cu} (1,109 \mu\text{g}\cdot\text{m}^{-2}) > \text{Pb} (1,038 \mu\text{g}\cdot\text{m}^{-2}) > \text{Zn} (893 \mu\text{g}\cdot\text{m}^{-2}) > \text{Mn} (199 \mu\text{g}\cdot\text{m}^{-2})$.

The presence of SRNOM and PEX-A pipe leaching organics hindered metals adsorption onto LDPE pellets. More metal-bonding functional groups in SRNOM induced more metal loading reduction than plastic pipe organics. Among mixed metals, Cu loading resulted up to 70% reduction that mainly due to Cu^{2+} was more active and easily formed copper-organics complex in the solution. The free chlorine resulted up to 38% metal loading reduction. It was suspected that the excess ions (i.e., Na^+) and molecules (i.e., HOCl) in the solution would compete with target metals on plastics surfaces. And corrosion inhibitor (i.e., Na_2HPO_4) reduced metals adsorption in the order as $\text{Pb} > \text{Cu} > \text{Zn}$ and Mn. In addition, after adding Fe in the solution, resulted in 4% Cu and 4.5% Pb loadings reduction, which were likely affected by the metal species affinity to plastic surface. SEM-EDS analysis revealed that metal deposits were present on new LDPE. XPS analysis further confirmed the addition of Fe decreased other metals adsorption onto new LDPE pellets. Furthermore, the high resolution XPS spectra revealed copper, lead and zinc deposits were primarily Cu^{2+} , Pb^{2+} and Zn^{2+} hydroxides and oxides.

This bench-scale study provides insight into the factors that influence metal adsorption onto LDPE. Additional work should be carried-out using commercial plastic drinking water pipes coupled with other water, hydraulic conditions. The long term pilot scale experiment are recommended. It's also worth to study the role of microorganism and metals release into the bulk water.

2.5 References

- [1] U.S. EPA, Maximum contaminant level goals and national primary drinking water regulations for lead and copper, final rule, Federal Register, 56 (1991).

- [2] L. Patrick, Lead Toxicity, a review of the literature. Part I: Exposure, Evaluation, and treatment, *Alternative medicine review*, 11 (2006).
- [3] L.M. Gaetke, C.K. Chow, Copper toxicity, oxidative stress, and antioxidant nutrients, *Toxicology*, 189 (2003) 147-163.
- [4] U.S. EPA, National Primary Drinking Water Regulations, (2009).
- [5] F. Edition, Guidelines for drinking-water quality, *WHO chronicle*, 38 (2011) 104-108.
- [6] N.S. Grigg, Assessment and renewal of water distribution systems, *Journal-American Water Works Association. Journal*, 97 (2005) 58-68.
- [7] J.M. Cerrato, L.P. Reyes, C.N. Alvarado, A.M. Dietrich, Effect of PVC and iron materials on Mn (II) deposition in drinking water distribution systems, *Water Research*, 40 (2006) 2720-2726.
- [8] P. Sarin, V.L. Snoeyink, D.A. Lytle, W.M. Kriven, Iron corrosion scales: model for scale growth, iron release, and colored water formation, *Journal of environmental engineering*, 130 (2004) 364-373.
- [9] E.J. Kim, J.E. Herrera, Characteristics of lead corrosion scales formed during drinking water distribution and their potential influence on the release of lead and other contaminants, *Environmental science & technology*, 44 (2010) 6054-6061.
- [10] D.A. Lytle, T.J. Sorg, C. Frietch, Accumulation of arsenic in drinking water distribution systems, *Environmental science & technology*, 38 (2004) 5365-5372.
- [11] M.J. Friedman, A.S. Hill, S.H. Reiber, R.L. Valentine, G. Larsen, A. Young, G.V. Korshin, C.Y. Peng, Assessment of inorganics accumulation in drinking water system scales and sediments, *Water Research Foundation, Denver*, (2010).
- [12] J. Liu, H. Chen, Q. Huang, L. Lou, B. Hu, S.D. Endalkachew, N. Mallikarjuna, Y. Shan, X. Zhou, Characteristics of pipe-scale in the pipes of an urban drinking water distribution system in eastern China, *Water Science and Technology: Water Supply*, 16 (2016) 715-726.
- [13] M. Salehi, X. Li, A.J. Whelton, Metal Accumulation in Representative Plastic Drinking Water Plumbing Systems, *Journal: American Water Works Association*, 109 (2017) 479-493.
- [14] C.E. Campbell, A.J. Whelton, R. Polera, A.M. Dietrich, The characteristics and chemical performance of polyethylene and poly (1-butene) pipes removed from a water distribution system, *VWRRC Special Report SR43-2008*, (2008) 1-13.
- [15] K. Ashton, L. Holmes, A. Turner, Association of metals with plastic production pellets in the marine environment, *Marine pollution bulletin*, 60 (2010) 2050-2055.
- [16] A. Turner, L.A. Holmes, Adsorption of trace metals by microplastic pellets in fresh water, *Environmental Chemistry*, 12 (2015) 600-610.
- [17] C.M. Rochman, B.T. Hentschel, S.J. Teh, Long-term sorption of metals is similar among plastic types: implications for plastic debris in aquatic environments, *PLoS One*, 9 (2014) e85433.
- [18] M. Eriksen, S. Mason, S. Wilson, C. Box, A. Zellers, W. Edwards, H. Farley, S. Amato, Microplastic pollution in the surface waters of the Laurentian Great Lakes, *Marine pollution bulletin*, 77 (2013) 177-182.
- [19] L.A. Holmes, A. Turner, R.C. Thompson, Adsorption of trace metals to plastic resin pellets in the marine environment, *Environmental Pollution*, 160 (2012) 42-48.
- [20] E. Nakashima, A. Isobe, S.i. Kako, T. Itai, S. Takahashi, Quantification of toxic metals derived from macroplastic litter on Ookushi Beach, Japan, *Environmental science & technology*, 46 (2012) 10099-10105.

- [21] M. Salehi, C.T. Jafvert, J.A. Howarter, A.J. Whelton, Investigation of the Factors that Influence Lead Accumulation onto Polyethylene: Implication for Potable Water Plumbing Pipes, *Journal of Hazardous Materials*, 347 (2017) 242-251.
- [22] J. Wang, J. Peng, Z. Tan, Y. Gao, Z. Zhan, Q. Chen, L. Cai, Microplastics in the surface sediments from the Beijiang River littoral zone: Composition, abundance, surface textures and interaction with heavy metals, *Chemosphere*, 171 (2017) 248-258.
- [23] L.A. Holmes, A. Turner, R.C. Thompson, Interactions between trace metals and plastic production pellets under estuarine conditions, *Marine Chemistry*, 167 (2014) 25-32.
- [24] D.E. Robertson, The adsorption of trace elements in sea water on various container surfaces, *Analytica Chimica Acta*, 42 (1968) 533-536.
- [25] A. Fischer, J. Kroon, T. Verburg, T. Teunissen, H.T. Wolterbeek, On the relevance of iron adsorption to container materials in small-volume experiments on iron marine chemistry: 55 Fe-aided assessment of capacity, affinity and kinetics, *Marine Chemistry*, 107 (2007) 533-546.
- [26] A.J. Whelton, T. Nguyen, Contaminant migration from polymeric pipes used in buried potable water distribution systems: a review, *Critical reviews in environmental science and technology*, 43 (2013) 679-751.
- [27] Y. Zhang, M. Edwards, Accelerated chloramine decay and microbial growth by nitrification in premise plumbing, *American Water Works Association. Journal*, 101 (2009) 51-62.
- [28] J.C. Montes, D. Cadoux, J. Creus, S. Touzain, E. Gaudichet-Maurin, O. Correc, Ageing of polyethylene at raised temperature in contact with chlorinated sanitary hot water. Part I—Chemical aspects, *Polymer degradation and stability*, 97 (2012) 149-157.
- [29] K.N. Fotopoulou, H.K. Karapanagioti, Surface properties of beached plastic pellets, *Marine environmental research*, 81 (2012) 70-77.
- [30] J.P. Gustafsson, Visual MINTEQ 3.0 user guide, KTH, Department of Land and Water Resources, Stockholm, Sweden, (2011).
- [31] J. Duruibe, M. Ogwuegbu, J. Ekwurugwu, Heavy metal pollution and human biotoxic effects, *International Journal of physical sciences*, 2 (2007) 112-118.
- [32] X. Huang, S. Zhao, M. Abu-Omar, A.J. Whelton, In-situ cleaning of heavy metal contaminated plastic water pipes using a biomass derived ligand, *Journal of Environmental Chemical Engineering*, 5 (2017) 3622-3631.
- [33] J. Coates, Interpretation of infrared spectra, a practical approach, *Encyclopedia of analytical chemistry*, 12 (2000) 10815-10837.
- [34] Y. Mato, T. Isobe, H. Takada, H. Kanehiro, C. Ohtake, T. Kaminuma, Plastic resin pellets as a transport medium for toxic chemicals in the marine environment, *Environmental science & technology*, 35 (2001) 318-324.
- [35] C. Faur-Brasquet, K. Kadirvelu, P. Le Cloirec, Removal of metal ions from aqueous solution by adsorption onto activated carbon cloths: adsorption competition with organic matter, *Carbon*, 40 (2002) 2387-2392.
- [36] J.H. Park, Y.S. Ok, S.-H. Kim, J.-S. Cho, J.-S. Heo, R.D. Delaune, D.-C. Seo, Competitive adsorption of heavy metals onto sesame straw biochar in aqueous solutions, *Chemosphere*, 142 (2016) 77-83.
- [37] R.G. Pearson, Absolute electronegativity and hardness: application to inorganic chemistry, *Inorg. Chem.:(United States)*, 27 (1988) 734-740.
- [38] B.K. Xiao, K.M. Thomas, Competitive adsorption of aqueous metal ions on an oxidized nanoporous activated carbon, *Langmuir*, 20 (2004) 4566-4578.

- [39] J.H. Crocket, J.W. Winchester, Coprecipitation of zinc with calcium carbonate, *Geochimica et Cosmochimica Acta*, 30 (1966) 1093-1109.
- [40] J. Zachara, J.A. Kittrick, J. Harsh, The mechanism of Zn²⁺ adsorption on calcite, *Geochimica et Cosmochimica Acta*, 52 (1988) 2281-2291.
- [41] H.A. Aziz, M.S. Yusoff, M.N. Adlan, N.H. Adnan, S. Alias, Physico-chemical removal of iron from semi-aerobic landfill leachate by limestone filter, *Waste management*, 24 (2004) 353-358.
- [42] J.A. Davis, Complexation of trace metals by adsorbed natural organic matter, *Geochimica et Cosmochimica Acta*, 48 (1984) 679-691.
- [43] L. Perelomov, D. Pinskiy, A. Violante, Effect of organic acids on the adsorption of copper, lead, and zinc by goethite, *Eurasian Soil Science*, 44 (2011) 22-28.
- [44] J. Rangel-Mendez, R. Monroy-Zepeda, E. Leyva-Ramos, P. Diaz-Flores, K. Shirai, Chitosan selectivity for removing cadmium (II), copper (II), and lead (II) from aqueous phase: pH and organic matter effect, *Journal of Hazardous Materials*, 162 (2009) 503-511.
- [45] A.K. Pandey, S.D. Pandey, V. Misra, Stability constants of metal-humic acid complexes and its role in environmental detoxification, *Ecotoxicology and environmental safety*, 47 (2000) 195-200.
- [46] K.M. Kelley, A.C. Stenson, R. Dey, A.J. Whelton, Release of drinking water contaminants and odor impacts caused by green building cross-linked polyethylene (PEX) plumbing systems, *Water research*, 67 (2014) 19-32.
- [47] V. Lund, M. Anderson-Glenna, I. Skjevrak, I.-L. Steffensen, Long-term study of migration of volatile organic compounds from cross-linked polyethylene (PEX) pipes and effects on drinking water quality, *Journal of water and health*, 9 (2011) 483-497.
- [48] D.A. Lytle, M.R. Schock, Formation of Pb (IV) oxides in chlorinated water, *Journal (American Water Works Association)*, 97 (2005) 102-114.
- [49] P. Bose, M.A. Bose, S. Kumar, Critical evaluation of treatment strategies involving adsorption and chelation for wastewater containing copper, zinc and cyanide, *Advances in Environmental Research*, 7 (2002) 179-195.
- [50] O.J. Hao, A.P. Davis, P.H. Chang, Kinetics of manganese (II) oxidation with chlorine, *Journal of Environmental Engineering*, 117 (1991) 359-374.
- [51] X. Cao, L.Q. Ma, M. Chen, S.P. Singh, W.G. Harris, Impacts of phosphate amendments on lead biogeochemistry at a contaminated site, *Environmental Science & Technology*, 36 (2002) 5296-5304.
- [52] F. Boyle, W. Lindsay, Diffraction Patterns and Solubility Products of Several Divalent Manganese Phosphate Compounds 1, *Soil Science Society of America Journal*, 49 (1985) 761-766.
- [53] M.C. Biesinger, L.W. Lau, A.R. Gerson, R.S.C. Smart, Resolving surface chemical states in XPS analysis of first row transition metals, oxides and hydroxides: Sc, Ti, V, Cu and Zn, *Applied Surface Science*, 257 (2010) 887-898.
- [54] A.V. Naumkin, A. Kraut-Vass, S.W. Gaarenstroom, C. Powell, NIST X-ray Photo-electron Spectroscopy Database, NIST Standard Reference Database 20, Version 4.1, (2012).
- [55] V. Nefedov, Y.V. Salyn, P. Solozhenkin, G.Y. Pulatov, X - ray photoelectron study of surface compounds formed during flotation of minerals, *Surface and Interface Analysis*, 2 (1980) 170-172.

- [56] C. Xiong, W. Wang, F. Tan, F. Luo, J. Chen, X. Qiao, Investigation on the efficiency and mechanism of Cd (II) and Pb (II) removal from aqueous solutions using MgO nanoparticles, *Journal of hazardous materials*, 299 (2015) 664-674.

CHAPTER 3. CORROSION OF UPSTREAM METAL PLUMBING COMPONENTS IMPACTS ON DOWNSTREAM PEX PIPE SURFACE DEPOSITS AND DEGRADATION

3.1 Introduction

Plastic drinking water pipes are being increasingly installed for building water service lines and commercial and residential plumbing [1]. A survey of 59 U.S. homeowners who replumbed their homes documented that 54% preferred to install crosslinked polyethylene (PEX) pipes, instead of applying an epoxy coating to the existing pipes or installing metallic plumbing materials [2]. When buildings are renovated sometimes only part, not all, of the existing metallic plumbing is replaced with new plastic pipes [3-5]. As a result, these buildings contain metal-plastic hybrid plumbing networks, where released metals may interact with plastic materials. Such hybrid plumbing networks can also be observed at the service line, where the utility installs a new plastic pipe and the customer does not replace the older piping material. PEX piping can also be located downstream of metallic service line and water distribution system pipes. Even when building owners install PEX piping throughout the household plumbing, metal fittings such as brass valves and couplings can be present.

While studies have investigated the leaching of metals into water from metallic plumbing components [6-9], few studies have investigated metal fate within plastic plumbing [4, 5, 10]. Brass leaching has been identified as a major source of metal release within plastic plumbing systems, and can be influenced by the product's composition [11, 12], drinking water characteristics [8, 13-15], water temperature [16], galvanic current [17, 18], and hydraulic conditions [11, 16, 19]. For example, compared to incoming building water metal concentrations, brass-related metals such as copper, lead, and zinc were higher within the plastic household

plumbing [4]. Another study examined metal deposits on indoor PEX plumbing pipes from a 1 year old single family U.S. home. Here, surface analysis revealed orders of magnitude different metal loadings on the exhumed pipes [20]. Calcium (Ca), Iron (Fe), magnesium (Mg), manganese (Mn), lead (Pb), and zinc (Zn) were the most abundant metals [20], which were hypothesized to have originated from the source water, water treatment chemicals, and/or plumbing components [4, 21]. Researchers also found abundant Fe deposits on one high-density polyethylene (HDPE) residential service line [22], Fe, Ca, and Zn deposits on PVC water mains [21], and Ca, Mn, and Zn deposits on HDPE water mains [23]. In contrast, a PVC water main exhumed from a U.S. water distribution system had “no or very small corrosion deposits” [24]. In Honduras, Mn deposits on exhumed PVC water mains were about 1.8 times greater than on iron water mains from the same distribution system [25]. In response to more than 100 black and yellow water complaints received by one utility in China, PVC and polyethylene (type not specified) water mains were exhumed and found to contain high loadings of aluminum (Al), Mn, silicon (Si), and Fe [26]. Thus, metal loading on plastic plumbing materials have been observed and the composition and amount of metal deposits present on plastic pipe surfaces likely originated from the drinking water source, water treatment processes, water distribution system materials, and environmental and hydraulic conditions. Further research is needed to characterize deposition throughout the plumbing network, including building plumbing, as it is closer to the consumer’s point of use.

The impact of metal deposition on plastic pipe service life has received little scrutiny, but field and laboratory evidence suggest there may be a relationship. In 2018, the U.S. Plastic Pipe Institute described concerns regarding use of copper pipe with polypropylene (PP-R) pipe. It was claimed that “dissolved copper levels below 0.1 mg/L will not adversely affect PP-R piping materials,” but at or above 0.1 mg/L this copper concentration could have negative impacts on PP-

R pipe integrity [27]. That same year, a PP-R pipe manufacturing company stated that copper ions could attack downstream PP-R pipes and PEX pipes [28]. In 2014, bench-scale experiments lead others to conclude that polyethylene (i.e., PE) exposure to “copper ion” at $> 60^{\circ}\text{C}$ increased crystallization and surface roughness [29]. In 2012, a researcher declared that copper salts can deposit on the surface of PP-R, PEX, and polybutylene water pipes and catalyze plastic pipe degradation [30]. Unfortunately, data was not available to support these claims. It was reported that copper ions and high temperatures for a hot water recirculation system depleted PP pipe stabilizers. A 2001 study reported that copper in a hot water PP pipe system catalyzed failures after 4 to 5 years installation in a German hospital [31]. As far back as 1974, carbonyl functional groups ($>\text{C}=\text{O}$) were found to be caused by the exposure of low density polyethylene to polished copper plates at high temperature ($> 55^{\circ}\text{C}$) [32]. Because PEX piping is increasingly being installed downstream of metallic components and metal deposits can accumulate on plastic pipes, understanding of metal-plastic interactions is warranted.

Field- and bench-scale tests were conducted further understand metal deposits on PEX piping installed in a residential building and deposition caused by upstream metallic components. Specific objectives were to: (i) characterize scales from galvanized iron and downstream PEX drinking water pipes exhumed from the residential building (ii) examine the influence of water conditions, temperature and pipe apparatus on metal leaching and metal deposition, and (iii) evaluate plastic degradation phenomenon due to metal loading.

3.2 Materials and methods

3.2.1 Characterizing metal scale and deposition on exhumed pipes

On May 10, 2018, six galvanized iron pipes (GIP) that were upstream of PEX piping sections (ranging from 3-12 feet each) were exhumed from a 4 bedroom, 1.5 bath, 204 m² area

single-family home in West Lafayette, Indiana USA. All sections were removed from the basement ceiling by a plumbing contractor and separated into hot and cold water sections. The exhumed PEX pipes were approximately 6 months old, while the GIPs were originally installed in 1928. One GIP-PEX pipe section was from the hot water system, while the other 5 GIP-PEX pipe sections were from cold water system. No water softener was in use or present at the time the pipes were exhumed. To prevent pipe section dry out during transport, pipes ends were covered with Parafilm[®]. Characteristics of the drinking water that entered the building have been described in detail elsewhere [20]. In brief, the drinking water source was groundwater, followed by chemical treatment that included KMnO_4 , free chlorine as the residual disinfectant, and 70% orthophosphate and 30% polyphosphate for corrosion control. The water that entered the residential plumbing was very hard (about 400 mg/L as CaCO_3).

An Inductively Coupled Plasma-Optical Emission Spectroscopy (ICP-OES) (Perkin Elmer) was used to characterize metal scales and deposits on: (1) six GIPs (GIP-1 to GIP-6) and PEX pipes (PEX-1 to PEX-6) each 3 cm length ($n=12$ pipes) and (2) one PEX piping section cut into 15 cm length ($n=3$). Scales on the GIPs (0.2-0.4 g) were scraped and solids digested at 55°C for 48 hr in 40 ml solution, which contained 2% nitric acid and 2% hydroxylamine as described by others [7, 15, 33]. The exhumed PEX pipes were filled with the 2% nitric acid and 2% hydroxylamine solution, plugged with PTFE wrapped silicon stoppers, and agitated for minimum of 48 hr [12, 33]. After, a 100 μL of digested solution was extracted and diluted to 10 ml (i.e., contain 1% HNO_3) with nanopure water and nitric acid before the ICP-OES measurement. PEX metal loadings from the current field work was compared with the neighboring house, as these residential buildings shared the same incoming water but had different plumbing material and device installed [20].

3.2.2 Bench-scale experiment on metals leaching and deposition on PEX pipe surfaces

3.2.2.1 Materials and pipe apparatus

Four plumbing rigs were assembled (Figure B.1): (1) P rig: PEX pipe only (1.905 cm \varnothing , 30 cm length), (2) C rig: copper pipe only (1.905 cm \varnothing , 30 cm length), (3) PBP rig: PEX pipe (1.905 cm \varnothing , 15 cm length) + brass valve + PEX pipe (1.905 cm \varnothing , 15 cm length) and (4) CBP rig: copper pipe (1.905 cm \varnothing , 15 cm length) + brass valve + PEX pipe (1.905 cm \varnothing , 15 cm length). Lead-free (<0.25% of lead based on weighted surface area) ball valves (1.905 cm \varnothing) were purchased from a local plumbing supplier and 1.905 cm PEX-A pipe (cross-linked medium density polyethylene) was purchased from SupplyHouse.com (product No. F1040750). Among these four rigs, P and C rigs were used as controls. PBP rig was examined the impact of brass fittings on downstream plastic pipe surface deposits while CBP rig examined the impact of upstream copper pipes on downstream plastic pipe surface deposits [29, 30]. All testing was conducted with four replicates.

3.2.2.2 Water conditions

Two water pH and alkalinity conditions and two temperatures conditions were selected ($n=4$ water conditions) based on a prior study [12] (Table B.1). Specifically, an aggressive water (pH 4 with <5 mg/L as CaCO₃ alkalinity and 100 mg/L as CaCO₃ hardness) and a moderately aggressive water (pH 7.5 with 175 mg/L as CaCO₃ alkalinity and 100 mg/L as CaCO₃ hardness) were used. These two water conditions were examined at cold (23°C) and hot (55°C) water temperatures.

3.2.2.3 Sample collection and analytical methods

The leaching experiment was conducted over a three-week period, and water quality parameters were measured on days 3, 6, 9, 12, 15, 18, 21. Every three days, water was freshly prepared and filled into rigs. Water samples were first collected in 125 mL HDPE bottles and water volume and pH were measured. A 20 ml of sample was collected for the total organic carbon (TOC) measurement (TOC-LCPH analyzer, Shimadzu). A 10 ml aliquot was withdrawn for total metals

analysis. Dissolved metals were obtained by filtering 30 mL of water sample through the 0.45 μm Nylon filter. Metal samples were acidified containing 2% HNO_3 before ICP-OES analysis. The TOC method reporting limit (MRL) was determined to be 0.2 mg/L from seven replicates [34]. Whereas, using the same method, target metal MRLs were Al (2 $\mu\text{g/L}$), barium (Ba; 1 $\mu\text{g/L}$), Ca (5 mg/L), cadmium (Cd; 1 $\mu\text{g/L}$), copper (Cu; 1 $\mu\text{g/L}$), Fe (2 $\mu\text{g/L}$), Mg (1 $\mu\text{g/L}$), Mn, (1 $\mu\text{g/L}$), nickel (Ni; 1 $\mu\text{g/L}$), phosphorus (P; 5 $\mu\text{g/L}$), Pb (2 $\mu\text{g/L}$), Si (2 $\mu\text{g/L}$), and Zn (1 $\mu\text{g/L}$). Measured values less than the corresponding MRL were not reported.

3.2.2.4 Characterization

At the end of 21-day exposure period, a 7 cm segment of PEX-A pipe was cut from the location nearest to the brass valve, filled with 2% HNO_3 solution and analyzed on the ICP-OES. The chemical composition of new brass valves and copper pipe was determined using a portable x-ray fluorescence (pXRF) instrument (Tracer III-SD, Bruker). The pXRF measurement was conducted at voltage and current of 40 keV and 10 μA , respectively. The standard titanium and aluminum filter was used for metals analysis, which allowed X-rays (i.e., 12-40 keV) to reach the samples. The running time was set to 100 s for each sample measurement. A 1 cm \times 1 cm PEX-A segment was analyzed by Attenuated Total Reflectance (ATR) - Fourier Transform Infrared (FTIR) spectroscopy (TravellR HazMat FTIR spectrometer) (scan range was 650 to 4000 cm^{-1} , with resolution of 2 cm^{-1}). ATR-FTIR was applied to identify the formation of oxygen containing functional groups (i.e., -OH, $>\text{C}=\text{O}$, and $>\text{C}=\text{O}<$). The morphology of metal deposits on the PEX-A pipe surface was examined by scanning electron microscopy-energy dispersive X-ray spectroscopy (SEM-EDS) (Hitachi S-4800 Field Emission SEM). Because the plastic had very low conductivity, all samples (1 cm \times 1 cm) were coated with a thin platinum film and fixed with the conductive tape. The measurement was operated at 20 keV and with a working distance of about 15 mm. The chemical composition and metal deposit speciation for select exhumed PEX

pipes was explored using a Kratos AXIS Ultra DLD Imaging X-ray Photoelectron Spectroscopy (XPS) with monochromatic Al K- α radiation ($h\nu=1486.6$ eV). Both survey and high resolution XPS spectra were obtained and the charge effect was corrected setting the main C1s peak at 284.8 eV.

3.2.2.4 Statistical methods

Since the experimental data were not following the normal distribution (Shapiro-Wilk; $p < 0.05$), nonparametric statistics were used. The strength of a relationship between distance (i.e., three 15 cm length plastic pipe sections from the tee) and metal loadings was measured by the Spearman's correlation coefficient (ρ). The Wilcoxon test was used to compare medians between monitored water quality data (e.g., metal and organic carbon leaching and metal deposition) under difference conditions [15].

3.3 Results and discussion

3.3.1 Chemical composition of exhumed residential plumbing pipe surface deposits

Metal deposits were found on both GIP and PEX pipe inner walls (Figure B.2). The most abundant metals on GIPs scales were Fe (48.0-86.7 wt%), Ca (3.1-27.2 wt%), Mn (0.3-21.0 wt%), and Zn (1.0-10.6 wt%) (Table B.2). Fe is a major GIP component [35], water supplier reported 0.05 mg Fe/L in their drinking water, and ductile iron water mains conveyed water to the service line [20, 36]. Ca likely originated from the hard water (i.e., about 400 mg/L hardness as CaCO_3) [37]. Mn was added to the drinking water as part of disinfection (KMnO_4) and the water supplier reported 0.02 mg Mn/L entering the distribution system [20]. Zn is a major GIP component (i.e., 10 wt%) [35] and brass fittings (34.9 wt%) in present study. Phosphorous (4.0-9.9 wt%) may have originated from the utility's phosphate-based corrosion inhibitor (70% orthophosphate/30% polyphosphate) and leached from PEX pipes, if present [10]. Other metals were also found at lesser

loadings (Si (< 3.0 wt%), Ba (<3.0 wt%), Al (<1.0 wt%), Ni (<0.6 wt%), Mg (<0.6 wt%), Cu (<0.6 wt%), Pb (<0.1%), and Cd (<0.01 wt%)) may have originated from the source water, metallic water distribution, and/or plumbing components [36, 38-40].

Similar as GIP scales, PEX pipe inner wall deposits contained Fe (25.6-60.0 wt%), Mn (0.6-28.2 wt%), Ca (6.0-17.0 wt%), P (2.4-15.4 wt%), and Zn (0.9-10.6 wt%) (Table 3.1). However, the maximum loadings of Cu (1.4-15.6 wt%) and Si (2.8-10.4 wt%) were much greater on PEX pipes compared to GIPs. Among all examined PEX pipes, PEX1-cold and PEX2-cold pipe deposits contained the greatest loadings of all metals. The observation might result from the aged upstream metallic materials leaching and the excess biofilm growth under certain circumstances. It is worth noting that Mn loading was more than 100 times greater on PEX1-cold and PEX2-cold pipes compared to the other four PEX pipe sections. These two PEX pipes had blackish deposits, which were easily removed by a finger wipe (Figure 3.1). Whereas, a light yellowish color was observed on the inner pipe wall for a hot water pipe (PEX3-hot) and cold water pipe (PEX6-cold) (Figure 3.1).

Ba, Ca, Fe, Mg, Mn, P, Si and Zn loadings along the length of a PEX section decreased as the distance from a brass tee increased (ρ ranged from -0.87 to -1) (Figure 3.2). For other detected metals (i.e., Al, Cu, Ni and Zn), there was either a weak or a positive correlation with distance (ρ ranged from -0.5 to 1). Overall, the pipe section closest to the brass tee had the highest total metal loadings, which reduced by 28.3% and 39.4% on the pipe sections further away from the brass tee. SEM-EDS results confirmed that a greater amount of metal deposits were present closer to the tee (Figure B.3). Compared to the 1 year old PEX cold and hot water pipes from a neighboring home [20], deposits on these 6 month old PEX pipes were 1 to 3 orders of magnitude greater, depending on the metal. These differences may be attributed to the water softener and type of plumbing

material installed. The neighboring home had a softener installed and the household plumbing was PEX pipes with brass fittings, except for one 5 ft long GIP conveyed hot water from the basement to the first and second floors. Additional work is suggested to characterize deposited metals within plastic plumbing systems and focus on pipe location, hydraulic, temperature, and fixture use factors.

Deposits on subset of PEX pipes were examined by XPS and found to contain a variety of oxidized metals: CuO, Cu(OH)₂, FeOOH, Fe₂O₃, and MnO₂. These metal contaminants have previously been found in metallic piping scales [21, 41] and in PVC water main deposits [21]. CuO and Cu(OH)₂, found in PEX pipe deposits, were characterized by the Cu 2p_{3/2} peak at 933.57 and 934.75 eV, respectively, and additional satellite peaks [42] (Figure 3.3). Based on Fe 2p peak locations (Fe 2p_{3/2} at 711.4 eV and Fe 2p_{1/2} at 725.5 eV) and peak shapes (i.e., with shake up satellites), the Fe deposits were likely Fe₂O₃ (Fe 2p_{3/2} at 711.6 eV) and FeOOH (Fe 2p_{3/2} at 711.3 eV and Fe 2p_{1/2} at 724 eV) [43, 44]. According to the NIST database and the work conducted by Li et al. (2018), the Mn 2p_{3/2} peak at 642.5 eV revealed MnO₂ was the dominant Mn species [26]. This study seems to be the first reporting these contaminants inside household plumbing and confirmed many of the metals detected by ICP-OES analysis were also present on the surface. For these pipes, the greater amount of metals detected on the surface (PEX1-cold (23.5%) > PEX3-hot (14.5%) > PEX6-cold (6.3%)), resulted a greater O 1s peak intensity (PEX1-cold (43.5%) > PEX3-hot (34.4%) > PEX6-cod (14.2%)) (Table B.3).

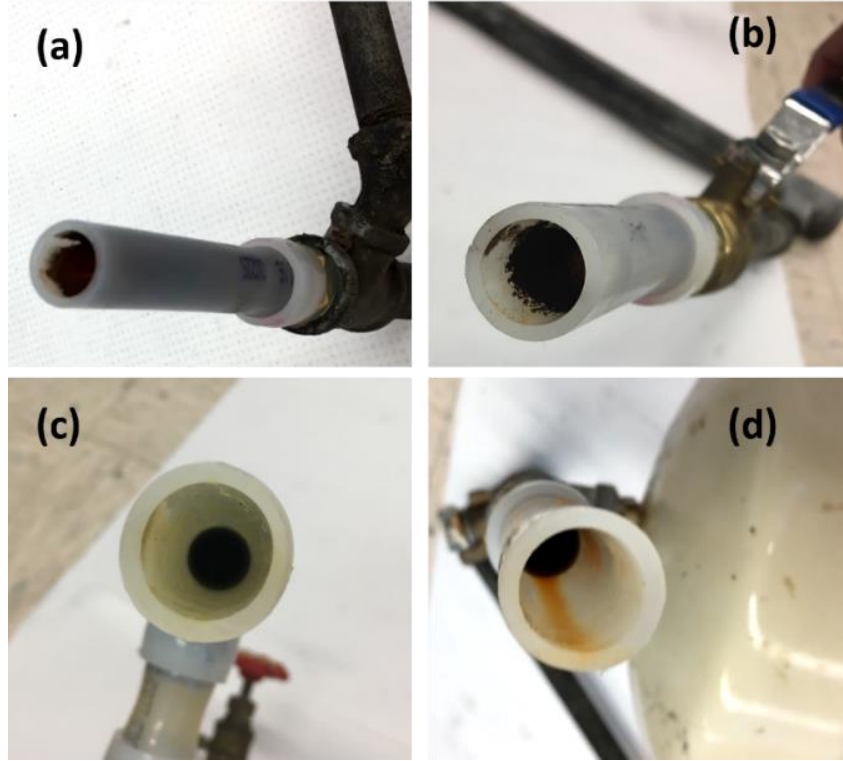


Figure 3.1 Image of inner wall metal scales on exhumed (a) PEX1-cold, (b) PEX2-cold, (c) PEX3-hot and (d) PEX6-cold pipes.

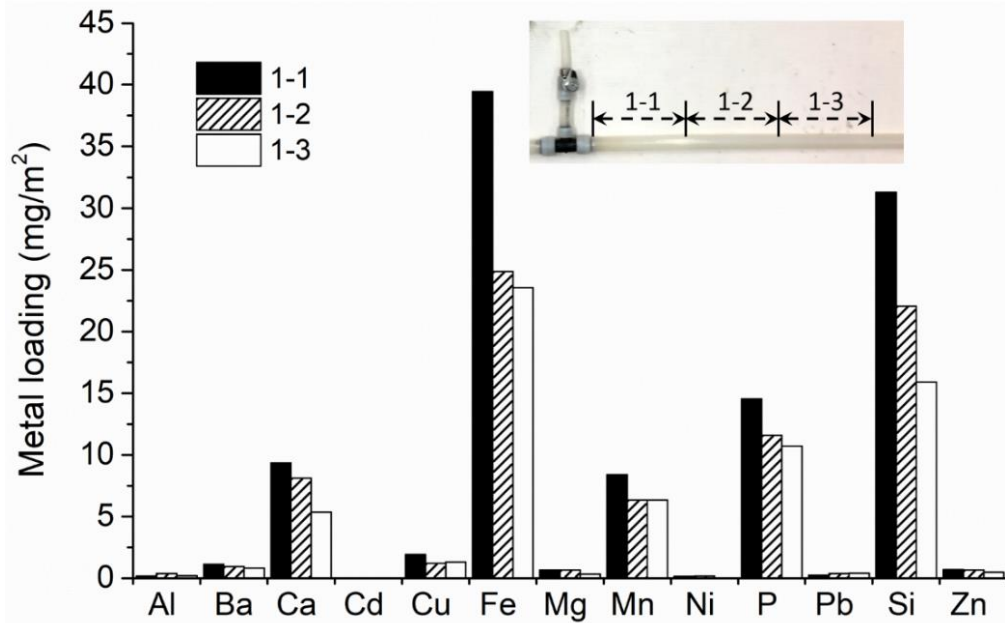


Figure 3.2 Element distribution along the same length of an exhumed PEX cold water pipe. Each pipe section was cut into 15 cm length. The tee on the left side of the image delivered water vertically to the refrigerator on the first floor.

Table 3.1 Chemical composition of GIP scales and the connected PEX pipe deposits removed from the residential housing.

Study	Sample Name	Element												
		Al	Ba	Ca	Cd	Cu	Fe	Mg	Mn	Ni	P	Pb	Si	Zn
Present	<i>Found on Galvanized Iron pipes (GIPs) by Scraping and Digestion, mg/g</i>													
	GIP1-cold	0.04	2.5	19.2	0.03	1.3	500.6	1.6	2.4	3.67	30.2	0.1	11.6	10.8
	GIP2-cold	0.5	16.6	38.8	0.01	3.4	353.2	3.6	122.7	0.10	27.3	0.4	11.7	5.6
	GIP3-hot	6.4	0.8	168.5	0.07	1.5	297.3	2.9	3.6	0.29	61.5	0.2	11.0	65.9
	GIP4-cold	0.7	2.9	29.9	0.02	1.4	479.2	2.2	1.8	0.11	37.8	0.3	12.4	17.8
	GIP5-cold	0.2	2.2	18.4	0.04	0.8	485.8	1.6	5.9	nd	23.6	1.2	13.2	36.4
	GIP6-cold	0.5	2.0	26.8	0.02	0.8	535.0	1.7	1.8	nd	26.8	0.1	12.5	9.1
	<i>Found on Crosslinked Polyethylene (PEX) Pipes by Digestion, mg/m²</i>													
	PEX1-cold	2.1	88.4	399.9	0.64	578.0	2,048.5	35.9	1,368.5	4.09	149.6	135.2	150.5	437.8
	PEX2-cold	2.6	44.6	245.7	0.38	493.0	807.5	20.6	888.3	2.03	76.5	135.2	103.7	335.8
	PEX3-hot	0.2	0.4	9.3	nd	2.7	22.3	0.7	3.0	0.05	8.4	nd	4.8	2.8
	PEX4-cold	0.6	2.5	30.1	nd	5.0	163.6	8.6	7.5	0.35	27.8	0.9	18.9	7.1
	PEX5-cold	0.3	3.5	47.2	nd	5.1	197.6	12.5	2.2	0.37	44.2	0.2	36.6	3.3
	PEX6-cold	8.5	8.0	33.5	nd	15.5	326.0	3.0	38.3	0.28	41.4	1.2	26.7	58.2
Neighbor's 1 Year Old PEX Home‡	Cold lines	0.1-0.3	nq	0.1-1.6	nd	0-2.4	0.7-19.7	0.1-0.6	1.3-5.9	0-0.017	0.1-2.3	0.1-0.5	nq	0.5-2.1
	Hot lines	0.1-1.3	nq	nd-0.4	nd	0.3-3.7	1.4-6.6	0.2-0.3	0.1-1.1	0-0.015	0.1-0.7	nd-0.2	nq	0.4-1.9

nd: represents elements were below the method report limit. In the Supplementary Information section results are reported as wt%.

‡In 2015, PEX pipes were removed from a 1 year old single-family residential building that was next door to the study house and results were reported by Salehi et al. (2017) [20].

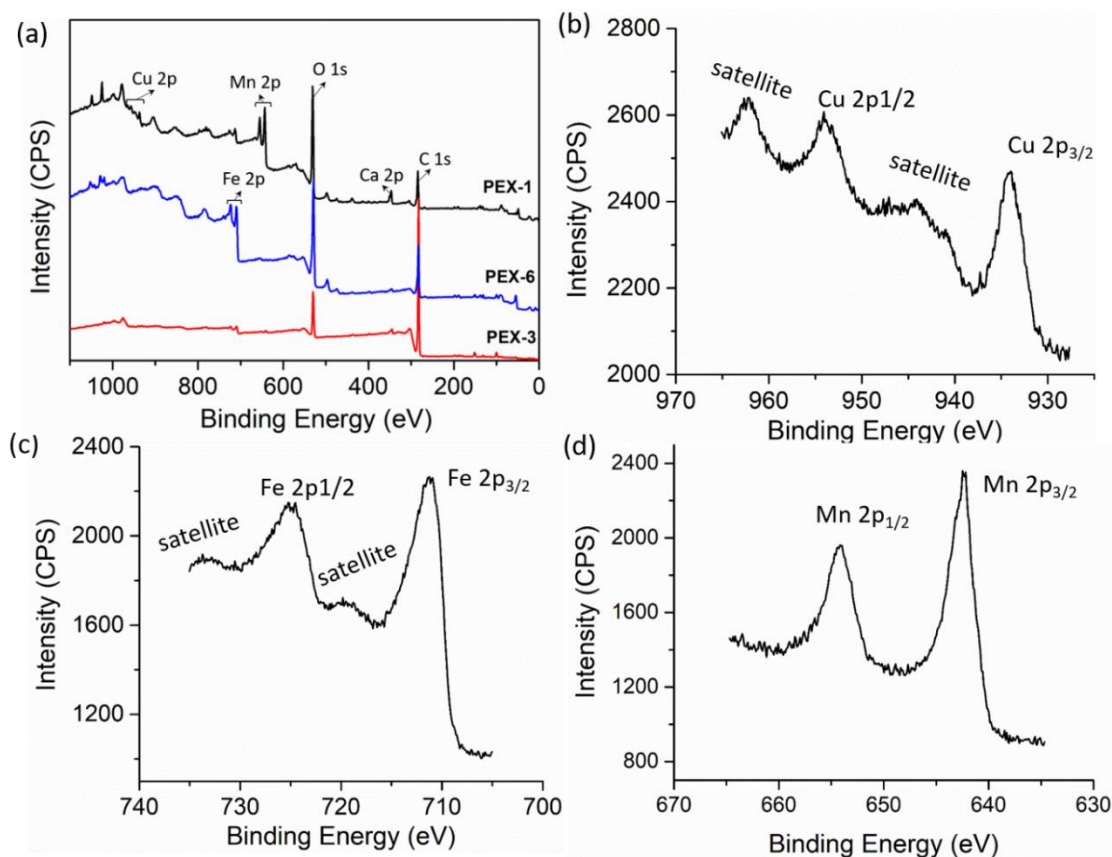


Figure 3.3 XPS wide scan spectra of (a) metal deposits on exhumed PEX pipe surfaces. XPS high resolution spectra of (b) Cu 2p, (c) Fe 2p and (d) Mn 2p detected from exhumed PEX pipe deposits.

3.3.2 Metals in aqueous phase and PEX pipe surface deposits were influenced by water pH, temperature, and brass and copper composition

A bench-scale experiment was conducted to investigate the influence of water conditions and plumbing materials on metal leaching. Through this experiment, greater aqueous metal concentrations were nearly always found when pipe rigs were exposed to the aggressive pH 4 water (Table 3.2 and Figure 3.4). Statistical analysis showed both water condition and temperature played a significant role on metals releasing into aqueous phase (Wilcoxon Test, $p < 0.05$) (Table B.4 and B.5). XRF analysis of brass fittings and copper pipes indicated Cu and Zn originated from the metallic components. Brass valves contained Cu ($64.3 \pm 0.5\%$) and Zn ($34.9 \pm 0.6\%$), and copper pipes were made of Cu ($99.8 \pm 0.0\%$) (Table B.6). Pb was not detected by XRF, though

the 'lead free' brass valves can release Pb to the water [7]. Other metals, such as, Fe, Mg, and Ni were also detected in metallic components, water samples and deposits (Figure B.4 and Table B.7). The galvanic connection (i.e., CBP rig) seemed promoted Pb and Zn in aqueous phase up to 3.7 times and inhibited Cu release (Table 3.2) [16, 18, 45]. Prior studies have shown higher temperature resulted in greater Pb release from brass fitting/copper pipe loops [16], Zn release from brass [46] and Cu release from copper pipes [13].

In contrast to metal aqueous concentration results, evidence suggested that metal surface deposits on PBP and CBP rigs were primarily affected by pH at hot water conditions (Wilcoxon test, $p < 0.05$) (Table B.8 and B.9). At the end of the 21 day exposure period, 15 of 16 metal deposition data had greater metal loadings on PEX surfaces in the hot water than the cold water condition (Table 3.2). However, this was not the case for the field study and study of a neighboring house [20], where hot water lines often had less metal deposits than cold water lines (Table 3.1). The bench scale testing also showed metal loading on PEX was up to four magnitudes lower than observed in the field. For instance, 9.3-399.9 mg Ca/m² and 2.8-437.8 mg Zn/m² were found on PEX surfaces in the field, compared as only 0.05-1.86 mg Ca/m² and 0.02-5.46 mg Zn/m² were detected on PBP and CBP rigs. These differences could be contributed to the different upstream metallic components installed, various water and hydraulic conditions, and the plastic aging effect. In the bench-scale test, the pH 7.5 hot water condition resulted the greatest metal loadings in PBP and CBP rigs (Table 3.2). Among all deposited metals, Zn loading in CBP rigs had the greatest differences (i.e., 21.3 µg/m² [pH 4 cold water] vs 5464.3 µg/m² [pH 7.5 hot water]). High pH and hot water may have enabled metal oxide and oxyhydride formation and deposition, whereas at low pH and cold water a greater amount of metals remained in solution (Table B.10). SEM images indicated that more metal deposits were present on the PEX pipe bottom sections compared to the

top sections (Figure B.5). In addition, alkalinity in the pH 7.5 water (i.e., 175 mg/L alkalinity as CaCO₃) may have also influenced metal deposition formation on PEX pipe surfaces. The effect of alkalinity on plastic drinking water pipe deposit received little study, but scales formed under lower alkalinity condition can be less dense (i.e., bulk density: 1.7-2.2 < 2.2-2.3 g/cm³) and with higher porosity (i.e., 44-54 > 40-43%) than those formed under higher alkalinity conditions [47].

Table 3.2 Total mass of Ca, Cu, Pb and Zn leached in water samples and deposited on PEX surfaces during the 21 day exposure period

Exp. Group	Metal Element	<i>In water, µg</i>				<i>On pipe surface, µg/m²</i>			
		pH 4		pH 7.5		pH 4		pH 7.5	
		Cold	Hot	Cold	Hot	Cold	Hot	Cold	Hot
P rig	Ca ^a	ns	ns	ns	ns	37.7	170.4	275.9	647.9
	Cu	2.2	2.4	nd	nd	31.0	18.9	20.9	19.2
	Pb	nd	nd	nd	nd	2.8	2.5	3.9	4.3
	Zn	2.4	2.1	nd	nd	19.3	13.6	14.9	17.1
C rig	Ca	ns	ns	ns	ns	ns	ns	ns	ns
	Cu	355.3	416.7	123.7	16.5	ns	ns	ns	ns
	Pb	nd	nd	nd	nd	ns	ns	ns	ns
	Zn	3.3	3.9	1.3	nd	ns	ns	ns	ns
PBP rig	Ca	ns	ns	ns	ns	51.6	280.0	424.2	1,115.5
	Cu	169.4	16.4	7.7	4.0	45.6	47.4	43.2	366.6
	Pb	3.1	18.1	nd	nd	5.9	24.6	4.4	92.9
	Zn	659.7	1518.9	31.0	95.3	17.0	50.5	27.7	442.7
CBP rig	Ca	ns	ns	ns	ns	78.7	367.9	466.6	1,856.2
	Cu	108.8	18.6	16.4	15.7	57.3	205.5	54.8	1,751.9
	Pb	4.8	66.7	nd	nd	7.3	29.2	5.7	105.5
	Zn	1,666.1	2,245.7	594.8	154.6	21.3	107.7	39.4	5,464.3

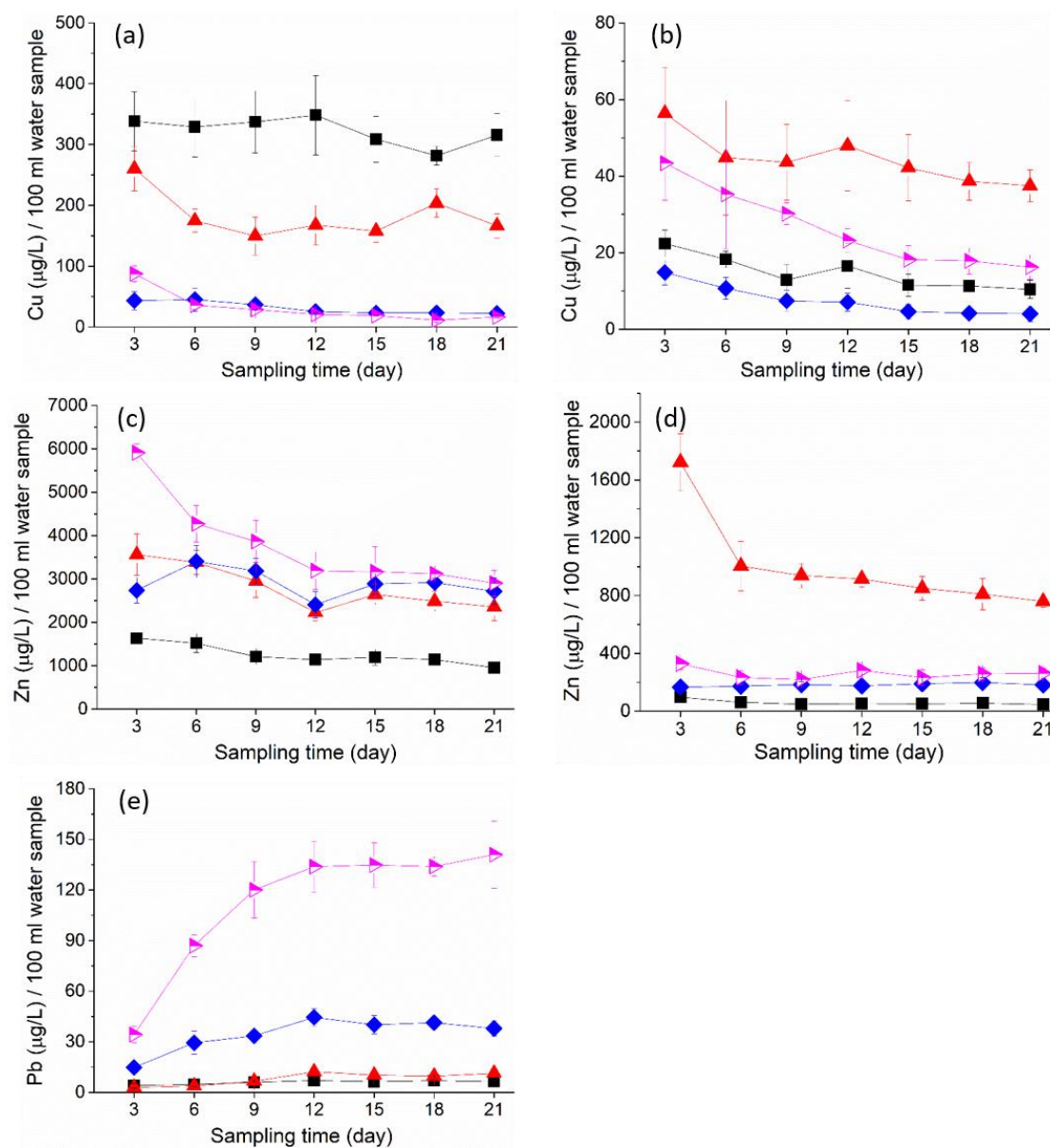


Figure 3.4 (a) Cu, (c) Zn, and (e) Pb levels when plumbing rigs exposed to the pH 4 water and (b) Cu, (d) Zn levels when they were exposed to the pH 7.5 water. —■— PBP @ 23°C, —▲— CBP @ 23°C, —◆— PBP @ 55°C, —▶— CBP @ 55°C. Pb levels were not detected under pH 7.5 water condition.

3.3.3 PEX pipe organic carbon release was influenced by water temperature

In the current work, organic carbon release was documented because the role of organic carbon on metal fate in PEX plumbing had not been previously investigated. Organic contaminants (i.e., NOM) can influence metal fate in drinking water treatment process and metallic pipe

corrosion [48, 49]. Results showed that organic carbon levels were influenced by temperature and exposure time. The greatest organic carbon levels were detected at the beginning of the experiment in rigs exposed to hot water compared to those exposed to cold water, and levels decreased with time (Figure 3.5 and Figure B.6). On day 3, the difference between hot and cold water organic carbon levels was as much as 16.5 mg/L, whereas, on day 21, the difference was as little as 0.5 mg/L. Hot water exposure likely accelerated PEX pipe organic compound release [50, 51]. The typical range of TOC level in plumbing system water has been reported to be 1-6 mg/L [6, 50, 52]. Additional work is needed to determine if the degree leached organic carbon influences heavy metal interaction under cold and hot water plastic piping applications.

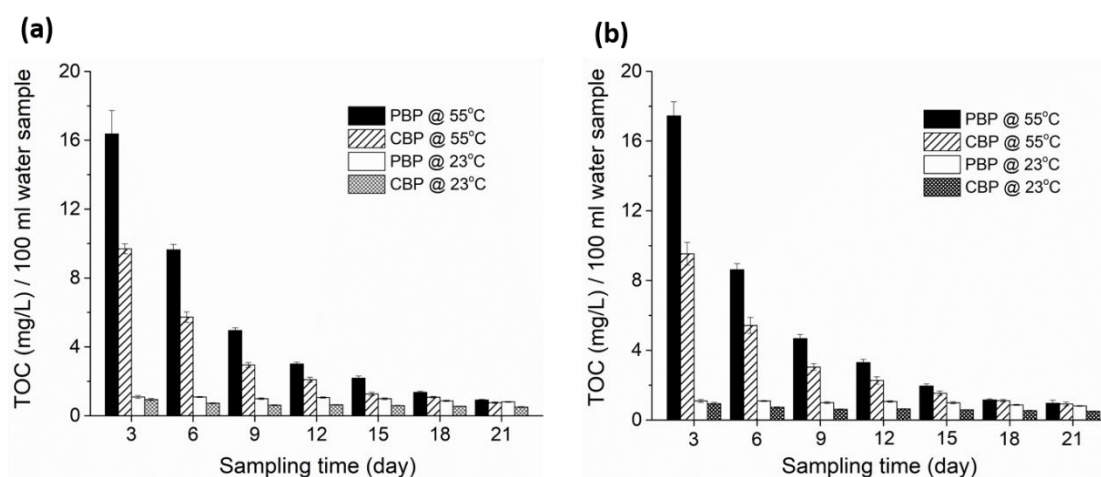


Figure 3.5 PBP and CBP organics leaching during the three weeks experimental period at 55°C and 23°C under (a) pH 4, and (b) pH 7.5 water conditions.

3.3.4 Indications of PEX pipe degradation

New PEX pipes were translucent, but after three weeks of water exposure at 55°C, the PEX pipes inner and outer walls were discolored (Figure 3.6). PEX pipes contained in PBP and CBP rigs were more yellowed than the P rigs. The yellow discoloration was not observed for the PEX pipes exposed to water at 23°C. Discoloration has been reported in 1 year old PEX hot water pipes installed in a residential building closer to brass fittings [20]. Gill et al. (1999) mentioned that PEX

pipe had a yellowish tint after it had completed ~40% of its lifetime [53], but a direct relationship between discoloration and mechanical integrity was not provided. To further investigate the discolored PEX pipes, PEX pipe inner wall surfaces were examined for oxygen containing functional groups. At the end of the 21 day study, no new bonds were detected for the new PEX pipe and PEX pipe that was in the P rig group at 55°C (Figure 3.7). However, for PEX pipes in the PBP and CBP rigs, several functional groups were detected: $>C-O-O-C<$ (796 cm^{-1}), $>C-O<$ (1020 and 1091 cm^{-1}) and $>C-O-C<$ (1259 cm^{-1}). These functional groups have been previously associated with PEX pipe surface oxidation [20, 54, 55]. Evidence suggests the connection of metallic plumbing components to PEX pipes may contribute to surface oxidation. The exact mechanism of oxidation is unclear but could be caused by: (1) eroded in aqueous environment, (2) elevated temperature, and (3) chlorinated water exposure [20, 55-57]. Further studies are recommended to better understand the degree and interaction of deposited metals, dissolved metals, temperature, and organic carbon-metal complexes influence on PEX pipe degradation.

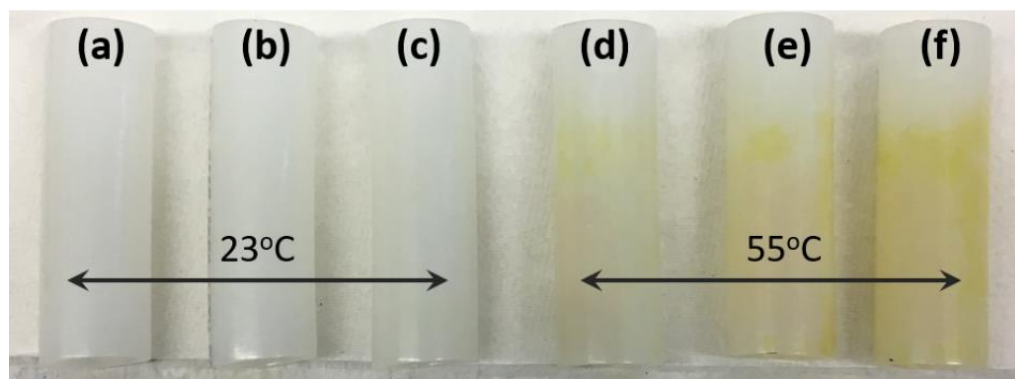


Figure 3.6 Images of PEX pipes that harvested at the end of 21 days from (a) P rig at 23°C (b) PBP rig at 23°C, and (c) CBP rig at 23°C, (d) P rig at 55°C (e) PBP rig at 55°C, and (f) CBP rig at 55°C. Images represent pipes exposed to pH 4 solution.

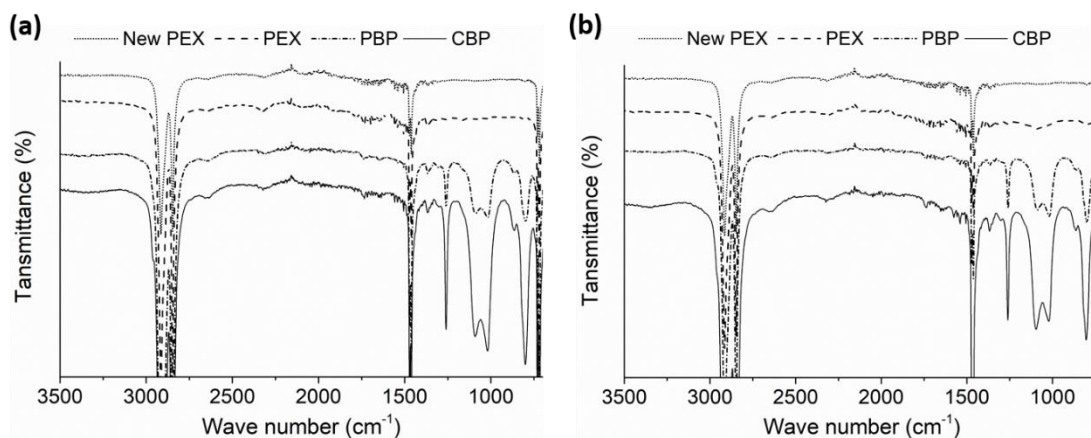


Figure 3.7 FTIR spectra for PEX pipe surfaces removed after 21 days of exposure to (a) aggressive pH 4 water and (b) moderate pH 7.5 water at 55°C.

3.4 Conclusion

Field- and bench-scale tests were conducted to characterize metal deposits on 6 month old PEX piping from a residential building and understand the degree upstream metallic components contribute to metal deposits. Fe, Ca, Mn, Zn and P were most abundant elements found on the six exhumed GIPs and six PEX pipes. These compounds likely originated from plumbing components, water distribution materials, source water, and water treatment plant. Both SEM images and the ICP-OES results confirmed metal deposits differed down the length of a single PEX pipe. The greatest metal loadings were found nearest to the tee and decreased with distance. CuO , $\text{Cu}(\text{OH})_2$, Fe_2O_3 , FeOOH , and MnO_2 were identified as the major metal species on exhumed PEX pipe surfaces using XPS analysis. Levels found on PEX pipes were 10- to 1000-fold greater than metal deposits found on PEX pipes removed from the neighboring home [20]. In that home, softener was installed after the service line, GIP was not often used, and the 1 year old plumbing only contained PEX pipe and brass fittings.

Bench-scale experiments revealed that plumbing configuration, water conditions, and temperature influenced the amount of metal released into aqueous phase and deposited on

downstream PEX pipe. While the aggressive water condition induced greater aqueous metal concentrations, the moderate hot water condition resulted in greater metal deposits on PEX pipes. SEM revealed a greater amount of metal deposits on the bottom of PEX pipes compared to the top section. Organic carbon release was significant for hot water pipes (up to 17.4 mg/L), but much less for cold water conditions (0.2-1.2 mg/L). The role of organic carbon leaching from plastic pipes on metal fate requires study.

PEX pipes exposed to hot water became discolored after the 21 day exposure period. Discoloration was not found for cold water exposure. In addition, PEX pipes that were connected to brass valves and copper pipes (i.e., CBP) had the greatest degree of oxygen containing functional groups formed on their inner pipe wall (i.e., $>C-O-O-C<$, $>C-O<$, and $>C-O-C<$).

Study results indicate a need to explore inorganic contaminant fate within plastic plumbing systems. Additional work is recommended to understand metal deposit processes on plastic plumbing pipes and whether these deposits impact drinking water quality at the tap. For example, the impact of leached organic carbon on metal fate, other water chemistries (pH, hardness, disinfectants and corrosion inhibitor), environmental factors (constant vs. intermittent hot temperature), hydraulic conditions (velocity and pressure) and the biofilm impact should be considered. It is notable that any change of water quality (i.e., blending and switching to a different source) or upstream plumbing material may impact metal deposits on downstream PEX pipes.

3.5 References

- [1] A.J. Whelton, T. Nguyen, Contaminant migration from polymeric pipes used in buried potable water distribution systems: a review, *Critical reviews in environmental science and technology*, 43 (2013) 679-751.
- [2] J. Lee, E. Kleczyk, D.J. Bosch, A.M. Dietrich, V.K. Lohani, G. Loganathan, Homeowners' decision-making in a premise plumbing failure-prone area, *Journal-American Water Works Association*, 105 (2013) E236-E241.

- [3] W.J. Rhoads, A. Pruden, M.A. Edwards, Survey of green building water systems reveals elevated water age and water quality concerns, *Environmental Science: Water Research & Technology*, 2 (2016) 164-173.
- [4] M. Salehi, M. Abouali, M. Wang, Z. Zhou, A.P. Nejadhashemi, J. Mitchell, S. Caskey, A.J. Whelton, Case study: Fixture water use and drinking water quality in a new residential green building, *Chemosphere*, 195 (2018) 80-89.
- [5] D.E. Kimbrough, Brass corrosion as a source of lead and copper in traditional and all-plastic distribution systems, *Journal (American Water Works Association)*, 99 (2007) 70-76.
- [6] Y. Tam, P. Elefsiniotis, Corrosion control in water supply systems: Effect of pH, alkalinity, and orthophosphate on lead and copper leaching from brass plumbing, *Journal of Environmental Science and Health Part A*, 44 (2009) 1251-1260.
- [7] C. Elfland, P. Scardina, M. Edwards, Lead-contaminated water from brass plumbing devices in new buildings, *American Water Works Association. Journal*, 102 (2010) 66-76.
- [8] M. Edwards, L. Hidmi, D. Gladwell, Phosphate inhibition of soluble copper corrosion by-product release, *Corrosion science*, 44 (2002) 1057-1071.
- [9] M. Lasheen, C. Sharaby, N. El-Kholy, I. Elsherif, S. El-Wakeel, Factors influencing lead and iron release from some Egyptian drinking water pipes, *Journal of hazardous materials*, 160 (2008) 675-680.
- [10] J. Inkinen, T. Kaunisto, A. Pursiainen, I.T. Miettinen, J. Kusnetsov, K. Riihinen, M.M. Keinänen-Toivola, Drinking water quality and formation of biofilms in an office building during its first year of operation, a full scale study, *Water research*, 49 (2014) 83-91.
- [11] D.A. Lytle, M.R. Schock, Stagnation time, composition, ph, and orthophosphate effects on metal leaching from brass, National Risk Management Research Laboratory, Office of Research and Development, US Environmental Protection Agency, (1996).
- [12] K.J. Pieper, L.A. Krometis, M. Edwards, Quantifying Lead-Leaching Potential From Plumbing Exposed to Aggressive Waters, *Journal-American Water Works Association*, 108 (2016) 458-466.
- [13] N. Boulay, M. Edwards, Role of temperature, chlorine, and organic matter in copper corrosion by-product release in soft water, *Water research*, 35 (2001) 683-690.
- [14] M. Edwards, A. Dudi, Role of chlorine and chloramine in corrosion of lead-bearing plumbing materials, *Journal (American Water Works Association)*, 96 (2004) 69-81.
- [15] K.J. Pieper, M. Tang, M.A. Edwards, Flint water crisis caused by interrupted corrosion control: Investigating “ground zero” home, *Environmental science & technology*, 51 (2017) 2007-2014.
- [16] E. Sarver, M. Edwards, Effects of flow, brass location, tube materials and temperature on corrosion of brass plumbing devices, *Corrosion Science*, 53 (2011) 1813-1824.
- [17] S. Triantafyllidou, M. Raetz, J. Parks, M. Edwards, Understanding how brass ball valves passing certification testing can cause elevated lead in water when installed, *Water research*, 46 (2012) 3240-3250.
- [18] A. Dudi, Reconsidering lead corrosion in drinking water: product testing, direct chloramine attack and galvanic corrosion, Doctoral dissertation, Virginia Tech, (2004).
- [19] Y. Zhang, Dezincification and brass lead leaching in premise plumbing systems: effects of alloy, physical conditions and water chemistry, Doctoral dissertation, Virginia Tech, (2009).
- [20] M. Salehi, X. Li, A.J. Whelton, Metal Accumulation in Representative Plastic Drinking Water Plumbing Systems, *Journal-American Water Works Association*, 109 (2017) 479-493.

- [21] D.A. Lytle, T.J. Sorg, C. Frietch, Accumulation of arsenic in drinking water distribution systems, *Environmental science & technology*, 38 (2004) 5365-5372.
- [22] C.E. Campbell, A.J. Whelton, R. Polera, A.M. Dietrich, The characteristics and chemical performance of polyethylene and poly (1-butene) pipes removed from a water distribution system, VWRRC Special Report SR43–2008, (2008) 1-13.
- [23] M.J. Friedman, A.S. Hill, S.H. Reiber, R.L. Valentine, G. Larsen, A. Young, G.V. Korshin, C. Peng, Assessment of inorganics accumulation in drinking water system scales and sediments, Water Research Foundation, Denver, (2010).
- [24] Z. Tang, S. Hong, W. Xiao, J. Taylor, Characteristics of iron corrosion scales established under blending of ground, surface, and saline waters and their impacts on iron release in the pipe distribution system, *Corrosion Science*, 48 (2006) 322-342.
- [25] J.M. Cerrato, L.P. Reyes, C.N. Alvarado, A.M. Dietrich, Effect of PVC and iron materials on Mn (II) deposition in drinking water distribution systems, *Water Research*, 40 (2006) 2720-2726.
- [26] G. Li, Y. Ding, H. Xu, J. Jin, B. Shi, Characterization and release profile of (Mn, Al)-bearing deposits in drinking water distribution systems, *Chemosphere*, 197 (2018) 73-80.
- [27] Plastic Pipe Institute, Proper Integration of Copper Tubing and Components with PP-R Piping Materials for Plumbing Applications, (2018).
- [28] Aquatherm Technical Bulletin, Mixing Copper Tubing and Aquatherm Piping, Aquatherm, (2012).
- [29] D. Tanemura, K. Yamada, H. Nishimura, K. Igawa, Y. Higuchi, Investigation of degradation mechanism by copper catalytic activity and mechanical property of polyethylene pipes for hot water supply, *Society of Plastic Engineers 2014*, (2014) 2022-2026.
- [30] G. Graeme, Expert opinion: performance of polyolefin (PP-R, PEX and PB) piping and fittings in recirculating hot water systems under Australian operating conditions, Queensland University of Technology, Brisbane, (2012).
- [31] D. Wright, Failure of plastics and rubber products: causes, effects and case studies involving degradation, iSmithers Rapra Publishing, (2001).
- [32] M. Chan, D. Allara, Infrared reflection studies of the mechanism of oxidation at a copper—polyethylene interface, *Journal of colloid and interface science*, 47 (1974) 697-704.
- [33] X. Huang, S. Zhao, M. Abu-Omar, A.J. Whelton, In-situ cleaning of heavy metal contaminated plastic water pipes using a biomass derived ligand, *Journal of Environmental Chemical Engineering*, 5 (2017) 3622-3631.
- [34] C.J.O. Childress, W.T. Foreman, B.F. Connor, T.J. Maloney, New reporting procedures based on long-term method detection levels and some considerations for interpretations of water-quality data provided by the US Geological Survey National Water Quality Laboratory. US Geological Survey Open-File Report, 99 (1999).
- [35] ASTM, B6-13, Standard Specification for Zinc, (2013).
- [36] S. Gonzalez, R. Lopez-Roldan, J.-L. Cortina, Presence of metals in drinking water distribution networks due to pipe material leaching: a review, *Toxicological & Environmental Chemistry*, 95 (2013) 870-889.
- [37] Indiana American Water, 2017 Annual Water Quality Report - West Lafayette Operations, in, American Water Works Company, (2017).
- [38] D.E. Kimbrough, Source identification of copper, lead, nickel, and zinc loading in wastewater reclamation plant influents from corrosion of brass in plumbing fixtures, *Environmental pollution*, 157 (2009) 1310-1316.

- [39] V. Rondeau, H. Jacqmin-Gadda, D. Commenges, C. Helmer, J.-F. Dartigues, Aluminum and silica in drinking water and the risk of Alzheimer's disease or cognitive decline: findings from 15-year follow-up of the PAQUID cohort, *American journal of epidemiology*, 169 (2008) 489-496.
- [40] World Health Organization (WHO), Barium in Drinking Water, WHO, (2004).
- [41] J. Liu, H. Chen, Q. Huang, L. Lou, B. Hu, S.-D. Endalkachew, N. Mallikarjuna, Y. Shan, X. Zhou, Characteristics of pipe-scale in the pipes of an urban drinking water distribution system in eastern China, *Water Science and Technology: Water Supply*, 16 (2016) 715-726.
- [42] M.C. Biesinger, L.W. Lau, A.R. Gerson, R.S.C. Smart, Resolving surface chemical states in XPS analysis of first row transition metals, oxides and hydroxides: Sc, Ti, V, Cu and Zn, *Applied Surface Science*, 257 (2010) 887-898.
- [43] M.C. Biesinger, B.P. Payne, A.P. Grosvenor, L.W. Lau, A.R. Gerson, R.S.C. Smart, Resolving surface chemical states in XPS analysis of first row transition metals, oxides and hydroxides: Cr, Mn, Fe, Co and Ni, *Applied Surface Science*, 257 (2011) 2717-2730.
- [44] P. Chagas, A.C. Da Silva, E.C. Passamani, J.D. Ardisson, L.C.A. de Oliveira, J.D. Fabris, R.M. Paniago, D.S. Monteiro, M.C. Pereira, δ -FeOOH: a superparamagnetic material for controlled heat release under AC magnetic field, *Journal of nanoparticle research*, 15 (2013) 1544.
- [45] C.K. Nguyen, Interactions between copper and chlorine disinfectants: chlorine decay, chloramine decay and copper pitting, *Doctoral Dissertation, Virginia Tech*, (2005).
- [46] D.M.F. Nicholas, Dezincification of brass in potable waters, *Urban Water Research Association of Australia*, (1994).
- [47] P. Sarin, V. Snoeyink, J. Bebee, W. Kriven, J. Clement, Physico-chemical characteristics of corrosion scales in old iron pipes, *Water Research*, 35 (2001) 2961-2969.
- [48] P. Westerhoff, Y. Yoon, S. Snyder, E. Wert, Fate of endocrine-disruptor, pharmaceutical, and personal care product chemicals during simulated drinking water treatment processes, *Environmental science & technology*, 39 (2005) 6649-6663.
- [49] G.V. Korshin, S.A. Perry, J.F. Ferguson, Influence of NOM on copper corrosion, *Journal-American Water Works Association*, 88 (1996) 36-47.
- [50] K.M. Kelley, A.C. Stenson, R. Dey, A.J. Whelton, Release of drinking water contaminants and odor impacts caused by green building cross-linked polyethylene (PEX) plumbing systems, *Water research*, 67 (2014) 19-32.
- [51] V. Lund, M. Anderson-Glenna, I. Skjevrak, I.-L. Steffensen, Long-term study of migration of volatile organic compounds from cross-linked polyethylene (PEX) pipes and effects on drinking water quality, *Journal of water and health*, 9 (2011) 483-497.
- [52] M.J. Lehtola, I.T. Miettinen, M.M. Keinänen, T.K. Kekki, O. Laine, A. Hirvonen, T. Vartiainen, P.J. Martikainen, Microbiology, chemistry and biofilm development in a pilot drinking water distribution system with copper and plastic pipes, *Water research*, 38 (2004) 3769-3779.
- [53] T. Gill, R. Knapp, S.W. Bradley, W. Bradley, Long term durability of crosslinked polyethylene tubing used in chlorinated hot water systems, *Plastics, Rubber and Composites*, 28 (1999) 309-313.
- [54] J. Coates, Interpretation of infrared spectra, a practical approach, *Encyclopedia of analytical chemistry*, 12 (2000) 10815-10837.

- [55] J.C. Montes, D. Cadoux, J. Creus, S. Touzain, E. Gaudichet-Maurin, O. Correc, Ageing of polyethylene at raised temperature in contact with chlorinated sanitary hot water. Part I– Chemical aspects, *Polymer degradation and stability*, 97 (2012) 149-157.
- [56] A.J. Whelton, A.M. Dietrich, D.L. Gallagher, Impact of chlorinated water exposure on contaminant transport and surface and bulk properties of high-density polyethylene and cross-linked polyethylene potable water pipes, *Journal of Environmental Engineering*, 137 (2011) 559-568.
- [57] K.N. Fotopoulou, H.K. Karapanagioti, Surface properties of beached plastic pellets, *Marine environmental research*, 81 (2012) 70-77.

CHAPTER 4. IN-SITU CLEANING OF HEAVY METAL CONTAMINATED PLASTIC WATER PIPES USING A BIOMASS DERIVED LIGAND

4.1 Introduction

Much of the aging U.S. drinking water infrastructure consists of metal components. Cast iron, copper, ductile iron, lead, galvanized iron and steel pipes, along with valves and appurtenances are some of the metal conveyance materials in use. A challenge with metal pipes is that they corrode and release heavy metals into drinking water such as Al, As, Cd, Cr, Cu, Fe, Mn, Pb and Zn. This is a concern because these compounds have health and aesthetic based drinking water standards. Also problematic is that metal scales can form on the inner pipe walls due to precipitation. Scales can decrease disinfectant residual meant to limit microbial growth, can provide surface area for biofilm growth, and scale constituents can adsorb other metals present (i.e., U, Ra-226 and As) [1-3]. Water chemistry and hydraulic changes can cause scale release and prompt an exceedance of primary or secondary drinking water standards. Because metal scales can affect drinking water quality, scale formation on metal water infrastructure materials has been studied.

As metal drinking water pipes near the end of their service-life, many are being replaced with plastic pipes. Plastic pipes are also being installed for new construction because they are inexpensive, do not corrode, and have estimated 20 year service-lives. An emerging body of evidence however indicates that plastic drinking water pipe surfaces can accumulate heavy metal scales [4-8]. A few studies have indicated that copper deposited on the plastic pipe surface can prompt polymer degradation and lead to premature failure [8-10]. Metals found on plastic water pipe surfaces have originated from upstream metal piping components, water treatment processes (i.e., $\text{Al}(\text{OH})_3$, FeCl_3 , KMnO_4) and drinking water sources. Several researchers have reported that

heavy metals deposited onto polyvinylchloride (PVC) and high density polyethylene (HDPE) water distribution plastic pipes (Table 4.1). To better control drinking water heavy metal concentrations, a better understanding of scale formation on plastic pipe is needed.

Table 4.1 Mass of metal deposits ($\mu\text{g/g}$ solid scale) found on plastic water distribution pipes

Metal	Type of Plastic Water Pipe ^[Reference]							DWS?
	PVC ^[11]	PVC ^[11]	PVC ^[11]	PVC ^[11]	PVC ^[4]	HDPE ^[12]	PVC ^[5]	
Al	1,906	1,025	2,329	574	19.72 w%	641	106	SMCL
As	13,650	1,416	7,842	2,008	nr	49.9	nr	MCL
Ca	22,939	28,859	4,455	3,541	1.29 w%	2,856	nr	-
Cd	<4.8	36	375	19	nr	34.1	35	MCL
Cr	nr	nr	nr	nr	nr	nr	35	MCL
Cu	nr	nr	nr	nr	nr	nr	35	AL
Fe	442,528	77,030	237,293	46,137	1.42 w%	5.5 w%	5,159	SMCL
Mg	1,492	1,736	442	371	0.1 w%	2,435	nr	-
Mn	5,142	290	1,267	1,143	6.12 w%	2,324	671	SMCL
Ni	6	110	137	30	nr	330	nr	-
Pb	210	4,667	9,681	2,009	0.96 w%	25.1	141	AL
Si	1,0452	8,719	4,074	5,420	19.26 w%	nr	nr	-
Zn	8,915	535,783	541,564	84,002	0.35 w%	1,846	1,873	SMCL

nr: stands for the value was not reported in the cited paper; “-“represents no drinking water standard (DWS) for the corresponding metal; SMCL is the secondary maximum contaminant level; MCL is the maximum contaminant level; AL is the action level; Lytle et al. (2004) examined pipe scales from four PVC samples at different locations [11].

Heavy metal accumulation on large diameter water distribution pipes (≥ 5.08 cm diameter) can be managed by *in-situ* mechanical, hydraulic, and chemical methods [13-15]. Although, methods for cleaning small diameter service line and building water pipes (< 5.08 cm diameter) have received little scrutiny. Mechanical and hydraulic cleaning approaches are extensively used for water distribution pipes, but can damage pipe surfaces and scales are not always removed [16, 17]. While water distribution pipes are commonly cleaned by flushing and mechanical scraping, small diameter water pipes pose unique challenges. Flowrates for small diameter pipes can be limited due to headloss, the presence of low-flow fixtures, and physical access can be difficult. Studies that report scale removal by chemical methods are limited. For one cement-lined ductile

iron pipe, a KMnO_4 solution coupled with flushing removed 72% to 96% of Hg [14]. Other researchers discovered that a greater amount of As was released from water distribution system solids, when water pH was increased from 7 to 9 [15, 18]. In addition, low pH water (< 3) showed effective desorption of Co from Fe particulates [19]. In one instance, citric acid has been recommended for cleaning copper pipes [20]. The cleaning process involved a pipe flush for 1.5 h with a warm 10% citric acid tap water solution, followed by a tap water rinse, and then pipe flush with a 10% NaHCO_3 tap water solution for another 1 h. Another chelating agent, ethylenediaminetetraacetic acid (EDTA), has also been proposed for removing radionuclides from water infrastructure [15], but no water pipe cleaning data were found in the literature. EDTA has been used for removing metals from contaminated soils, groundwater, urban and industrial sludge, wastewater, and hard surfaces (e.g., glass, ceramic, and metallic materials) [21], but it is reported as environmentally persistent [22].

Biomass derived agents show promise as water pipe cleaning agents because some of them have been used to remove and recover metals from wastewater and contaminated soils [23, 24]. These compounds are created from raw materials such as sawdust, algae, chitin, chitosan and lignin etc. [25, 26]. Especially, as an abundant and low-cost biomass waste, lignin can be depolymerized into various phenol derivatives (e.g., 2-methoxy-4-propylphenol, DHE). [27] Through reasonable chemical modifications, lignin derivatives could be converted to water soluble reagents that may be used for water pipe cleaning. For example, reaction of DHE with iminodiacetic acid via the Mannich reaction has the potential to enhance the synthesized ligand's water solubility and metal chelating capacity [28].

The study goal was to synthesize a lignin derived ligand and explore its effectiveness for removing heavy metals from plastic drinking water pipes. Plastic drinking water pipes were from

a one year old residential plumbing system. The specific research objectives were to 1) determine the Fe^{3+} -DHEL complex association constant and reaction stoichiometry, 2) quantify total heavy metal loading on the exhumed plastic pipe surfaces, 3) explore the DHEL heavy metal removal kinetics and performances, and 4) propose heavy metal-DHEL reaction mechanisms.

4.2 Materials and methods

4.2.1 Materials and conditions

A 10 mM Fe^{3+} stock solution was prepared using $\text{FeCl}_3 \cdot 6\text{H}_2\text{O}$ (> 99% for analysis; Sigma Aldrich, St. Louis, MO). Dihydroeugenol (DHE) ($\geq 99\%$; Sigma Aldrich, St Louis, MO), iminodiacetic acid ($\geq 98\%$; Sigma Aldrich, St Louis, MO), ethanol (200 proof; Decon Labs, Inc., King of Prussia, PA), and formaldehyde solution (37%; Macron Fine Chemicals, Center Valley, PA) were used without further purification. 0.1N HCl and 0.1N NaOH solutions were adopted to adjust the solution's pH. HNO_3 (TraceMetal™ Grade) was used for ICP-MS analysis and digestions. In addition, solutions were prepared by using deionized water (DI) and were adjusted to pH 7. All experiments were conducted at room temperature.

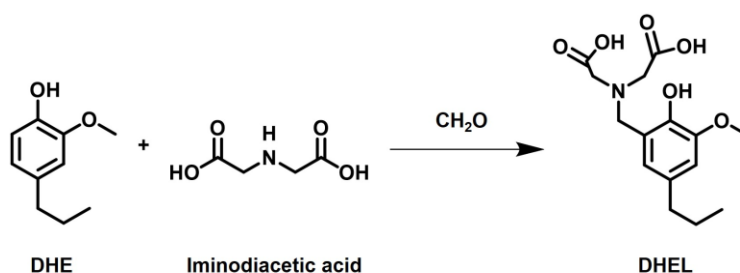
4.2.2 Equipment

An Accumet AB 150 pH/mV benchtop meter (Fisher Scientific, Pittsburgh, PA) was used to measure pH values. The Fe^{3+} -DHEL complex concentration was measured by a UV-vis spectrophotometer (Shimadzu UV-2700) by using the scanning mode. Metal concentrations were measured by inductively coupled plasma-mass spectrometry (ICP-MS) (Perkin Elmer II). The structure of DHEL was determined by nuclear magnetic resonance spectroscopy (NMR, Bruker Avance ARX-400 spectrometer), in which deuterated water was used as the solvent. Metal deposits of exhumed plastic pipe surfaces before and after decontamination process were examined by the field emission scanning electron microscopy-energy dispersive X-ray spectroscopy

(FESEM-EDS) (Hitachi S-4800 SEM, Japan). Pipe samples were coated with a thin layer of carbon under vacuum to increase the electrical conductivity [29].

4.2.3 Synthesis of lignin derived DHEL

A solution mixture of DHE (3.32 g, 20 mmol), iminodiacetic acid (2.92 g, 22 mmol), 37% aqueous formaldehyde (1.63 g, 20 mmol) and NaOH (1.6 g, 40 mmol) in H₂O/ethanol (1:2 v/v, 40 mL) was stirred and refluxed overnight. The reaction scheme is shown below (Scheme 4.1). The resulting white precipitate was collected via filtration. The substance was dried in an oven at 60 °C for 24 h and yielded DHEL as a white solid (5.3 g, 86% yield).



Scheme 4.1 Synthesis of DHEL

4.2.4 Bench scale metal-DHEL complexation experiment

Iron was selected for this study because it is one of the most abundant metals found on plastic drinking water pipe scales [5, 11]. In this experiment, Fe³⁺ was selected as the representative metal and it was hypothesized to chelate with the synthesized DHEL. The Fe³⁺-DHEL complex stability constant was determined through the Benesi-Hildebrand method [30]. A DHEL solution (50 mL of 1 mM) was prepared in a 100 mL beaker, another 50 mL of 1 mM FeCl₃ solution was filled in a 50 mL burette for titration. Various volumes of the metal solution were titrated into the DHEL solution. After solutions were mixed, the pH was adjusted at the pre-determined values (i.e., pH 4 or 7). In addition, the volume of titrated metal solution was recorded and the Fe³⁺-DHEL complex absorbance was measured using a UV spectrophotometer.

With the assumption of 1:1 stoichiometry (Fe: DHEL), the adopted Benesi-Hildebrand equation used was [31, 32]:

$$\frac{1}{A - A_0} = \frac{1}{K_f(A_{max} - A_0)[Fe^{3+}]} + \frac{1}{A_{max} - A_0}$$

where A represents the absorbance of Fe³⁺-DHEL complex during continuous titration of Fe³⁺ solution, A₀ is the absorbance of the original DHEL solution without Fe³⁺ solution added, A_{max} is the maximum absorbance during the continuous titration experiment, K_f is the association constant (M⁻¹) and [Fe³⁺] represents the added Fe³⁺ concentration. Then the graph could be generated as 1/(A-A₀) vs 1/[Fe³⁺]. Through linear fit, the association constant (K_f) would be determined from the slope ($K_f = \frac{1}{slope \times (A_{max} - A_0)}$).

The method of continuous variation was performed to generate a Job's plot to determine the stoichiometry of Fe: DHEL binding. The same concentration of DHEL (1 mM) and FeCl₃ (1 mM) was prepared for these experiments and the total volume of the mixture was set to be 10 mL. The volume ratio between DHEL and Fe solutions was varied from 0.1 to 0.9 and the complex absorbance value was recorded for each condition. After placing the certain parts of Fe³⁺ and DHEL solutions in the 50 ml centrifuge tube, the tube was vigorously mixed by shaking. After mixing, the solution pH was adjusted to 4 and 7.

4.2.5 Performance of DHEL to remove heavy metals from exhumed pipes

DHEL metal removal performance was examined using a one year old, 1.91 cm diameter, and 1.22 m long PEX pipe. This pipe represented the buried water service line removed from the single-family residential property located in Indiana, USA. While other indoor plumbing PEX pipes were also removed as part of a parallel study, preliminary experiments indicated that the service line contained the greatest loading of metals [33]. Cu, Fe, Pb, Zn and a variety of other

metals found on the pipe surface were also present in the drinking water. In the present study, the service line PEX pipe was used for all kinetic and other metal removal experiments. Before use, the pipe was triple rinsed with deionized water (DI) to remove loose debris.

Experiments were conducted to determine DHEL metal removal kinetics and to determine if DHEL concentration influenced metal removal efficiency. Pipe segments were cut into 3 cm length and all solutions were adjusted to pH 7. After filling pipe segments with the dilute DHEL-DI water solution or control water (DI only), each pipe was plugged with Teflon[®] wrapped silicon stoppers. Metal removal kinetics were examined for 0.1 mM, 1 mM, and 5 mM DHEL concentration, during a 7 day period. For each DHEL level, eight pipe segments were prepared. Periodically, the pipe segment was sacrificed and the water sample's volume and pH was characterized. Water samples were acidified using HNO₃ and removed metal concentrations were analyzed by ICP-MS. The remaining metals on each pipe segment was determined by filling pipes with 2.5 % of HNO₃ and allowing stagnation for a minimum of 48 h. The experimental data was used to fit kinetic models stated as following:

First order kinetic model [34, 35]:

$$\frac{m_t}{m_0} = e^{-k_{R1}t}$$

$$1 - \frac{m_R}{m_0} = e^{-k_{R1}t}$$

$$\text{Metal removal \%} = 1 - e^{-k_{R1}t}$$

Where m_t is the remaining metals on the plastic segment at time t , m_0 is the total amount of metals detected on exhumed plastic pipe's inner wall at time zero, k_{R1} is the first order metal removal rate constant (h^{-1}), m_R is the amount of removed metals from plastic pipe surfaces and Metal removal % = $\frac{m_R}{m_0} \times 100\%$.

Second order kinetic model [36, 37]:

$$\frac{m_t}{m_0} = \frac{1}{\beta_2 + k_{R2}t}$$

$$1 - \frac{m_R}{m_0} = \frac{1}{\beta_2 + k_{R2}t}$$

$$\text{Metal removal \%} = 1 - \frac{1}{\beta_2 + k_{R2}t}$$

Where β_2 and k_{R2} are the second order kinetic metal removal constant and rate (h^{-1}), respectively.

By plotting Metal removal % vs time and fitting kinetic models, k_{R1} and k_{R2} should be obtained.

The DHEL performance was evaluated over a range of concentrations (i.e., 0.01-10 mM) during a 7 day period at pH 7. Under each condition, triplicate pipe segments were used. Water and pipe samples were acidified and analyzed as stated in the kinetic experiment. ICP-MS calibration curves were developed for a total of 19 metals. For the more abundant elements (Ca, Fe, Mg, Na and P), the concentration range was set from 25 to 1000 ppb, whereas, other metals (Al, As, Be, Cd, Co, Cr, Cu, Hg, Mn, Ni, Pb, Se, V and Zn) the concentration range was 5 to 200 ppb. The recovery percentage for all metals was $\geq 85\%$. All calibration curves had regression coefficient R^2 values of > 0.98 .

4.2.6 Statistical analysis

NCSS statistical software was applied to conduct the single factor one way analysis of variance (ANOVA) and multivariate analysis of variance (MANOVA) in order to examine interaction effects. The significant level of all data set was set as 0.05. For each experimental condition, arithmetic mean and standard deviation values were reported.

4.3 Results and discussion

4.3.1 Characterization of DHEL structure

^1H and ^{13}C NMR spectra revealed DHEL's chemical structure (Figure 4.1). The proton peak at 3.9 ppm corresponded to the methylene linkage (f), which indicated successful DHE coupling with iminodiacetic acid (Figure 4.1 (A)). Aromatic protons were found at 6.5 and 6.7 ppm. The methylene groups (d) connecting to carboxylic acid were observed at 3.3 ppm, while DHE's methyl and propyl groups were found at 3.7, 2.3, 1.4 and 0.8 ppm, respectively. The appearance of characteristic methylene linkage (f) was also confirmed by ^{13}C NMR. This linkage was detected at 55.5 ppm (Figure 4.1 (B)). Carboxylic acid, methylene (d) and methoxy were also observed at 176.1, 57.3 and 56.5 ppm, respectively.

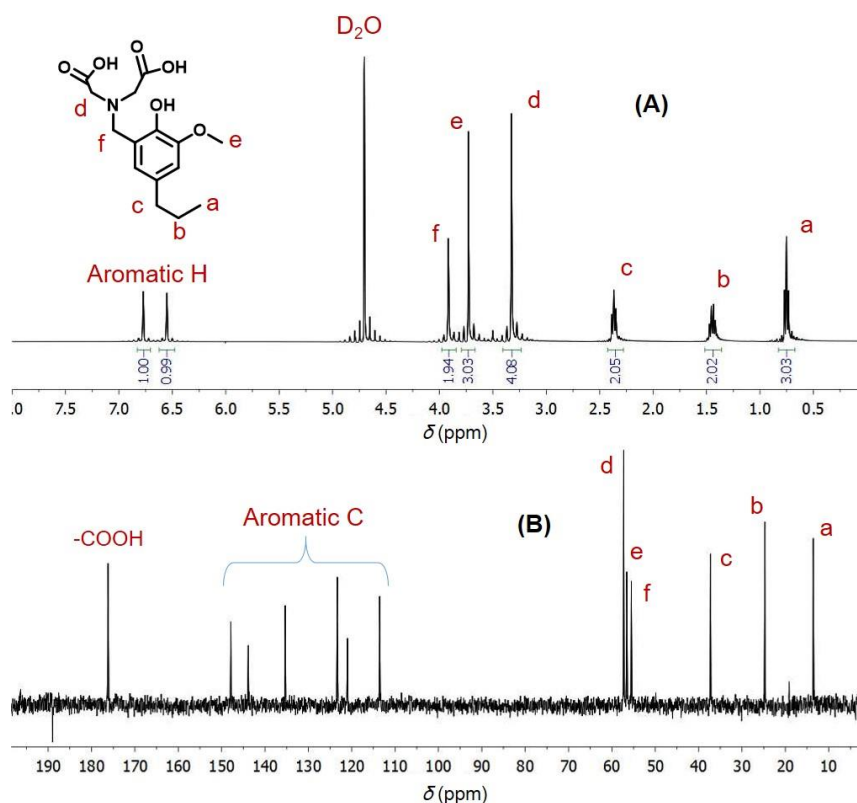


Figure 4.1 Proton and carbon NMR spectra of DHE based DHEL.

4.3.2 Fe^{3+} -DHEL complex stability constant and binding ratio

Results showed that Fe^{3+} (ranged from $1.96 \times 10^{-5} M$ to $5.83 \times 10^{-4} M$) bound with DHEL and pH conditions did not significantly affect the complex's stability (Figure 4.2 (b) and (d)). According to the Benesi-Hildebrand equation, the K_f values obtained for pH 4 and pH 7 were $(2.25 \pm 0.07) \times 10^3 M^{-1}$ and $(2.14 \pm 0.10) \times 10^3 M^{-1}$, respectively. UV spectra indicated that upon continuous titration of Fe^{3+} , the peak absorbance gradually increased until the molar ratio of Fe^{3+} and DHEL was close to 1:1 (Figure 4.2 (a) and (c)). This observation inferred the potential reaction stoichiometry, and no shift in maximum wavelength was detected.

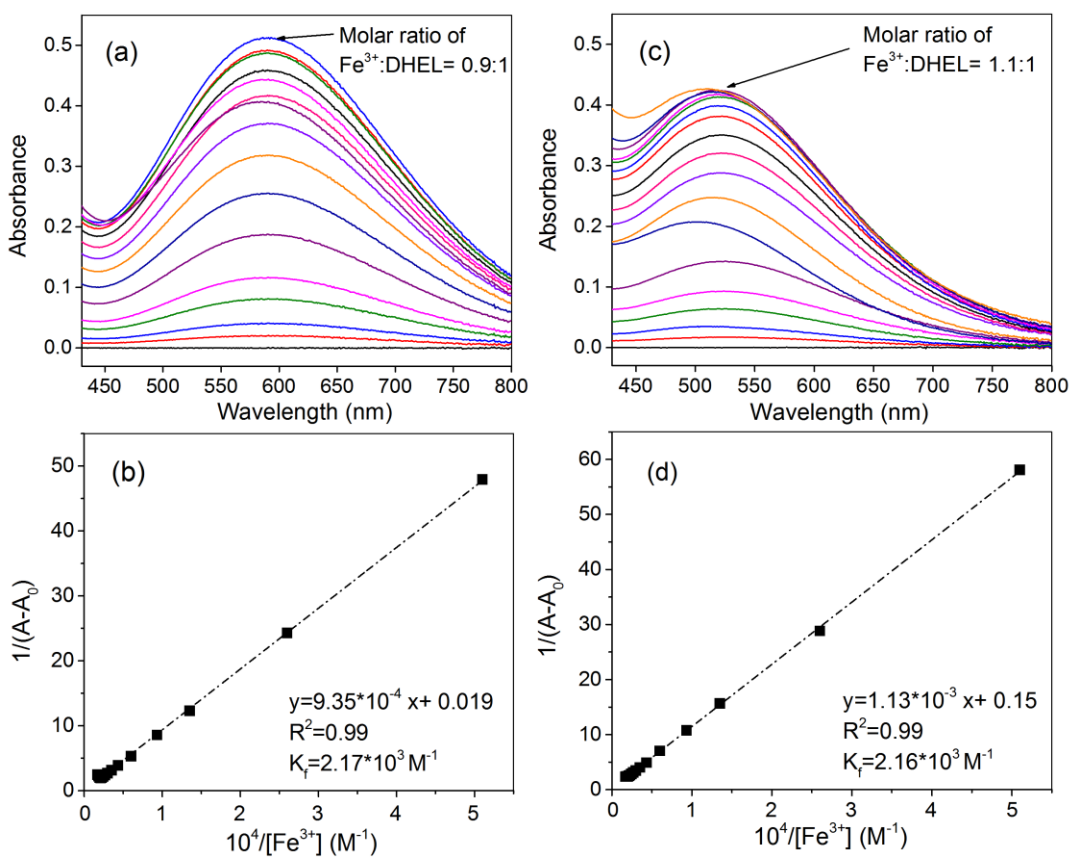


Figure 4.2 UV-spectra of Fe^{3+} -DHEL complex upon increasing of $[Fe^{3+}]$ at pH 4 (a) and pH 7 (c); Benesi-Hildebrand plot of DHEL with Fe^{3+} at pH 4 (b) pH 7 (d).

Job's plot experiments confirmed the 1:1 reaction ratio between Fe and DHEL at pH 4 and pH 7. As shown in Figure 4.3, the maximum absorbance at 588 nm and 523 nm wavelength for pH 4 and pH 7 was plotted against the DHEL mole fraction. The peak absorbance value was observed when the molar fraction value was 0.5 which indicated a 1:1 reaction ratio. A 1:1 stoichiometry of Fe: ligand complex has been found in other studies in the aqueous phase [38, 39]. However, the magnitude of association constants in the literature varied (10^3 vs. 10^{20}) likely because of ligand property and experimental condition differences (i.e., solvent solution, temperature and pH). In the present work, absorbance values shifted upward (i.e., when ligand mole fraction < 0.5) for the pH 7 condition compared to the pH 4 condition. This shift likely occurred due to the formation of iron hydroxides or oxides in solution at greater pH (i.e., FeOH^{2+} , $\text{Fe}(\text{OH})_{2(s)}$, $\text{Fe}(\text{OH})_3$). Because the ionic radii for iron hydroxides and oxides were greater than ferric ion's radius, this may have retarded the Fe and DHEL reaction [40].

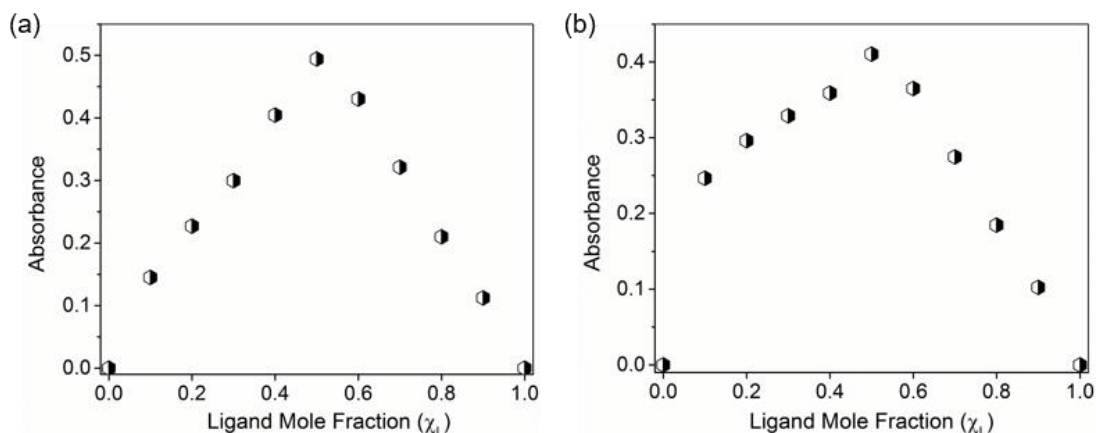


Figure 4.3 Job's plot of a 1:1 Fe-DHEL complex at a) pH 4 and b) pH 7, where the absorbance was measured at 588 nm and 523 nm, respectively.

4.3.3 Variation of metal loading on the service line plastic pipe material

Total metal loadings differed across pipe segment samples, which indicated metal loadings differed down the length of the service line pipe (probability value, $p < 0.01$) (Figure 4.4). The metal's abundance found in the plastic pipe scale was: $\text{Fe} > \text{Mn} > \text{Ca} > \text{Zn} > \text{Mg}$, $\text{Cu} > \text{Pb} > \text{Al}$.

While P is not a metal, a notable amount of P ($19.13 \pm 3.25 \mu\text{g}/\text{dm}^2$) was also detected in the scale and is likely due to the orthophosphate/polyphosphate blend corrosion inhibitor added by the local water utility to treated drinking water. The metals detected in the current work were similar to those found by others. Liu et al. (2016) found the most abundant heavy metals on a PVC water distribution system pipe scale were $\text{Fe} > \text{Zn} > \text{Mn} > \text{Pb} > \text{Al} > \text{Cu}$ [5]. Cerrato et al. (2006) also found Fe and Mn were present on PVC water distribution pipe scale, but Mn was in greater abundance [4]. For the present study, the water distributed by the water utility contained low levels of Fe (0.05 mg/L) and Mn (0.02 mg/L) exiting the water treatment plant [41]. In addition, drinking water that entered the building was very hard (248 to 416 mg/L as CaCO_3). As a result, Ca, Fe, Mg and Mn from the plastic pipe scales likely originated from the source water. Other metals (Al, Pb and Zn) detected on plastic pipe surfaces, as well as additional amount of Fe and Mn, were likely released from water conveyance components (i.e., pipes, fixtures and fittings). The reasons for unequal metal deposits on the plastic service line remain unclear and no studies were found that explained this phenomenon in much detail. Unequal metal deposits on the service line could be due to hydraulic condition changes (i.e., hydraulic force and residence time), pipe surface morphology (i.e., scratches and oxidative condition), and biofilm activity. Additional work should be considered to examine scale formation on plastic pipe surfaces.

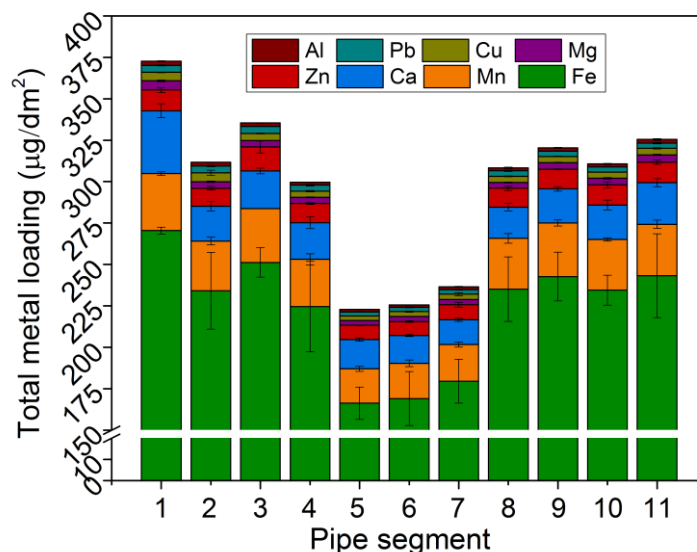


Figure 4.4 Total metal loading along the same length of exhumed PEX-A pipes: initial pH was 7; error bars are representing standard deviations from triplicate 3 cm length pipe segments.

4.3.4 Preliminary test and SEM-EDS analysis of DHEL interaction with exhumed plastic pipe

A screening experiment was conducted to determine DHEL's heavy metal removal effectiveness. Triplicate pipe segments were exposed to solutions and the DHEL concentration was varied from 0 to 5 mM. The exposure duration was up to 48 h. After the exposure procedure, the exhumed pipe segments were visually observed to be scale-free for experimental groups, but deposits were still visible for the control group (Figure 4.5). SEM images and accompanying EDS spectra of the original exhumed plastic pipe surfaces and after decontamination process were compared in Figure 4.6. The SEM image indicated that DHEL removed most metal deposits (Figure 4.6 (a) and (b)). The original metal deposits were mainly shown as aggregates, whereas, the size of remaining metals on plastic pipe surface was much smaller after decontamination procedure. Further confirmation of DHEL's effectiveness was found by EDS analysis (Figure 4.6 (c) and (d)). Results showed that, the most abundant element was C, followed by O, which was mainly due to the polymer properties and the metal forms on the plastic surface (i.e. oxides), respectively. After decontamination, the peak intensity for metals (i.e., Fe) was much less than

those before DHEL exposure. Ca and Zn were not detected after DHEL treatment. Based on these observations, additional tests were conducted to explore reaction kinetics and evaluate DHEL removal effectiveness.

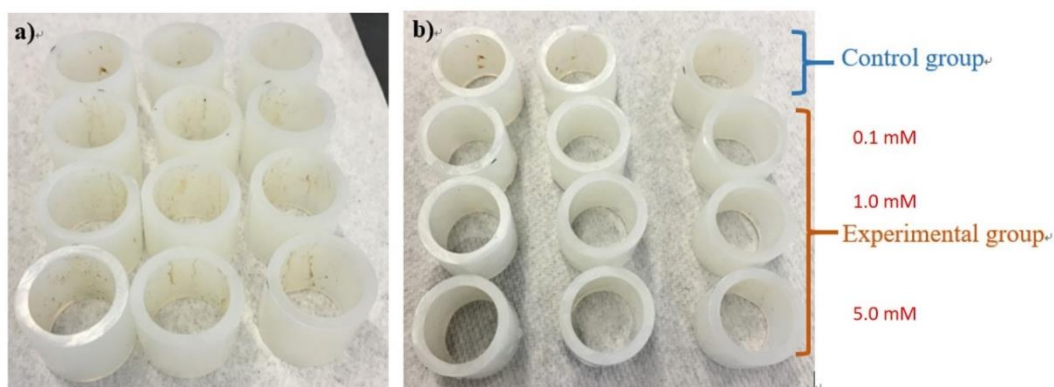


Figure 4.5 Cross-section images of one year old PEX-A potable water pipe segments removed from residential plumbing: a) original, b) after treated with biomass derived DHEL.

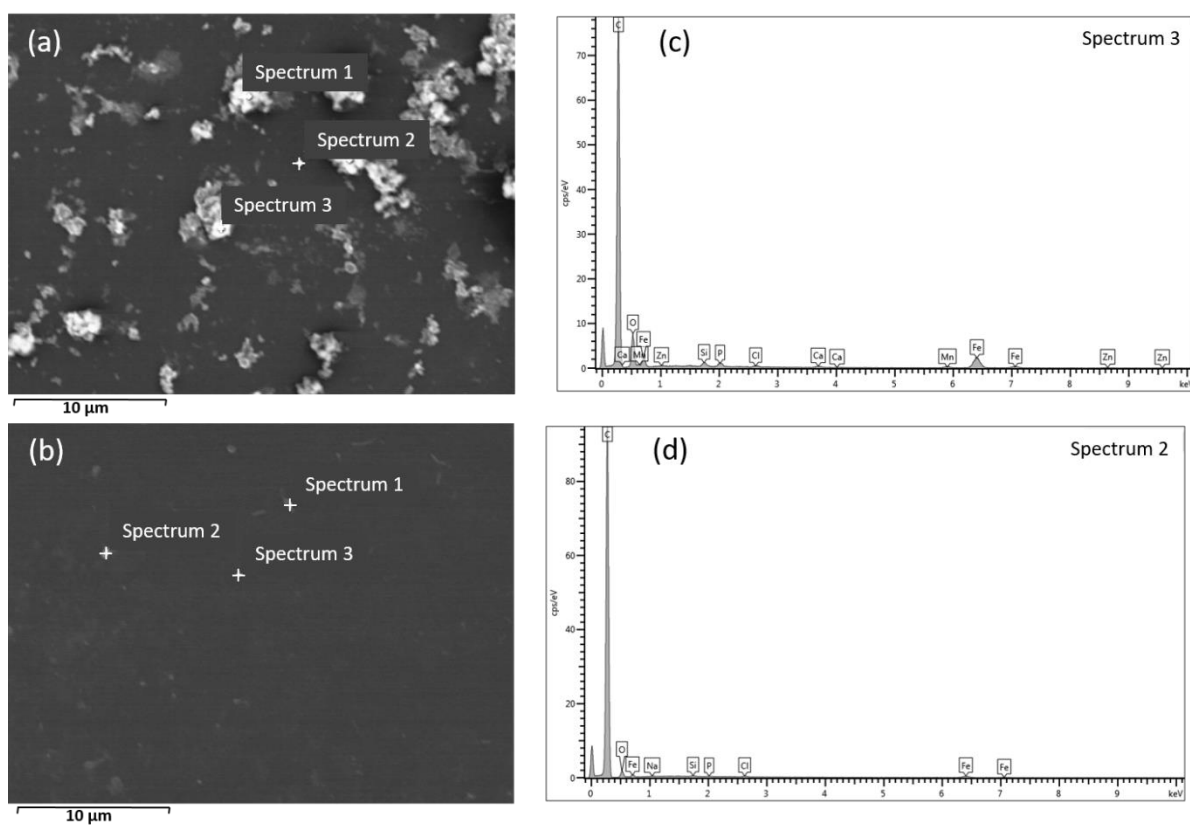


Figure 4.6 SEM and EDS analysis of metals on exhumed plastic pipe surfaces: (a) and (b) SEM images, (c) and (d) EDS analysis before and after decontamination process (i.e., 5 mM DHEL for 48 h).

4.3.5 Kinetic study of DHEL interaction with exhumed plastic pipe

Kinetic study results showed that the DHEL solution exposure time and DHEL concentration significantly influenced metal removal from pipe segments (Figure 4.7). DHEL's performance was examined for five target metals: Cu, Fe, Mn, Pb, and Zn. These metals were chosen based on their abundance on the pipe segments and they had U.S. drinking water standards. Considering the unequal distribution of heavy metals along the pipe (refer to section 3.3), the metal removal % ($\frac{mass_{removed}}{mass_{original}} \times 100\%$) was adopted instead of the metal loading ($\mu\text{g}/\text{dm}^2$). As shown in Figure 4.7, for the first 80 h, the DHEL metal removal rate was the greatest for all metals and then it's decreased with time. By day 7, the 5 mM DHEL concentration removed $\geq 95\%$ of Cu Fe, Mn, Pb and Zn from the pipe surface. Among five target metals, Fe, Mn, and Pb exhibited similar removal behavior ($p = 0.64$) vs Zn and Cu ($p = 0.43$) (Figure 4.7). The DHEL was more favorable for Cu and Zn rather than Fe, Mn, and Pb, even though Cu and Zn were not the most abundant metals present on the pipe surface (Figure 4.4). Under the control condition (DI only, no DHEL), except for Zn (about 30% released into the water), less than 5% of the total metals were released.

Both first and second kinetic models were fitted and compared with the experimental data (Figure 4.7). In general, both kinetic models had a good agreement with Fe, Mn and Pb metal removal data (R^2 was as high as 0.99). However, Cu and Zn data fitted poorly with kinetic models and may be due to the rapid release of metals into the water. The first and second order kinetic parameters and the corresponding R^2 are presented in Table 4.2. More specifically, when DHEL concentration was high (i.e., 5.0 mM), the first order kinetic model showed the better fit than and second order kinetic model. Whereas, the second order kinetic model could represent the data better within the lower range of DHEL concentrations (i.e. 0.1mM and 1.0 mM).

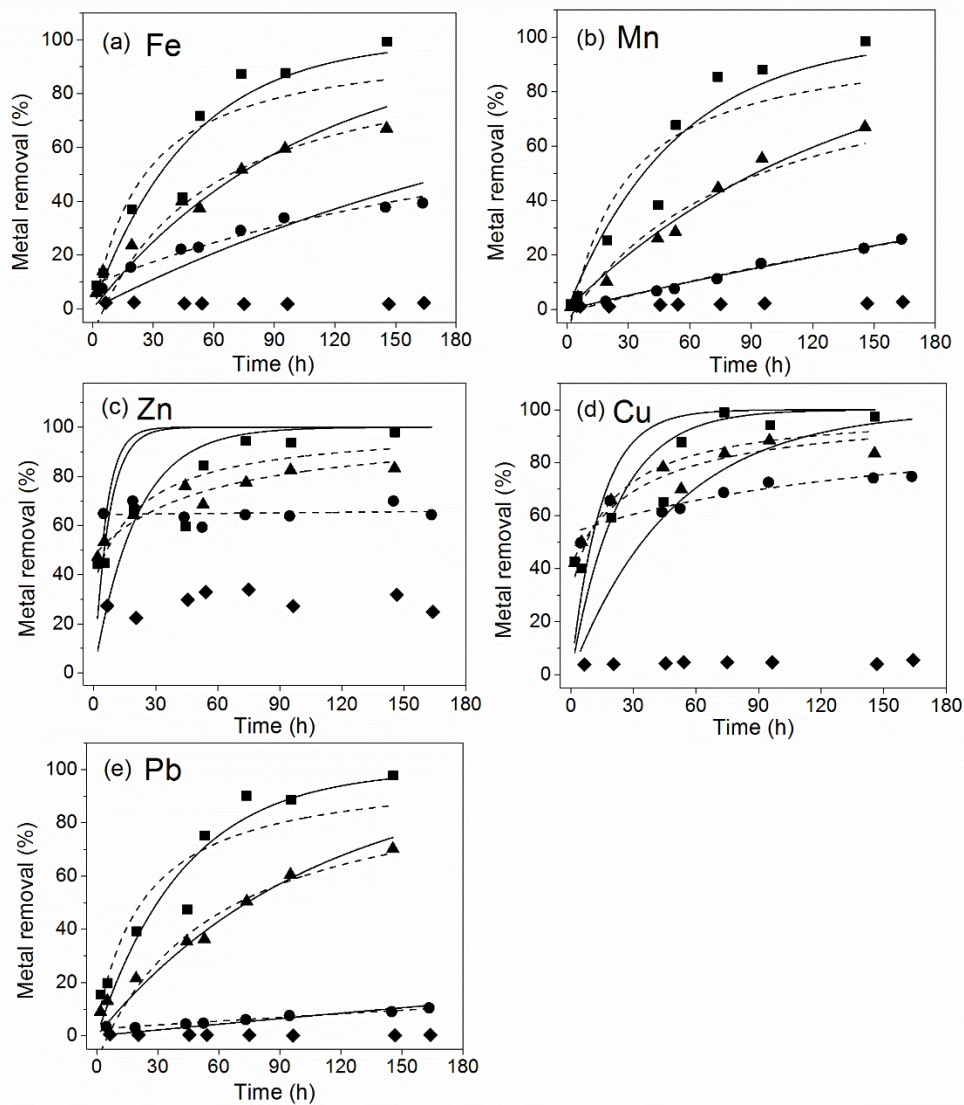


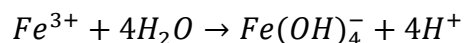
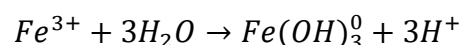
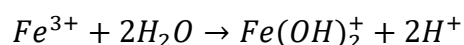
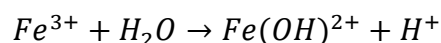
Figure 4.7 Percentage of metal removed kinetic test (7 days) a) Fe, b) Mn, c) Zn, d) Cu, e) Pb: room temperature at 22 ± 1 °C ; initial pH was 7; (◆) blank, (●) 0.1 mM, (▲), 1 mM, (■) 5mM. (—) first kinetic model fit, (---) second kinetic model fit.

Table 4.2 Kinetic parameters and regression coefficients for DHEL metal removal from exhumed plastic pipe.

Target metals and conditions		First order kinetic fit		Second order kinetic fit	
Metals	DHEL Conc. (mM)	k_{R1} (h^{-1})	R^2	k_{R2} (h^{-1})	R^2
Fe	0.1	0.23	0.67	0.23	0.96
	1.0	0.57	0.92	0.96	0.98
	5.0	1.25	0.94	2.40	0.87
Mn	0.1	0.11	0.99	0.13	0.99
	1.0	0.45	0.99	0.66	0.95
	5.0	1.11	0.95	2.11	0.87
Pb	0.1	0.04	0.63	0.03	0.97
	1.0	0.56	0.95	0.94	0.98
	5.0	1.40	0.92	2.62	0.87

4.3.6 DHEL metal removal performance with exhumed plastic pipes

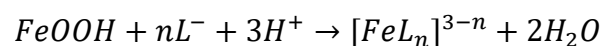
DHEL's metal removal performance agreed well with kinetic experiment observations where two different behavior groups were identified: Fe, Mn and Pb ($p = 0.77$) and Cu and Zn ($p = 0.33$) (Figure 4.8). DHEL was more favorable to removing Cu and Zn than Fe, Mn and Pb. For the low range DHEL concentrations (i.e., <5 mM), metal removal efficiency increased as the amount of DHEL increased. However, when DHEL concentrations exceeded 5 mM, metal removal efficiency ($\geq 95\%$) did not increase further. This phenomenon is likely due to the fact that when DHEL concentration reached 5 mM, a maximum amount of metals had been removed; above 5 mM, DHEL became the excess reagent. In addition, during the pipe exposure experiment, the final pH ranged from 6.3 to 7.3 (Figure 4.8) depending on DHEL concentration. The lower final pH value (pH <7) likely resulted from Fe^{3+} hydrolysis of the scale that released protons into the solution (i.e. Fe^{3+}) [42]:



Or the reaction of ions with hydroxide [43]:



However, $pH > 7$ could be explained by the ligand promoted mineral dissolution process where H^+ was acting as the reactant (i.e., $FeOOH$), where L stands for the ligand [44]:



The favorability of DHEL for Cu and Zn may have been influenced by the metal's ionic radius, absolute electronegativity, and complex stability. For metal cations, according to the charge-to-radius ratio (Z/r), the favorability sequence was expected to be Fe^{3+} (4.69) $>$ Fe^{2+} (3.28) $>$ Cu^{2+} (2.74) \approx Zn^{2+} (2.70) $>$ Mn^{2+} (2.50) $>$ Pb^{2+} (1.55) [45, 46]. Except for Fe, the observed metal favorability was proportional to the Z/r ratio. Metal ions with higher absolute electronegativity would have a stronger attraction to the lone pair electrons in the functional groups (i.e., $-COOH$ and $-OH$). This might have led to the observed higher favorability. Pearson (1988) calculated the absolute electronegativity of metal cations as Fe^{3+} (42.73 eV) $>$ Zn^{2+} (28.84 eV) \approx Cu^{2+} (28.56 eV) $>$ Pb^{2+} (26.18 eV) $>$ Mn^{2+} (24.66 eV) $>$ Fe^{2+} (23.42 eV) [47]. Except for Fe^{3+} , the work of Pearson (1988) also agrees with the observed DHEL metal favorability in the present study.

The metal complex stability constant is another factor that could impact ligand favorability. Irving and Williams (1953) examined complex stability constants for a number of natural or synthetic ligands and concluded the general order as $Mn < Fe < Co < Ni < Cu, > Zn$ [48]. However, as one of the most common used metal chelators, metal-EDTA complex stability was found to be Fe^{3+} (25.00) $>$ Cu^{2+} (18.70) $>$ Pb^{2+} (17.88) $>$ Zn^{2+} (16.44) $>$ Mn^{2+} (13.56) [49]. Metal ligand complex formation is a complicated process, which cannot be predicted from only considering Z/r , electronegativity, or complex stability. Other factors that could influence metal removal from the plastic pipe are ionic radii, the replacement of water by more polarized ligand molecules, metal

coordination states and orbital theory [48]. Furthermore, the form of metal and hydrolyzed metal species on the plastic pipe surface or in the aqueous solution could also have influenced the result. For instance, under the certain circumstances (i.e., pH 5.5 and initial metal concentration as 100 mM), Bhattacharyya (1998) found Pb was about 50% Pb^{2+} and 40% $[Pb_4(OH)_4]^{4+}$, whereas, Cu was about 80% Cu^{2+} and 20% $[Cu_2(OH)_2]^{2+}$ [50]. The presence of different metal species in solution could potentially affect metal-ligand complex formation, reaction molar ratio and bonding capacities. Additional work should be considered to isolate which factors are most significant on influencing metal removal from plastic pipe surfaces.

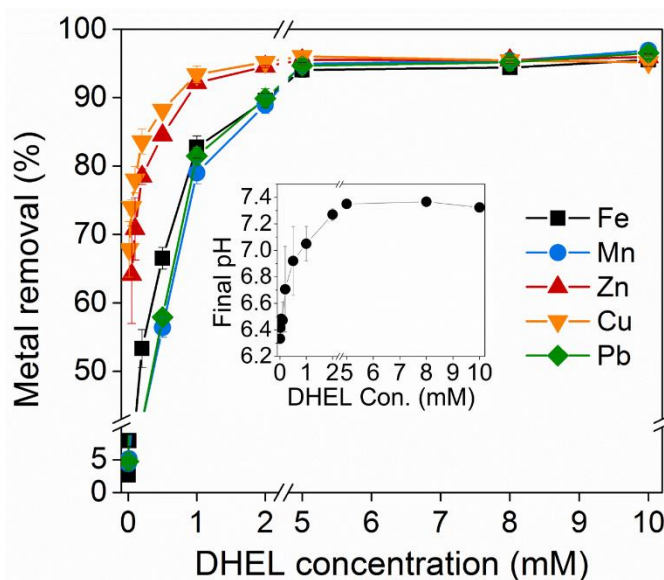


Figure 4.8 DHEL performance test as showing the percentage of metal removed from the pipe inner surface, 7 day exposure period: 22 ± 1 °C; initial pH 7; error bars represent standard deviation for triplicates

4.3.7 Relationship between total metal loading and total metal removed on pipe segments

The total metal removed by DHEL from each pipe segment was directly correlated to the initial metal loading on pipe segments, but this was not the case for the control group (no DHEL added) (Figure 4.9). Linear regression analysis showed correlation coefficients of 0.93 or greater when DHEL was present (Figure 4.9 (b)). In the absence of DHEL, the amount of metal leached

into the water was not correlated to the total metal loading (Figure 4.9 (a)). Only a noticeable amount of Zn ($R^2=0.95$) leached into control water from the exhumed plastic pipe surface.

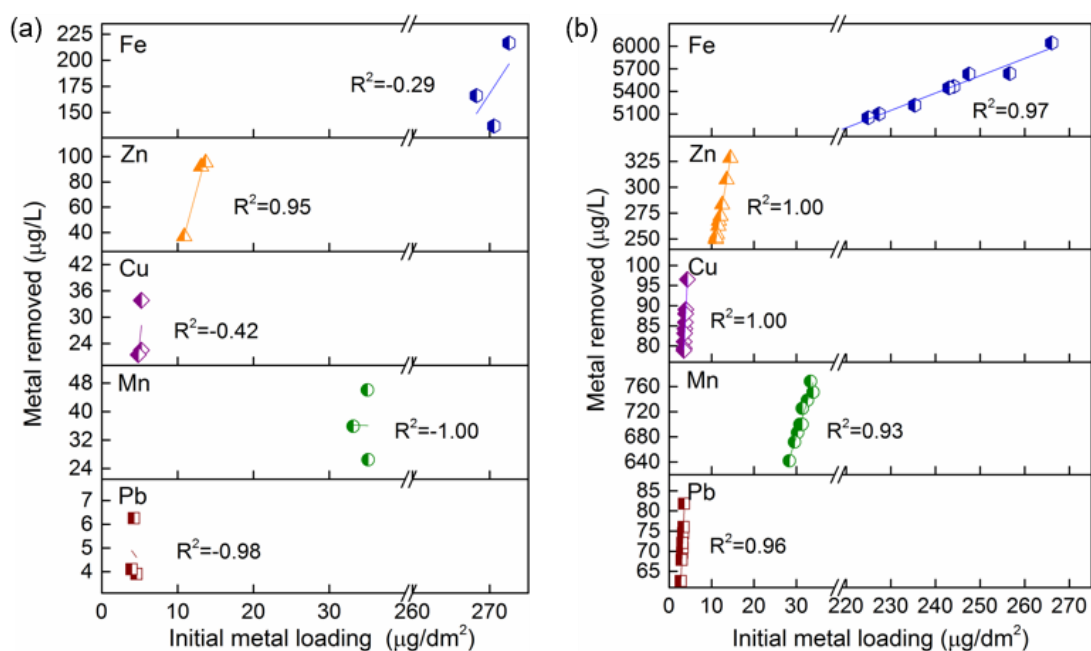


Figure 4.9 The correlation between metal desorption with amount of metal loadings (7 days): (a) blank group, (b) DHEL dosages varied from 5 mM to 10 mM: 22 ± 1 °C; initial pH 7.

4.3.8 Proposed reaction mechanism

Results from the present study indicate that plastic service lines can accumulate heavy metals on their surface, and the deposited metals were successfully removed by short-term exposure to a DHEL solution. While metal speciation and forms were not examined in this work, metal deposits found on metal drinking water pipes have been reported to contain Cu_2O , $\alpha\text{-FeOOH}$, Fe_3O_4 , MnO_2 , PbCO_3 and ZnO [51, 52]. Soluble metal forms coupled with minerals are also expected to be found on or releasing from the exhumed plastic pipes. Like past metal pipe scale characterization studies, additional work is needed to understand forms of metal deposits that are most common for plastic pipes.

The factors that control metal adsorption and release from plastic pipe surfaces have received limited scrutiny, but DHEL effectively removed metal deposits from the pipe surface. Past studies

have reported that aged plastics adsorbed higher amount of metals than new plastics [6, 33]. These phenomena have been hypothesized to occur due to increased surface porosity and presence of oxygen functional groups, as well as negatively charged plastic surface having induced metal ion adsorption and coprecipitation. Additional work is needed to further understand the mechanism of metal accumulation onto plastic drinking water pipes and effects of various water and hydraulic conditions (i.e., natural organic matter, hardness, flow velocity and pressure).

Several researchers have proposed that metal oxide dissolution can occur by proton-promoted, ligand-promoted, reductive, and synergistic pathways [53, 54]. Compared with proton-promoted dissolution, the rate of ligand-promoted dissolution process has been reported to be faster. Water pH, ionic strength, and the presence of organic ligands are some key factors which could significantly influence metal oxide solubility in the solution. Because experiments in the present study were conducted at pH 7, both the proton-promoted and reductive dissolution could be neglected [55]. Considering only a single type of ligand (i.e., DHEL) was examined, the synergistic pathway where multiple ligands act could be ignored. As stated above, the ligand-promoted minerals dissolution pathway should be the dominant mechanism that controls DHEL to remove metal deposits from exhumed plastic pipes. In addition, considering soluble metals that released from pipe scales, we also proposed the ligand-metal complex formation pathway. The complex formation process can through consuming metal ions in the solution to drive the minerals' dissolution process further (Figure 4.10).

Based on the literature, the following steps during the ligand-promoted mineral dissolution process were likely occurring [54]: (1) formation of surface complex, (2) detachment of the complex from mineral surface, and (3) re-adsorption of ligand on the oxide surface through ligand exchange mechanism. While ligand-mineral binding phenomena in solution phase has been

examined by others, the interactions between minerals, ligands, and plastic pipe has not been addressed.

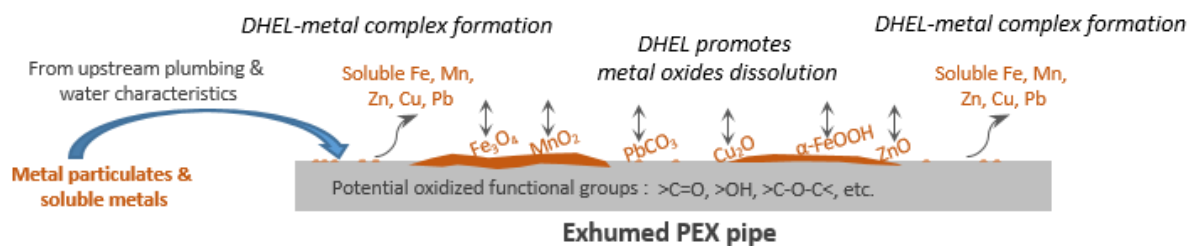


Figure 4.10 Proposed DHEL metal removal mechanism from exhumed plastic pipe.

4.4 Conclusion

In the current study, a biomass derived ligand (DHEL) was synthesized and used to remove heavy metals from exhumed plastic materials. First, the interaction of DHEL and Fe^{3+} was studied. The DHEL- Fe^{3+} complex constant was estimated to be $(2.25 \pm 0.07) \times 10^3 \text{ M}^{-1}$ and $(2.14 \pm 0.10) \times 10^3 \text{ M}^{-1}$ at pH 4 and 7 and a 1: 1 stoichiometry between DHEL and Fe was discovered. Characterization of plastic pipe surface revealed unequal metal distributions along the same length of exhumed plastic pipe. Fe was present in the greatest abundance, followed by Mn, Ca, Zn, Mg, Cu, Pb and Al. SEM-EDS analysis confirmed DHEL removed heavy metal deposits from the surface of exhumed plastic pipes. Further experiments (i.e., DHEL metal removal kinetic and performance evaluation) confirmed that when DHEL was $\geq 5 \text{ mM}$, more than 95% of target metals (i.e., Cu, Fe, Mn, Pb and Zn) could be removed. More specifically, the first order kinetic model fitted better for the higher DHEL concentration (i.e., 5 mM). In addition, DHEL showed higher favorability for Cu and Zn than Fe, Mn and Pb. A good correlation ($R^2 \geq 0.93$) between metal removal and total metal loadings supports the hypothesis that DHEL efficiently removed metals from exhumed plastic pipes. Two metal removal mechanisms were also hypothesized and include: (1) ligand-promoted mineral dissolution, and (2) formation of ligand-metal complexes. Work is

needed to identify the factors that control heavy metal accumulation onto plastic pipes. In addition, the types, amount, and speciation of metals on plastic water pipe surfaces should be considered for characterization in the future work. While the ligand-mineral binding phenomena in solution phase has been examined by others, the interactions between minerals, ligands, and plastic pipe has not been addressed. Understanding the application of biomass derived ligands as a cleaning agent for water infrastructure deserves further study.

4.5 References

- [1] L.S. MCNEILL, M. Edwards, Iron pipe corrosion in distribution systems, *Journal of the American Water Works Association* 93 (2001) 88-100.
- [2] Y. Zhu, H. Wang, X. Li, C. Hu, M. Yang, J. Qu, Characterization of biofilm and corrosion of cast iron pipes in drinking water distribution system with UV/Cl₂ disinfection, *Water Research* 60 (2014) 174-181.
- [3] Z. Zhang, J.E. Stout, L.Y. Victor, R. Vidic, Effect of pipe corrosion scales on chlorine dioxide consumption in drinking water distribution systems, *Water Research* 42 (2008) 129-136.
- [4] J.M. Cerrato, L.P. Reyes, C.N. Alvarado, A.M. Dietrich, Effect of PVC and iron materials on Mn (II) deposition in drinking water distribution systems, *Water Research* 40 (2006) 2720-2726.
- [5] J. Liu, H. Chen, Q. Huang, L. Lou, B. Hu, S.D. Endalkachew, N. Mallikarjuna, Y. Shan, X. Zhou, Characteristics of pipe-scale in the pipes of an urban drinking water distribution system in eastern China, *Water Science and Technology: Water Supply* 16 (2016) 715-726.
- [6] L.A. Holmes, A. Turner, R.C. Thompson, Adsorption of trace metals to plastic resin pellets in the marine environment, *Environmental Pollution* 160 (2012) 42-48.
- [7] C.Y. Peng, G.V. Korshin, Speciation of trace inorganic contaminants in corrosion scales and deposits formed in drinking water distribution systems, *Water Research* 45 (2011) 5553-5563.
- [8] G. Graeme, Expert opinion: performance of polyolefin (PP-R, PEX and PB) piping and fittings in recirculating hot water systems under Australian operating conditions, Queensland University of Technology, Brisbane, 2012.
- [9] D. Wagner, H. Siedlarek, M. Kropp, W.R. Fischer, *Plastic Pipes IX*, IOM, (1995) 497.
- [10] D. Wright, *Failure of plastics and rubber products: causes, effects and case studies involving degradation*, iSmithers Rapra Publishing, 2001.
- [11] D.A. Lytle, T.J. Sorg, C. Frietch, Accumulation of arsenic in drinking water distribution systems, *Environmental Science & Technology* 38 (2004) 5365-5372.
- [12] M.J. Friedman, A.S. Hill, S.H. Reiber, R.L. Valentine, G. Larsen, A. Young, G.V. Korshin, C.Y. Peng, *Assessment of inorganics accumulation in drinking water system scales and sediments*, Water Research Foundation, Denver, 2010.
- [13] American Water Works Association (AWWA), *M28 Rehabilitation of Water Mains*, Third Edition, American Water Works Association (AWWA), Denver, 2014.

- [14] U.S. Environmental Protection Agency (EPA), Pilot-scale tests and systems evaluation for the containment, treatment, and decontamination of selected materials from T&E building pipe loop equipment. https://cfpub.epa.gov/si/si_public_record_report.cfm?address=nhsrc/&dirEntryId=188411, 2008 (accessed 16. 10. 01). Washington, D.C.
- [15] U.S. Environmental Protection Agency (EPA), Decontamination of drinking water infrastructure: A literature review and summary. https://cfpub.epa.gov/si/si_public_file_download.cfm?p_download_id=519689, 2014 (accessed 16. 09. 05). Cincinnati, OH.
- [16] D.O. Siringi, P.G. Home, E. Koehn, Cleaning Methods for Pipeline Renewals, *International Journal of Engineering and Technical Research* 2 (2014) 44-47.
- [17] K.S. Casteloes, R.H. Brazeau, A.J. Whelton, Decontaminating chemically contaminated residential premise plumbing systems by flushing, *Environmental Science: Water Research & Technology* 1 (2015) 787-799.
- [18] R.C. Copeland, D.A. Lytle, D.D. Dionysious, Desorption of arsenic from drinking water distribution system solids, *Environmental Monitoring and Assessment* 127 (2007) 523-535.
- [19] A.D. Ebner, J.A. Ritter, J.D. Navratil, Adsorption of cesium, strontium, and cobalt ions on magnetite and a magnetite– silica composite, *Industrial & Engineering Chemistry Research* 40 (2001) 1615-1623.
- [20] G. P. Fritzke, A letter regarding copper pipe treatment, Copper Development Association (CDA) Inc., 1991.
- [21] D. Leštan, C.L. Luo, X.D. Li, The use of chelating agents in the remediation of metal-contaminated soils: a review, *Environmental Pollution* 153 (2008) 3-13.
- [22] C. Oviedo, J. Rodríguez, EDTA: the chelating agent under environmental scrutiny, *Quimica Nova* 26 (2003) 901-905.
- [23] S.S. Ahluwalia, D. Goyal, Microbial and plant derived biomass for removal of heavy metals from wastewater, *Bioresource Technology* 98 (2007) 2243-2257.
- [24] M.E. Argun, S. Dursun, C. Ozdemir, M. Karatas, Heavy metal adsorption by modified oak sawdust: Thermodynamics and kinetics, *Journal of Hazardous Materials* 141 (2007) 77-85.
- [25] S.E. Bailey, T.J. Olin, R.M. Bricka, D.D. Adrian, A review of potentially low-cost sorbents for heavy metals, *Water Research* 33 (1999) 2469-2479.
- [26] S.O. Lesmana, N. Febriana, F.E. Soetaredjo, J. Sunarso, S. Ismadji, Studies on potential applications of biomass for the separation of heavy metals from water and wastewater, *Biochemical Engineering Journal* 44 (2009) 19-41.
- [27] T.H. Parsell, B.C. Owen, I. Klein, T.M. Jarrell, C.L. Marcum, L.J. Hauptert, L.M. Amundson, H.I. Kenttämä, F. Ribeiro, J.T. Miller, M.M. Abu-Omar, Cleavage and hydrodeoxygenation (HDO) of C–O bonds relevant to lignin conversion using Pd/Zn synergistic catalysis, *Chemical Science* 4 (2013) 806-813.
- [28] M.M. Abu-Omar, B. Saha, I. Klein, Compounds and compositions for delivery of nutrients and micronutrients to plants, WO 2017004052, 2017.
- [29] K. Ashton, L. Holmes, A. Turner, Association of metals with plastic production pellets in the marine environment, *Marine Pollution Bulletin* 60 (2010) 2050-2055.
- [30] H.A. Benesi, J. Hildebrand, A spectrophotometric investigation of the interaction of iodine with aromatic hydrocarbons, *Journal of the American Chemical Society* 71 (1949) 2703-2707.

- [31] S. Goswami, D. Sen, N.K. Das, H.K. Fun, C.K. Quah, A new rhodamine based colorimetric 'off-on' fluorescence sensor selective for Pd 2+ along with the first bound X-ray crystal structure, *Chemical Communications* 47 (2011) 9101-9103.
- [32] X. Yu, T. Qin, P. Zhang, Q. Hu, J. Li, Novel Rhodamine-Coumarin Conjugate as an Effective Colorimetric Probe for Copper Ions in Aqueous Solution and Test Kits, *Sensor Letters* 12 (2014) 142-146.
- [33] M. Salehi, Exploring Contaminant Fate within Plastic Water Infrastructure: The Nexus of Environmental Engineering and Material Science Frontiers, Civil Engineering, Purdue University, West Lafayette, IN, 2017.
- [34] B. Özkaya, Adsorption and desorption of phenol on activated carbon and a comparison of isotherm models, *Journal of Hazardous Materials* 129 (2006) 158-163.
- [35] Z. Li, Sorption kinetics of hexadecyltrimethylammonium on natural clinoptilolite, *Langmuir* 15 (1999) 6438-6445.
- [36] Y.S. Ho, J.C.Y Ng, G. McKay, Kinetics of pollutant sorption by biosorbents: review, *Separation and Purification Methods* 29 (2000) 189-232.
- [37] N.K. Lazaridis, T.A. Pandi, K.A. Matis, Chromium (VI) Removal from Aqueous Solutions by Mg- Al- CO₃ Hydrotalcite: Sorption- Desorption Kinetic and Equilibrium Studies, *Industrial & Engineering Chemistry Research* 43 (2004) 2209-2215.
- [38] S. Andrianirinaharivelo, G. Mailhot, M. Bolte, Photodegradation of organic pollutants induced by complexation with transition metals (Fe³⁺ and Cu²⁺) present in natural waters, *Solar Energy Materials and Solar Cells* 38 (1995) 459-474.
- [39] C.A. Blanco, I. Caballero, A. Rojas, M. Gomez, J. Alvarez, Chelation of aqueous iron (III) by 2-acetyl-1, 3-cyclohexanedione and beer ageing, *Food Chemistry* 81 (2003) 561-568.
- [40] G.A. Parks, The isoelectric points of solid oxides, solid hydroxides, and aqueous hydroxo complex systems, *Chemical Reviews* 65 (1965) 177-198.
- [41] M. Salehi, X. Li, A.J. Whelton, Metal Accumulation in Representative Plastic Drinking Water Plumbing Systems, *Journal of the American Water Works Association*, accepted on May 30, 2017, in press.
- [42] A. Stefánsson, Iron (III) hydrolysis and solubility at 25 C, *Environmental Science & Technology* 41 (2007) 6117-6123.
- [43] Y. Yang, J.S. Jiang, Gradual phase and morphology transformation of Fe₃O₄ nanoparticles to α -FeOOH nanorods in alcohol/water media in the presence of surfactant F127, *Journal of Materials Science* 43 (2008) 4340-4343.
- [44] U. Schwertmann, Solubility and dissolution of iron oxides, in: *Iron nutrition and interactions in plants*, Springer Netherlands (1991) 3-27.
- [45] R. Lacomba-Perales, J. Ruiz-Fuertes, D. Errandonea, D. Martínez-García, A. Segura, Optical absorption of divalent metal tungstates: Correlation between the band-gap energy and the cation ionic radius, *Europhysics Letters* 83 (2008) 37002.
- [46] G. Bacquet, J. Dugas, C. Escribe, J. Gaite, J. Michoulier, Comparative electron paramagnetic resonance study of Fe³⁺ and Gd³⁺ ions in monoclinic zirconia, *Journal of Physics C: Solid State Physics* 7 (1974) 1551.
- [47] R.G. Pearson, Absolute electronegativity and hardness: application to inorganic chemistry, *Inorganic Chemistry* 27 (1988) 734-740.
- [48] H. Irving, R. Williams, 637. The stability of transition-metal complexes, *Journal of the Chemical Society (Resumed)* (1953) 3192-3210.

- [49] A.E. Martell, R.D. Hancock, Metal complexes in aqueous solutions, Springer Science & Business Media 2013.
- [50] D. Bhattacharyya, J.A. Hestekin, P. Brushaber, L. Cullen, L.G. Bachas, S.K. Sikdar, Novel poly-glutamic acid functionalized microfiltration membranes for sorption of heavy metals at high capacity, *Journal of Membrane Science* 141 (1998) 121-135.
- [51] Z. Tang, S. Hong, W. Xiao, J. Taylor, Characteristics of iron corrosion scales established under blending of ground, surface, and saline waters and their impacts on iron release in the pipe distribution system, *Corrosion Science* 48 (2006) 322-342.
- [52] E.J. Kim, J.E. Herrera, Characteristics of lead corrosion scales formed during drinking water distribution and their potential influence on the release of lead and other contaminants, *Environmental Science & Technology* 44 (2010) 6054-6061.
- [53] O.W. Duckworth, S.T. Martin, Surface complexation and dissolution of hematite by C 1-C 6 dicarboxylic acids at pH= 5.0, *Geochimica et Cosmochimica Acta* 65 (2001) 4289-4301.
- [54] B.A. Holmén, W.H. Casey, Hydroxamate ligands, surface chemistry, and the mechanism of ligand-promoted dissolution of goethite [α -FeOOH (s)], *Geochimica et Cosmochimica Acta* 60 (1996) 4403-4416.
- [55] S.F. Cheah, S.M. Kraemer, J. Cervini-Silva, G. Sposito, Steady-state dissolution kinetics of goethite in the presence of desferrioxamine B and oxalate ligands: implications for the microbial acquisition of iron, *Chemical Geology* 198 (2003) 63-75.

APPENDIX A

Isotherm and kinetic model fittings

The Langmuir and Freundlich isotherm models were adopted to study the effect of metal concentrations on metal adsorptions. The assumption for the Langmuir isotherm is the monolayer adsorption on a homogeneous plastic surface:

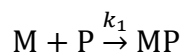
$$[MP]_e = \frac{k_L [MP]_{max} [M]_e}{1 + k_L [M]_e}$$

where $[MP]_e$ ($\mu\text{g}/\text{m}^2$) is the amount of metals adsorbed onto plastics surfaces at the equilibrium status, $[MP]_{max}$ is the maximum metal adsorption capacity, $[M]_e$ is the equilibrium metal concentration in the solution, k_L ($\text{L } \mu\text{g}^{-1}$) is the Langmuir isotherm constant. For the Freundlich model, the assumption is that multilayer adsorption occurs:

$$[MP]_e = k_F [M]_e^{1/n}$$

where n is the measurement of linearity and k_F ($\mu\text{g}^{1-1/n} \text{m}^{-2} \text{L}^{1/n}$) is the Freundlich constant.

The pseudo-first-order model has been applied to study the interaction of metals with micro-plastics [1]:



In which, M stands for metals in the solution, P represents the plastic surface, and MP is metal adsorbed onto plastic surfaces.

The reaction rate expression:

$$\frac{d[MP]}{dt} = k_1 ([MP]_e - [MP]_t)$$

Where k_1 is the pseudo-first order reaction constant, with unit hr^{-1} . $[\text{MP}]_e$ and $[\text{MP}]_t$ ($\mu\text{g}/\text{m}^2$) are amount of metals adsorbed onto plastic surfaces at the equilibrium status, and at time t (hr), respectively.

Apply the boundary condition, when $t=0$, $[\text{MP}]_0=0$:

$$\ln([\text{MP}]_e - [\text{MP}]_t)_{[\text{MP}]_0}^{[\text{MP}]_t} = -k_1 t$$

Final equation used for curve fitting as:

$$[\text{MP}]_t = [\text{MP}]_e(1 - e^{-k_1 t})$$

The first-order reaction half- life, $t_{1/2}$ (hr), is defined as when $[\text{MP}]_t=1/2 [\text{MP}]_e$. So

$$t_{1/2} = \frac{\ln 2}{k_1}$$

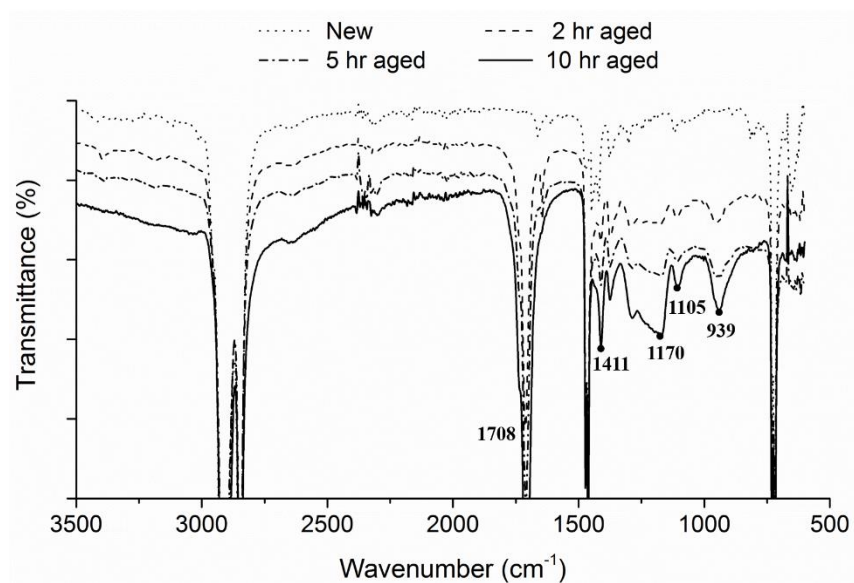


Figure A.1 FTIR spectra of new and aged LDPE pellets.

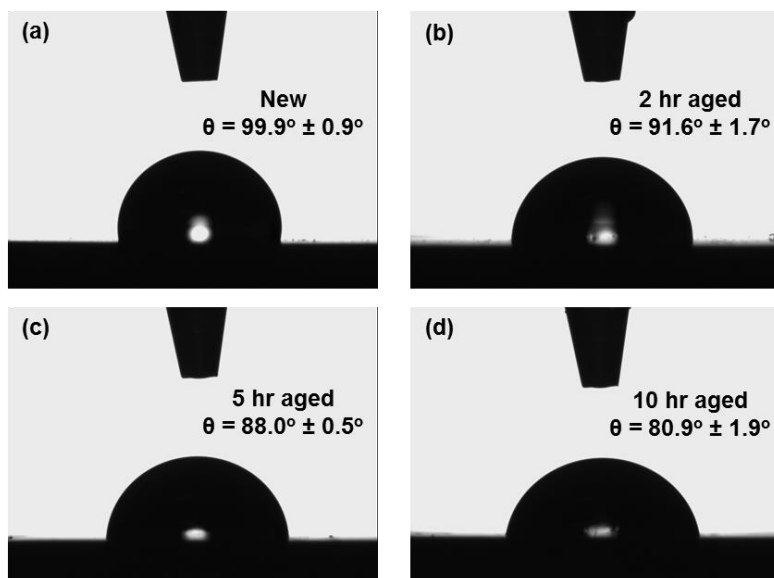


Figure A.2 Contact angle measurement images of (a) New LDPE segment, (b) 2 hr aged LDPE segment, (c) 5 hr aged LDPE segment, and (d) 10 hr aged LDPE segment.

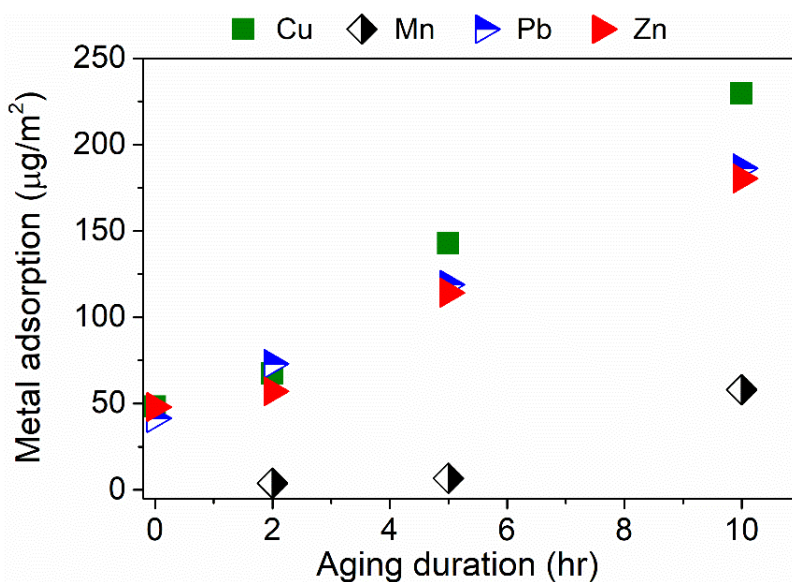


Figure A.3 Metal adsorption onto new and aged (i.e., 2, 5 and 10 hr aged) LDPE pellets. The exhibiting data was the adsorbed metal at the end of 24 hr (i.e., equilibrium point). Initial metal concentration was 30 ppb for each metal, equilibrium pH was at 6.8.

Table A.1 Use Minteq ver. 3.1 to predict metal speciation (% of total metal) in the solution as variation of equilibrium pH values^a.

Metal Type	Metal Speciation	<i>Equilibrium pH @</i>					
		5.5	6.4	6.8	7.2	7.5	9.3
Calcium	Ca ²⁺	88.9	88.8	88.7	88.7	88.6	50.2
	CaCO ₃ (aq)	< 1	< 1	< 1	< 1	< 1	1.1
	CaCO₃ (s)	< 1	< 1	< 1	< 1	< 1	42.1
	CaSO ₄ (aq)	10.9	10.9	10.9	10.8	10.8	6.4
Copper	Cu ²⁺	87.8	75.2	56.8	37.8	20.8	< 1
	Cu(OH) ⁺	< 1	5.0	9.7	14.1	17.8	7.4
	Cu(OH) ₂ (aq)	< 1	< 1	< 1	< 1	1.0	24.3
	Cu(OH)₂ (s)	< 1	< 1	< 1	< 1	< 1	53.1
	Cu(OH) ₃ ⁻ (aq)	< 1	< 1	< 1	< 1	< 1	1.9
	CuCO ₃ (aq)		9.6	25.4	42.3	57.1	12.2
	CuSO ₄ (aq)	10.8	9.2	7.0	4.6	2.5	< 1
Manganese	Mn ²⁺	91.2	90.9	90.5	90.0	88.8	55.0
	MnOH ⁺	< 1	< 1	< 1	< 1	< 1	2.1
	MnCO ₃ (aq)	< 1	< 1	< 1	< 1	2.1	37.1
	MnSO ₄ (aq)	8.7	8.7	8.6	8.5	8.4	5.4
Lead	Pb ²⁺	75.7	64.4	53.3	40.8	26.3	< 1
	PbOH ⁺	< 1	< 1	7.2	12.1	17.9	1.4
	Pb(OH)₂ (s)	< 1	< 1	< 1	< 1	< 1	96.0
	PbHCO ₃ ⁺ (aq)	2.8	9.7	11.0	9.6	6.7	< 1
	PbCO ₃ (aq)	< 1	4.7	13.7	26.2	41.6	1.7
	PbSO ₄ (aq)	19.9	16.9	14.0	10.7	6.9	< 1
Zinc	Zn ²⁺	89.2	88.6	87.9	86.7	83.8	2.6
	ZnOH ⁺	< 1	< 1	< 1	1.0	2.3	4.0
	Zn(OH) ₂ (aq)	< 1	< 1	< 1	< 1	< 1	90.3
	ZnCO ₃ (aq)	< 1	< 1	< 1	2.2	2.2	2.0
	ZnSO ₄ (aq)	10.5	10.4	10.3	10.1	9.8	< 1

a. Trace metal speciation (percentage < 1) was not shown in the table.

b. Experimental conditions: 30 ppb of Cu, Mn, Pb and Zn, equilibrium pH was at 6.

Table A.2 Isotherm model fitting (Langmuir and Freundlich models) summary of competitive metal adsorption (Cu, Mn, Pb and Zn) onto 10 hr aged plastic surfaces.

Metal	<i>Langmuir model</i>			<i>Freundlich model</i>		
	k _L (L.µg ⁻¹)	[MP] _{max} (µg.m ⁻²)	R _L ²	k _F (µg ^{1-1/n} m ⁻² L ^{1/n})	1/n	R _F ²
Cu	0.048	1109	0.95	48.23	0.81	0.99
Mn	0.015	199	0.98	5.39	0.70	0.98
Pb	0.021	1038	0.97	34.92	0.71	0.99
Zn	0.019	893	0.90	42.73	0.58	0.96

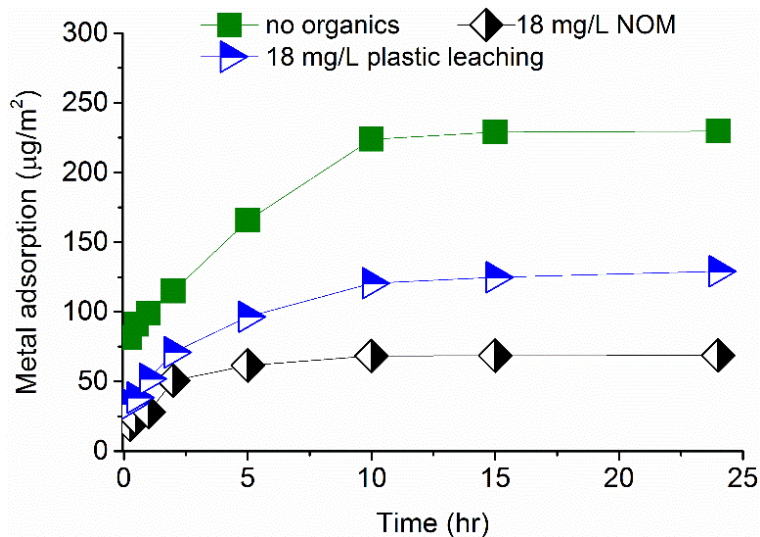


Figure A.4 Organic constitutes effect of Cu adsorption onto 10hr aged LDPE pellets. Initial metal concentration was 30 ppb of each metal (i.e., Cu, Mn, Pb and Zn), at pH 7.5. Initial metal concentration was 30 ppb, equilibrium pH was at 6.8.

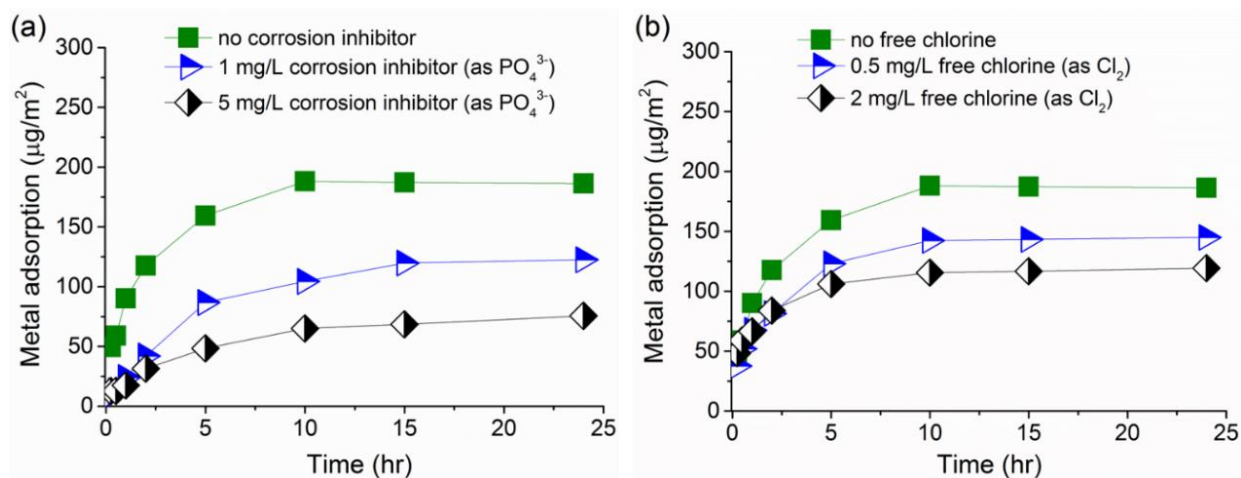


Figure A.5 The presence of the (a) corrosion inhibitor and (b) free chlorine reduced metal adsorption onto suspended 10 hr aged LDPE pellets. Initial metal concentration was 30 ppb of each metal (i.e., Cu, Mn, Pb and Zn), equilibrium pH was at 6.8.

Table A.3 Comparison of metals competitive adsorption onto plastic surfaces by using pseudo-first-order model fittings.

Metal	<i>Without Fe scenario</i>			<i>With Fe scenario</i>		
	k_1 (hr ⁻¹)	$t_{1/2}$ (hr)	R_1^2	k_1 (hr ⁻¹)	$t_{1/2}$ (hr)	R_1^2
Cu	0.55	1.26	0.73	0.79	0.88	0.74
Fe	-	-	-	0.76	0.91	0.73
Mn	0.15	4.62	0.95	0.11	6.30	0.94
Pb	0.64	1.08	0.95	0.57	1.22	0.92
Zn	0.25	2.77	0.86	0.41	1.69	0.89

- represents the data is not available.

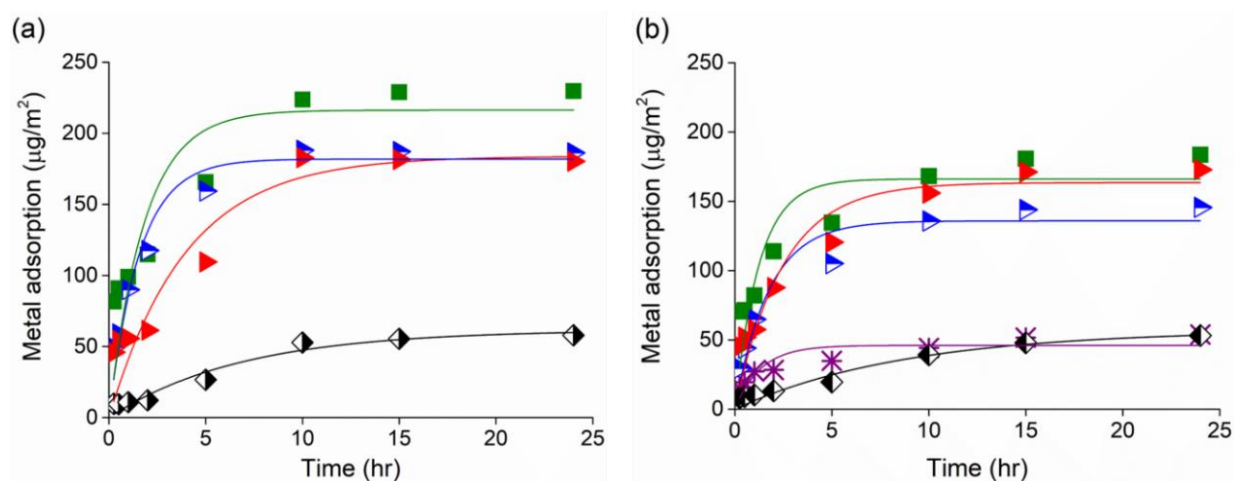


Figure A.6 Competitive metal adsorption onto 10 hr aged LDPE pellets surface (a) without Fe and (b) with Fe scenarios (■ Cu, * Fe, ◆ Mn, ▲ Pb, and ▲ Zn). Solid lines stand for the pseudo-first-order kinetic model fitting. Initial metal concentration was 30 ppb for each metal, equilibrium pH was at 6.8.

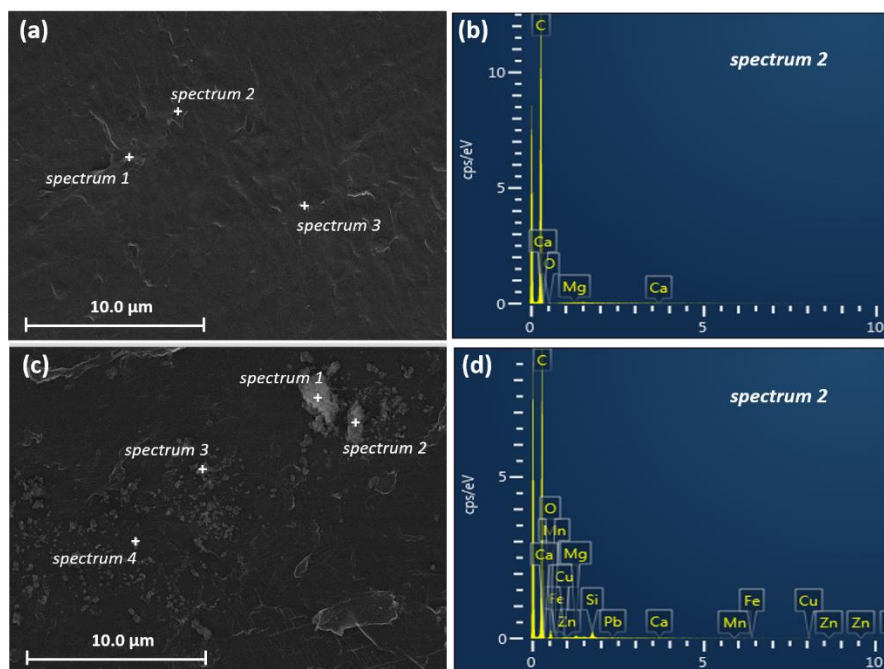


Figure A.7 (a) The SEM image and (b) the selected EDS spectrum of new LDPE segment from the blank solution (water only). (c) The SEM image and (b) the selected EDS spectrum of new LDPE segment from the metal solution (with 3 ppm of Cu, Fe, Mn, Pb, and Zn, respectively).

Table A.4 Elemental atomic concentration % from LDPE pellets.

<u>Sample name</u>	<u>Element composition (%)</u>					
	C 1s %	N 1s %	O 1s %	Cu 2p %	Pb 4f %	Zn 2p3/2 %
without Fe	91.34	2.03	6.30	0.15	0.06	0.13
with Fe	92.46	2.13	5.30	0.05	0.03	0.04

References:

- [1] A. Turner, L.A. Holmes, Adsorption of trace metals by microplastic pellets in fresh water, *Environmental Chemistry*, 12 (2015) 600-610.

APPENDIX B



Figure B.1 Illustration of pipe apparatus and experimental groups' layout: (1) P rig: PEX pipe only (1.905 cm diameter, 30 cm length), (2) C rig: copper pipe only (1.905 cm diameter, 30 cm length), (3) PBP rig: PEX pipe (1.905 cm diameter, 15 cm length) + brass valve + PEX pipe (1.905 cm diameter, 15 cm length) and (4) CBP rig: copper pipe (1.905 cm diameter, 15 cm length) + brass valve + PEX pipe (1.905 cm diameter, 15 cm length). Only 2 of the 4 replicates are shown.

Table B.1 End pHs and % of dissolved metals during the 21 days metal leaching test.

Water Type	Water condition	pH	Alkalinity mg/L as CaCO ₃	Temperature °C	Hardness mg/L as CaCO ₃
Aggressive	A	7.5	175	23	100
	B	7.5	175	55	100
Moderate	C	4	0	23	100
	D	4	0	55	100



Figure B.2 Image of metal scales on exhumed galvanized and PEX-A drinking water pipes from the cold city water supply line.

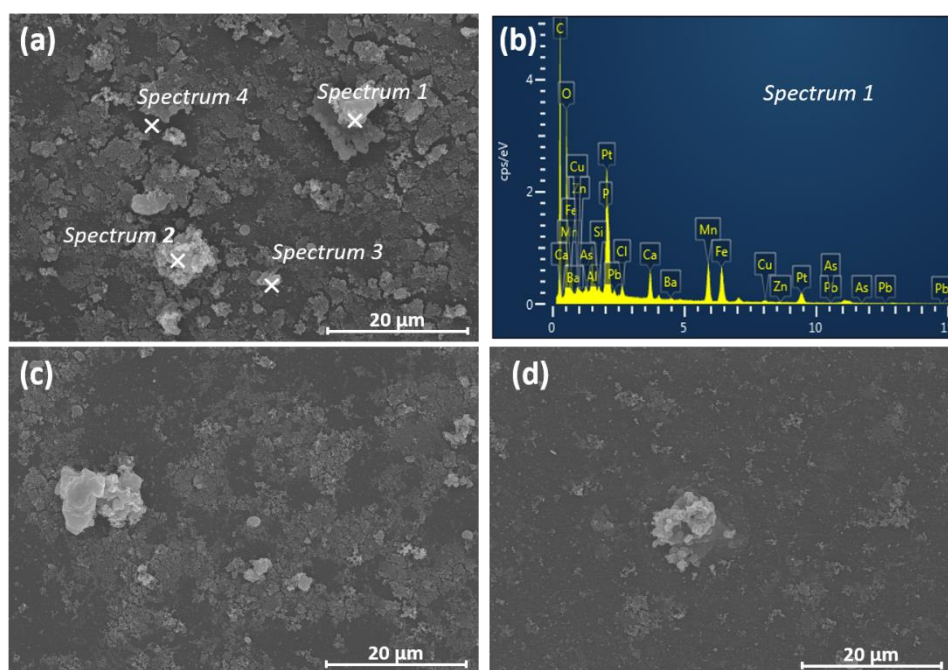


Figure B.3 SEM images and EDS spectrum of exhumed PEX piping surfaces at (a) section 1-1 (SEM), (b) 1-1 (EDS), (c) 1-2 and (d) 1-3.

Table B.2 End pHs and % of dissolved metals during the 21 days metal leaching test.

Sample Name	Element												
	Al	Ba	Ca	Cd	Cu	Fe	Mg	Mn	Ni	P	Pb	Si	Zn
<i>Found on Galvanized Iron Pipes (GIP) by scraping and digestion, %</i>													
GIP1-cold	0.01	0.44	3.29	0.01	0.22	85.73	0.27	0.40	0.63	5.17	0.01	1.99	1.84
GIP2-cold	0.08	2.84	6.65	-	0.58	60.48	0.61	21.02	0.02	4.68	0.06	2.01	0.96
GIP3-hot	1.03	0.13	27.18	0.01	0.25	47.95	0.47	0.58	0.05	9.92	0.03	1.78	10.63
GIP4-cold	0.12	0.50	5.09	-	0.23	81.71	0.38	0.31	0.02	6.44	0.05	2.11	3.04
GIP5-cold	0.03	0.37	3.11	0.01	0.13	82.46	0.27	0.99	-	4.01	0.20	2.24	6.18
GIP6-cold	0.08	0.32	4.35	-	0.13	86.69	0.28	0.29	-	4.35	0.02	2.03	1.48
<i>Found on Crosslinked Polyethylene (PEX) Pipes by digestion, %</i>													
PEX1-cold	0.04	1.64	7.41	0.01	10.71	37.94	0.66	25.35	0.08	2.77	2.50	2.79	8.11
PEX2-cold	0.08	1.41	7.78	0.01	15.62	25.59	0.65	28.15	0.06	2.42	4.28	3.29	10.64
PEX3-hot	0.40	0.71	16.98	-	5.02	40.90	1.29	5.48	0.10	15.35	-	8.73	5.04
PEX4-cold	0.21	0.93	11.03	-	1.82	59.95	3.16	2.74	0.13	10.20	0.33	6.91	2.58
PEX5-cold	0.08	1.00	13.36	-	1.44	55.98	3.54	0.63	0.11	12.52	0.07	10.35	0.92
PEX6-cold	1.52	1.42	5.98	-	2.77	58.14	0.54	6.84	0.05	7.38	0.22	4.76	10.39

- Represents the metal was below the method report limit or the percentage value was below 0.01.

Table B.3 Elemental composition (% atomic concentration) of exhumed PEX piping metal deposits.

Sample	C 1s	Ca 2p	Cu 2p	Fe 2p	Mn 2p	O 1s	P 2p	Pb 4f	Si 2p	Zn 2p
PEX-1	33.0 (0.9)	2.8 (0.1)	2.9 (0.2)	3.6 (0.3)	8.6 (0.4)	43.5 (0.6)	1.6 (0.1)	0.2 (0.0)	-	1.4 (0.1)
PEX-3	79.5 (3.5)	1.0 (0.3)	-	0.9 (0.1)	0.2 (0.0)	14.2 (2.5)	0.7 (0.1)	-	2.3 (0.3)	0.1 (0.0)
PEX-6	51.1 (2.0)	1.1 (0.6)	-	6.0 (1.0)	0.2 (0.1)	34.4 (1.2)	2.1 (1.1)	-	2.0 (0.7)	1.4 (0.2)

- represents the element was not detected.

Table B.4 Influence of water solutions on metal aqueous concentration.

Metal Element	<u>Cold pH 4 vs. 7.5 (p-value)</u>			<u>Hot pH 4 vs. 7.5 (p-value)</u>		
	C	PBP	CBP	C	PBP	CBP
Cu (n=4)	0.029	0.029	0.029	0.029	0.029	0.886
Pb (n=4)	-	0.021	0.021	-	0.021	0.021
Zn (n=4)	-	0.029	0.029	0.029	0.029	0.029

- represents the metal aqueous data was below the method report limit. The Wilcoxon test was not conducted.

Table B.5 Influence of temperatures on metal aqueous concentration.

Metal Element	<u>PH 4 water 23 vs 55°C (p-value)</u>			<u>PH 7.5 water 23 vs 55°C (p-value)</u>		
	C	PBP	CBP	C	PBP	CBP
Cu (n=4)	0.029	0.029	0.029	0.029	0.029	0.029
Pb (n=4)	-	0.029	0.029	-	-	-
Zn (n=4)	0.029	0.029	0.057	-	0.029	0.029

- represents the metal aqueous data was below the method report limit. The Wilcoxon test was not conducted.

Table B.6 Composition (wt%) of brass valve and copper pipe from XRF analysis.

Sample	As	Co	Cu	Fe	Mn	Ni	Pb	Zn
Brass value	0.0 (0.0)	0.1 (0.0)	64.3 (0.5)	0.4 (0.1)	0.1 (0.0)	0.2 (0.0)	-	34.9 (0.6)
Copper pipe	0.0 (0.0)	0.0 (0.0)	99.8 (0.0)	-	-	0.1 (0.0)	-	0.1 (0.0)

Data presented as averaged values from four replicates (with standard deviation).

- represents the element was not detected.

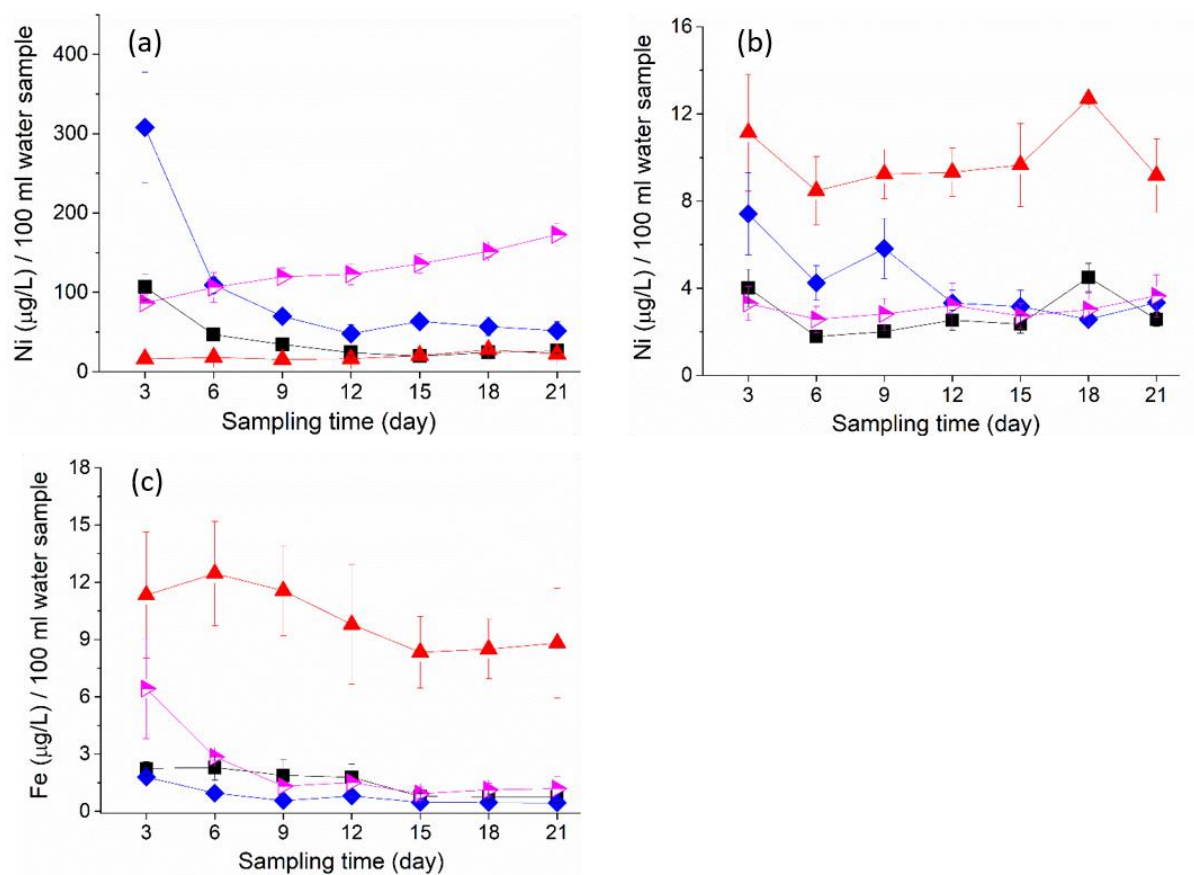


Figure B.4 (a) Ni and (c) Fe levels when plumbing rigs exposed to the pH 4 water and (b) Ni levels when they were exposed to the pH 7.5 water. —■— PBP @ 23°C, —▲— CBP @ 23°C, —◆— PBP @ 55°C, —▶— CBP @ 55°C. Fe levels were not detected under pH 7.5 water condition.

Table B.7 Total mass of Fe, Mg and Ni leached in water samples and deposited on PEX surfaces during the 21 day exposure period.

Exp. Group	Metal Element	<i>In water, µg</i>				<i>On pipe surface, µg/m²</i>			
		pH 4		pH 7.5		pH 4		pH 7.5	
		Cold	Hot	Cold	Hot	Cold	Hot	Cold	Hot
P rig	Fe	nd	nd	nd	nd	13.8	25.7	18.6	27.6
	Mg	ns	ns	ns	ns	10.0	6.2	8.8	6.8
	Ni	nd	nd	nd	nd	nd	nd	nd	nd
C rig	Fe	7.0	11.7	nd	nd	ns	ns	ns	ns
	Mg	ns	ns	ns	ns	ns	ns	ns	ns
	Ni	nd	nd	nd	nd	ns	ns	ns	ns
PBP rig	Fe	0.7	0.4	nd	nd	27.4	58.2	36.0	43.6
	Mg	ns	ns	ns	ns	31.3	79.4	51.3	110.8
	Ni	21.1	53.0	1.5	2.2	nd	nd	nd	nd
CBP rig	Fe	6.0	1.3	nd	nd	31.2	138.7	51.3	115.9
	Mg	ns	ns	ns	ns	39.8	89.9	76.1	[
	Ni	11.6	76.1	5.9	1.8	nd	nd	nd	nd

nd = the element was below the method report limit

ns = no sample/analysis was not conducted.

Table B.8 Influence of water solutions on metal surface deposits.

Metal Element	<u>Cold pH 4 vs. 7.5 (p-value)</u>			<u>Hot pH 4 vs. 7.5 (p-value)</u>		
	P	PBP	CBP	P	PBP	CBP
Ca (n=4)	0.029	0.029	0.029	0.029	0.029	0.029
Cu (n=4)	0.114	0.886	0.561	0.885	0.029	0.029
Pb (n=4)	0.029	0.029	0.114	-	0.029	0.029
Zn (n=4)	0.200	0.029	0.057	0.200	0.029	0.029

- represents the metal aqueous data was below the method report limit, thus the Wilcoxon test was not conducted.

Table B.9 Influence of temperatures on metal surface deposits.

Metal Element	<u>pH 4 water 23 vs 55oC (p-value)</u>			<u>pH 7.5 water 23 vs 55oC (p-value)</u>		
	P	PBP	CBP	P	PBP	CBP
Ca (n=4)	0.029	0.029	0.029	0.029	0.029	0.029
Cu (n=4)	0.029	0.886	0.029	0.886	0.029	0.029
Pb (n=4)	0.309	0.029	0.0289	0.468	0.029	0.029
Zn (n=4)	0.057	0.029	0.029	0.384	0.029	0.029

- represents the metal aqueous data was below the method report limit, thus the Wilcoxon test was not conducted

Table B.10 Averaged water pH and percent dissolved metals during 3 weeks exposure period.

Water cond.	Exp. group	End pH	Cu %	Fe %	Ni %	Pb %	Zn %
<u>23°C</u>							
pH 4	PEX	3.9 ± 0.0	99.2 ± 1.9	nd	nd	nd	98.5 ± 1.0
pH 7.5	PEX	7.7 ± 0.1	nd	nd	nd	nd	nd
pH 4	Copper	6.6 ± 0.2	97.3 ± 0.9	nd	nd	nd	98.3 ± 0.6
pH 7.5	Copper	3.9 ± 0.0	62.4 ± 0.7	10.2 ± 0.3	nd	nd	nd
pH 4	PBP	5.0 ± 0.2	95.6 ± 0.8	nd	98.1 ± 0.3	nd	97.9 ± 0.4
pH 7.5	PBP	7.8 ± 0.1	87.2 ± 3.7	nd	94.90 ± 0.5	nd	85.1 ± 2.0
pH 4	CBP	6.7 ± 0.1	96.0 ± 0.9	nd	98.2 ± 1.0	nd	97.3 ± 0.8
pH 7.5	CBP	7.9 ± 0.1	77.7 ± 3.37	nd	94.8 ± 1.3	nd	78.3 ± 1.8
<u>55°C</u>							
pH 4	PEX	4.0 ± 0.0	98.4 ± 1.5	nd	nd	nd	98.7 ± 0.9
pH 7.5	PEX	8.6 ± 0.0	nd	nd	nd	nd	nd
pH 4	Copper	5.4 ± 0.1	70.7 ± 0.8	nd	nd	nd	92.2 ± 1.4
pH 7.5	Copper	8.3 ± 0.1	62.1 ± 0.7	nd	nd	nd	nd
pH 4	PBP	7.0 ± 0.1	96.2 ± 0.6	nd	96.6 ± 1.6	35.5 ± 3.5	97.2 ± 1.8
pH 7.5	PBP	8.3 ± 0.1	78.9 ± 1.2	nd	93.5 ± 1.8	nd	77.7 ± 2.3
pH 4	CBP	7.4 ± 0.1	95.2 ± 1.7	nd	95.8 ± 0.5	21.1 ± 1.9	97.1 ± 1.3
pH 7.5	CBP	8.4 ± 0.1	67.0 ± 2.3	nd	93.4 ± 1.2	nd	71.4 ± 1.8

ND standards for the dissolved metal data was not detected or below the method report limit.

End pH and % dissolved metals were obtained from day 3 to day 21 data collection.

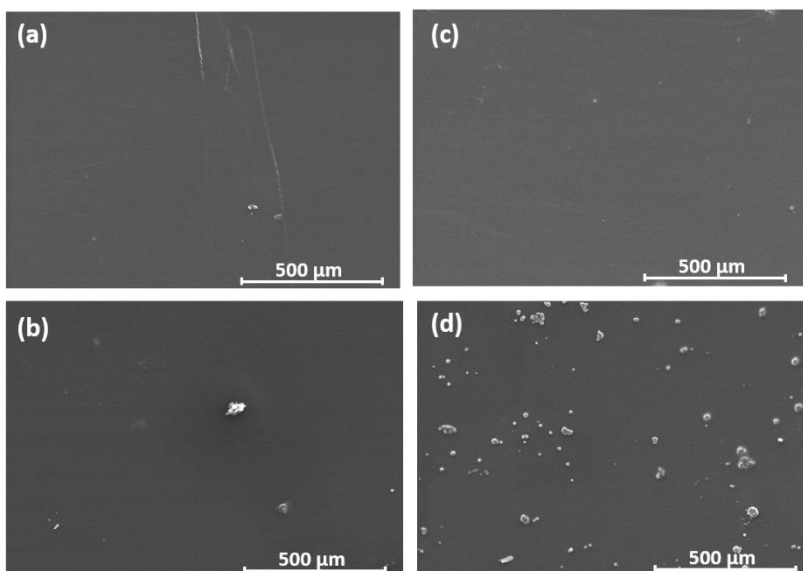


Figure B.5 SEM images of metal deposition onto PEX surfaces from CBP rigs at (a) 23°C top section (b) 23°C bottom section (c) 55°C top section and (d) 55°C bottom section. The pH 7.5 water conditions were used.

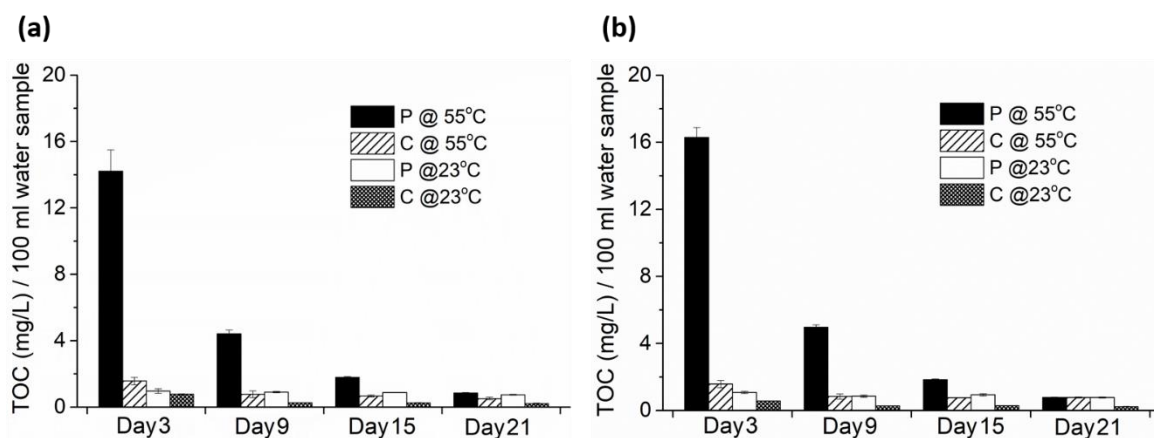


Figure B.6 P and C rigs organics leaching during the three weeks experimental period at 55°C and 23°C under (a) pH 4, and (b) pH 7.5 water condition.